University of Alberta

Synthesis and Biological Evaluation of Bacteriocin Analogues and the Analgesic Peptide Crotalphine

by

Darren J. Derksen

A thesis submitted to the Faculty of Graduate Studies and Research in partial fulfillment of the requirements for the degree of

Doctor of Philosophy

Department of Chemistry

Edmonton, Alberta

Spring 2008

Your file Votre référence
ISBN: 978-0-494-45416-9
Our file Notre référence
ISBN: 978-0-494-45416-9

ABSTRACT

This thesis is divided into four sections. The first section focuses on antimicrobial peptides and will address synthetic difficulties in the synthesis of the bacteriocins leucocin A (**1**), pediocin PA-1 (**2**) and a number of analogues prepared to examine structure activity relationships (SAR) of these two peptides. The SAR studies focus on the highly conserved disulfide ring and explore the possibility of replacing disulfide bonds with carbon-carbon double bonds as well as hydrophobic residues.

The next section deals with the preparation of induction peptides responsible for the production of piscicolin 126, carnobacteriocin A and enterocins A and B. Through chemical synthesis, the corresponding induction peptides PisN (**8**), CbaX (**9**), and EntF (**10**) are prepared and subjected to biological testing. In the CbaX and EntF peptides, hybrid peptides and fragments are closely examined to elucidate how these peptides function and interact with their cognate receptors.

Difficulties in the preparation of CbaX (**9**) inspired the development of the third project. Observation of a thiol eliminated byproduct inspired progress toward an alternative linker that fundamentally addresses the acidity of the C-terminal α-proton by incorporation of an orthoester. This study involves the synthesis and purification of a standard tripeptide using a variety of conditions to examine the effect of base on different resin linkers.

The final project involves a structure activity relationship study of crotalphine (**13**), a peptide that has reported biological activity as an orally administered analgesic. Through chemical synthesis, a variety of analogues that examine the disulfide bridge and the *N*-terminal pyroglutamic acid residue were prepared.

Dedicated to my best friend, companion and wife, Heather

ACKNOWLEDGEMENTS

I would like to acknowledge my research supervisor, Professor John C. Vederas, for his constant support, encouragement and seemingly endless supply of ideas. The time that I have spent in his research group has introduced me to new ideas and perspectives that have helped to prepare me for a future in science. Similarly, the people that I have met while in his group have made my time in the lab a tremendous learning experience and have helped me to develop not only as a scientist, but as a person. I would specifically like to thank Drs. Matt Clay and Viji Moorthie for the time they spent proofreading this manuscript as well as Ms. Emma Heydari (summer, 2007) and Ms. Landon Reid (401 project, 2007) for their assistance and hardwork.

This work would not have been possible without the tremendous support of our collaborators who spent time teaching me how to complete experiments and interpret results. I would particularly like to mention my gratitude for the assistance of Prof. Peter Smith, Prof. Alan Hudson, Prof. Bradley Taylor (Tulane University) and all of their research groups for enduring my endless stream of questions and hypotheses about the crotalphine project. I would like to thank the staff at the Department of Chemistry, especially those in analytical and spectral services for there technical assistance. I would like to thank all of the funding agencies for the financial support that has made my time in graduate school possible. The University of Alberta, the Natural Sciences and Engineering Research Council (NSERC), the Alberta Ingenuity Foundation, and the Advanced Foods and Materials Network are all gratefully acknowledged for their financial contributions.

I would like to acknowledge all of the young athletes at Paralympic Sport sledge hockey who have unknowingly taught me more about life then I could ever hope to teach them about hockey. My appreciation also goes out to my family and friends for their constant support and encouragement throughout my graduate studies. My parents deserve particular gratitude for their encouragement and for the skills that they taught me from a young age. The values, beliefs and dedication they have instilled in me have proven beneficial in every aspect of my life. My dad's insistence on hard work and my mom's caring heart have stood by me throughout my life and I cannot thank them enough for the influence they have had on me.

Finally, I would like to thank my wife Heather for her endless supply of encouragement, patience, smiles, and laughs. Your understanding throughout this entire time has been instrumental in getting me through each day with the motivation to tackle new challenges. I look forward to the next chapter of our lives together.

TABLE OF CONTENTS

LIST OF TABLES

LIST OF FIGURES

LIST OF SCHEMES

LIST OF ABBREVIATIONS

$[\alpha]_D^{25}$	specific rotation
A or Ala	alanine
Ac	acetyl
Acm	acetamidomethyl
Ac_2O	acetic anhydride
AcOH	acetic acid
ap	apparent
Apa	azidophenylalanine
APT	all purpose tween
Ar	aryl
atm	atmosphere
Bn	benzyl
Boc	*tert*-butoxycarbonyl
$(Boc)_2O$	di-*tert*-butyl dicarbonate
Bpa	benzoylphenylalanine
n-Bu	*normal*-butyl
t-Bu	*tertiary*-butyl
t-BuOH	*tertiary*-butanol
br	broad
c	concentration
C or Cys	cysteine

C-terminus	carboxy terminus
calc'd	calculated
CbaX	induction peptide of carnobacteriocin A
CbnB2	carnobacateriocin B2
Cbz	benzyloxycarbonyl
CCI	chronic constriction injury
CD	circular dichroism
CFA	complete Freund's adjuvant
COSY	correlation spectroscopy
CurA	curvacin A
δ	chemical shift in parts per million downfield from tetramethylsilane
d	doublet
D or Asp	aspartic acid
DBU	1,8-diazabicyclo[5.4.0]undec-7-ene
DCC	1,3-dicyclohexylcarbodiimide
DCM	dichloromethane
DIPEA	diisopropylethylamine
DMAP	4-dimethylaminopyridine
DMF	*N*,*N*-dimethylformamide
DMSO	dimethylsulfoxide
E or Glu	glutamic acid
EDT	1,2-ethane dithiol
EI	electron impact

EntF	induction peptide of enterocin A and B
eq.	equivalents
ES	electrospray
Et	ethyl
EtOCOCl	ethyl chloroformate
Et_3N	triethylamine
Et_2O	diethyl ether
EtOAc	ethyl acetate
EtOH	ethanol
F or Phe	phenylalanine
Fm	fluorenyl
Fmoc	9*H*-fluorenylmethoxycarbonyl
g	gram
g	local acceleration due to gravity
G or Gly	glycine
gCOSY	gradient correlation spectroscopy
gHMBC	gradient heteronuclear multiple bond correlation spectroscopy
gHMQC	gradient heteronuclear multiple quantum correlation spectroscopy
h	hour
H or His	histidine
HIV	Human immunonodeficiency virus
HPLC	high performance liquid chromatography
HRMS	high resolution mass spectrometry

I or Ile	isoleucine
IC_{50}	concentration causing 50% inhibition
IP	intraperitoneal
IR	infrared
J	coupling constant
K or Lys	lysine
kg	kilogram
L or Leu	leucine
LAB	lactic acid bacteria
LC	liquid chromatography
LeuA	leucocin A
lit.	literature reference
m	multiplet
M or Met	methionine
MALDI-TOF	matrix-assisted laser desorption ionization / time of flight
Me	methyl
MeCN	acetonitrile
MeOH	methanol
mer	number of reidues in a peptide chain
Mes	mesityl
MesY105	mesentericin Y105
min	minute(s)
mL	millilitre

mol	mole
mpt	mannose phosphotransferase
MHz	megahertz
MS	mass spectrometry
MW	molecular weight
MWCO	molecular weight cut-off
μ	micro
N or Asn	asparagine
N-terminus	amino terminus
NaOMe	sodium methoxide
NCL	native chemical ligation
Nle	norleucine
NlePed	pediocin PA-1 with M31Nle substitution
nm	nanometres
NMM	*N*-methylmorpholine
NMP	N-methyl pyrollidone
NMR	nuclear magnetic resonance
Nva	norvaline
OBO	4-methyl-trioxobicyclo[2.2.2]octanyl
P or Pro	proline
Ped	pediocin PA-1
PEG	polyethylene glycol
Ph	phenyl

PisA	piscicolin 126
PisN	induction peptide in production of PisA
pKa	acid dissociation constant
PMB	*para*-methoxybenzyl
i-Pr	*iso*-propyl
PyBOP	benzotriazole-1-yl-oxy-*tris*-pyrrolidino-phosphonium hexafluorophosphate
q	quartet
quin	quintet
Q or Gln	glutamine
R or Arg	arginine
RCM	ring closing metathesis
R_f	retention factor
RP	reverse phase
rt	room temperature
s	singlet
S or Ser	serine
SA	sinapinic acid, 3,5-dimethoxy-4-hydroxycinnamic acid
SAR	structure activity relationship
SakP	sakacin P
SNI	spared nerve injury
SPPS	solid phase peptide synthesis
t	triplet

T or Thr	threonine
TfO	trifluoromethylsulfonyl
TFA	trifluoroacetic acid
TFE	trifluoroethanol
THF	tetrahydrofuran
TIPS-H	triisopropylsilane
TLC	thin layer chromatography
Tmd	3-(trifluoromethyl)-3*H*-diazirin-3-yl
TMS	trimethylsilyl
TMSBr	bromotrimethylsilane
TMSI	iodotrimethylsilane
TMSOTf	trifluoromethylsulfonyltrimethylsilane
t_R	retention time
Tris	trishydroxymethylaminomethane
Trt	triphenylmethyl
UV	ultraviolet
V or Val	valine
W or Trp	tryptophan
Y or Tyr	tyrosine

1. INTRODUCTION

1.1 Synthetic Preparation of Peptides

The ability to synthesize large peptides is a challenge that has taunted chemists since the beginning of organic chemistry. It is reported that in 1905, Emil Fischer wrote a letter to Adolf Baeyer that contained the text, "My entire yearning is directed toward the first synthetic enzyme. If its preparation falls into my lap with the synthesis of a natural protein material I will consider my mission fulfilled."[1] Used throughout nature in many applications such as enzymes, antibacterial agents, pheromones, and signaling molecules, the diversity of peptides and their applications appear endless. These important biological effects have been exploited for human applications. As drug candidates, peptides have the ability to display high selectivity and potency while having minimal toxicity, tissue accumulation and drug-drug interactions.[2] Among the approved peptide-based drugs are natural peptides such as insulin, vancomycin, cyclosporine, calcitonin and leuprolide as well as synthetic peptides such as Fuzeon (enfuvirtide, a HIV drug) and Integrilin (eptifibatide, an anticoagulant).[2] The ability to make peptides on a large, industrial size scale has opened new possibilities for commercial application. According to a report in 2005, the 36 amino acid drug, Fuzeon, can be produced synthetically at a capacity of 3700 kg per year, clearly demonstrating that peptides can be prepared on an industrial scale.[3] As of July 2006, at least 20 companies have peptide or peptide-based drugs in Phase III development.[4] An important non-medical application of peptides is their use as food preservatives. One such bacterially produced peptide is nisin, which has been approved as a food preservative in over 48 countries.[5] Many other

bacterially produced peptides that target different organisms could potentially be employed in a similar fashion.

In a typical peptide preparation using solid phase peptide synthesis (SPPS), the first amino acid residue is loaded onto a solid support (Scheme 1). Next, removal of the *N*-terminal Fmoc protecting group with a solution of piperidine liberates the free amine group. The side product of this reaction is the dibenzofulvene-piperidine adduct that can be monitored by UV absorbance at 301 nm to ensure that the deprotection reaction has gone to completion. Following deprotection, addition of an appropriately activated amino acid solution to the resin extends the growing peptide chain by one residue. After this elongation step, addition of a solution of acetic anhydride acylates any unreacted amine groups while leaving the desired product unaffected. The growing peptide chain is then available for further rounds of deprotection-elongation to produce the desired peptide. Once the peptide has been completely prepared on the solid support, the final Fmoc removal is followed by acidic deprotection from the resin with concomitant removal of side chain protecting groups.

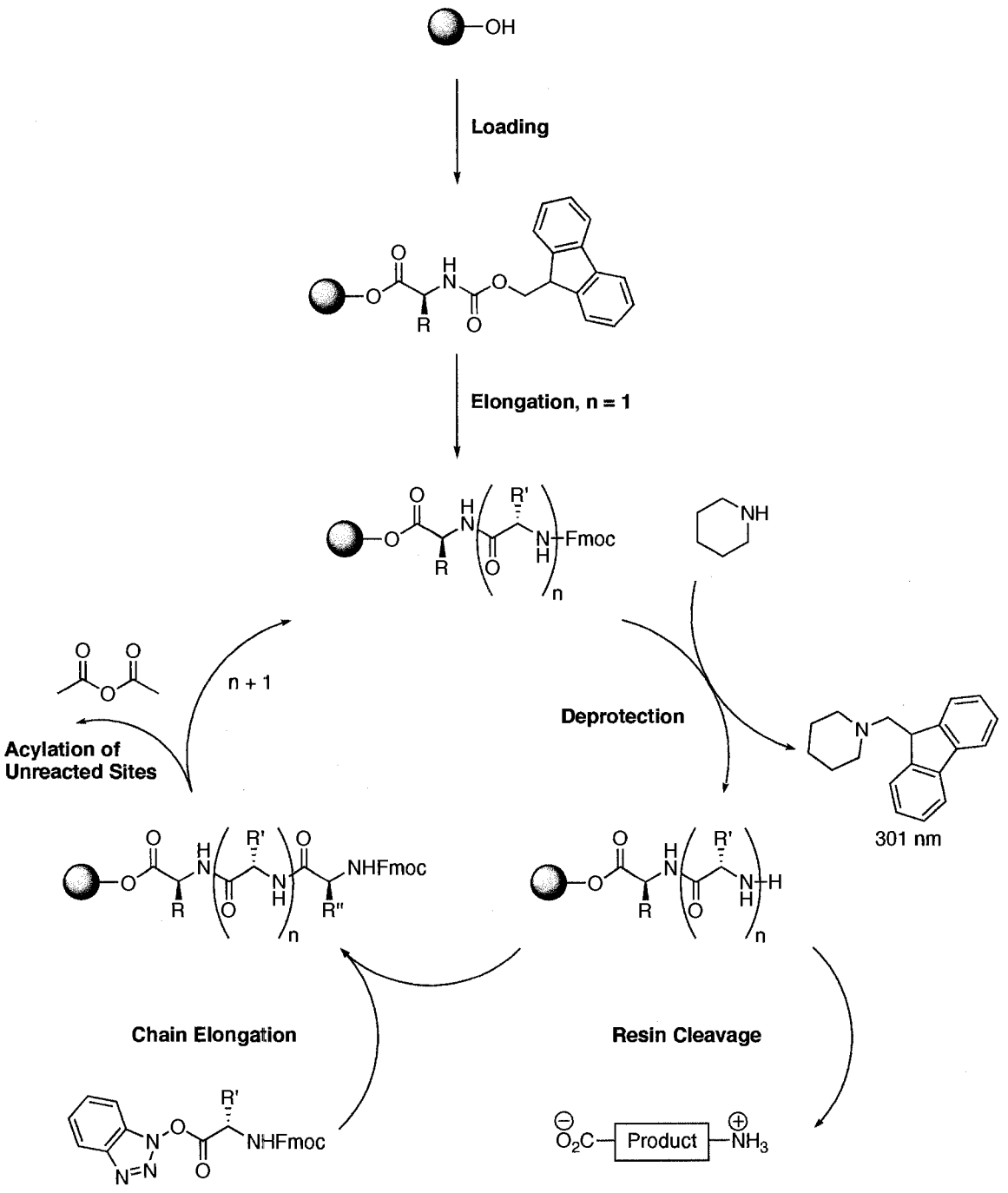

Scheme 1. Standard Fmoc-SPPS method of synthesizing peptides highlighting main steps.

Although significant advances have been made in peptide synthesis, there are still recurring problems that need to be overcome. One of the major difficulties in peptide synthesis is the preparation of hydrophobic peptides, particularly those greater than 30

residues in length, in good yield. Recent advances with native chemical ligation,[1, 6-11] pseudo prolines,[12-16] and backbone protection[17-19] have improved synthetic efficiencies but each must be applied in a case-dependant manner to the target peptide. For peptides greater than 50 residues, it can be difficult to obtain yields that are useful for further application. However, one major advantage of synthetic peptide preparation is the ability to easily incorporate unnatural (e.g. photoaffinity labels, amino acid surrogates) and unusual (e.g. natural post-translationally modified residues) amino acids that would be difficult or not yet possible to introduce via biological methods. Another advantage is the ability to rapidly prepare target compounds. According to one report, it is possible to "have a few hundred grams in the clinic in four to five months, whereas with a recombinant approach it would be 18 months before that is possible."[4] This is particularly helpful for structure activity relationship (SAR) studies when only a small amount of material is required, but a large number of peptides are necessary. Unfortunately, there are problems that make some peptides particularly challenging to synthesize. As mentioned previously, one common point of difficulty is the preparation of long, hydrophobic peptides with more than 30 residues. Incomplete removal of the *N*-terminal Fmoc group (Scheme 1, Deprotection) on a long peptide chain leads to truncated peptide fragments or deletion sequences that complicate purification. On-resin aggregation of hydrophobic peptides also makes other reactions, such as ring closing metathesis (RCM), difficult on long peptide chains. Another common problem with peptide synthesis is the introduction and protection of cysteine containing peptides, especially when this residue is located at the *C*-terminus. As peptides are generally immobilized via an ester linkage to a solid support, the acidity of the *C*-terminal α-proton

is higher than the internal α-protons. In examples where cysteine is at the *C*-terminus, the situation is further complicated by the protected thiol acting as a leaving group after deprotonation (Scheme 2).

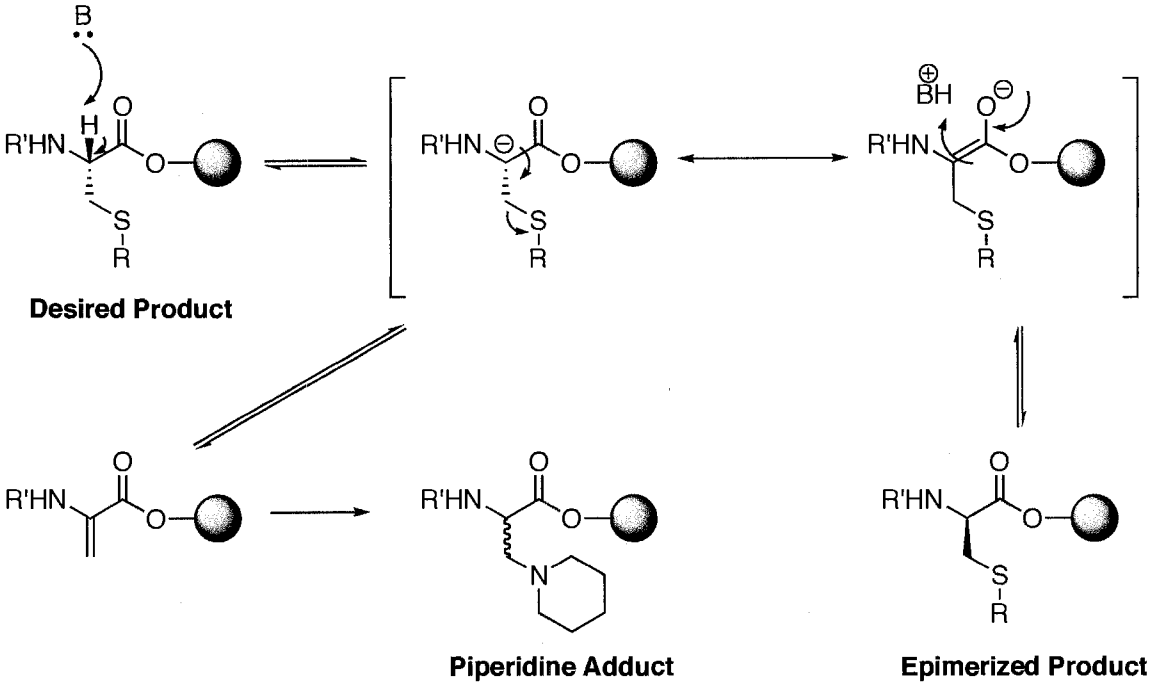

Scheme 2. Synthesis of *C*-terminal cysteine containing peptides leading to undesired side products.

This thesis is divided into studies that address the underlying problems associated with the synthesis of hydrophobic and cysteine containing peptides while simultaneously examining important biological applications.

1.2 Antimicrobial Peptides

The first section of this thesis will examine potent antimicrobial peptides named bacteriocins. Bacteriocins are ribosomally synthesized antimicrobial peptides produced by bacteria that are active against other bacterial strains.[5] With the rise of bacterial resistance to conventional antibiotics, the development of new antimicrobial agents remains an important task.[20]

Lactic acid bacteria (LAB) found in food are one of the emerging sources of antimicrobial agents.[21] There are a wide variety of peptides that fall under the classification of bacteriocins. It is important to note that multiple classification schemes exist, some are based on the presence of post-translational modifications and sequence conservation,[22, 23] some solely on the presence or absence of lanthionines,[5] and others on the resemblance to representative examples.[24] Based on the facts that the majority of the literature refers to the initial method proposed by Klaenhammer[25] and that the scientific community has not been particularly receptive to new methods of classification,[26, 27] the Klaenhammer scheme will be used throughout this thesis (Table 1). These peptides can be active against a narrow or wide range of organisms, and the producing organism is protected from its own bacteriocin via an immunity protein.[5, 23] Many bacteriocins are produced by LAB already found in food, suggesting potential application of these systems as natural preservatives against pathogenic bacteria. Some of these bacteriocin producing organisms include strains of *Carnobacterium*, *Lactococcus*, *Leuconostoc* and *Pediococcus* spp.[28]

Classification	Components	Sub Classification	Examples
Class I	Lantibiotics	Type A - elongated	Nisin A Lacticin 3147 A2
		Type B - globular	Mersacidin
Class II	Non-modified peptides	Type IIa - antilisterial	Pediocin PA-1 Leucocin A
		Type IIb -two peptide bacteriocins	Plantaricin EF
		Type IIc -other bacteriocins	Lactococcin 972
Class III	Heat labile, large proteins		Helveticin J

Table 1. Classification and examples of bacteriocins[29, 30]

Before these peptides or producing organisms can be used for general application in food preservation or as medical therapeutics, it is important to have a thorough understanding of how these systems are regulated and controlled. The Class I lantibiotic nisin A is thus far the benchmark for the level of understanding in antimicrobial peptides, as it has been examined by total synthesis,[31] NMR studies[32] and has been approved for use as a food additive in over 48 countries.[5] For studies on another Class I lantibiotic, Lacticin 3147 A2, see Appendix 1 of this thesis. Another group of antimicrobial peptides that has received attention for potential human applications are the type IIa bacteriocins (Figure 1).

```
                          1   5    10    15    20    25    30    35    40    45
(1) Leucocin A            KYYGN GVHCT KSGCS VNWGE AFSAG VHRLA NGGNG FW
(2) Pediocin PA-1         KYYGN GVTCG KHSCS VDWGK ATTCI INNGA MAWAT GGHQG NHKC
(3) Mesentericin Y105     KYYGN GVHCT KSGCS VNWGE AASAG IHRLA NGGNG FW
(4) Piscicolin 126        KYYGN GVSCN KNGCT VDWSK AIGII GNNAA ANLTT GGAAG WNKG
(5) Carnobacteriocin B2 VNYGN GVSCS KTKCS VNWGQ AFQER YTAGI NSFVS GVASG AGSIG RRP
(6) Curvacin A          ARSYGN GVYCN NKKCW VNRGE ATQSI IGGMI SGWAS GLAGM
(7) Sakacin P             KYYGN GVHCG KHSCT VDWGT AIGNI GNNAA ANWAT GWNAG G
```

Figure 1. Sequence alignment of some type IIa bacteriocins. Leucocin A (LeuA, 1), Pediocin PA-1 (Ped, 2), Mesentericin Y105 (MesY105, 3), Piscicolin 126 (PisA, 4), Carnobacteriocin B2 (CbnB2, 5), Curvacin A (CurA, 6) and Sakacin P (SakP, 7).

Many of the type IIa bacteriocins display potent activity against pathogenic bacteria, particularly strains of *Listeria*. These peptides have a highly conserved YGNGVXC sequence in the *N*-terminus where the cysteine residue is part of a disulfide bridge. Type IIa bacteriocins only contain common amino acids that are not post-translationally modified except for the disulfide bridge. Currently, the 3-D NMR structures of four type IIa bacteriocins have been published: leucocin A (LeuA, **1**),[32-34] carnobacteriocin B2 (CbnB2, **5**),[35] curvacin A (CurA, **6**),[36] and sakacin P (SakP, **7**) (Figure 1).[37] These peptides exist predominantly as random coil structures in water but assume defined conformations in trifluoroethanol (TFE) or membrane mimicking environments. All of these structures are similar with the general features of a three strand β-sheet in the *N*-terminus and an α-helical portion in the *C*-terminal region.[30] LeuA (**1**) contains a three-strand antiparallel β-sheet in the *N*-terminus (residue 2-16) that is rigidified by a disulfide bond.[33] The *C*-terminal portion of the type IIa bacteriocins is much less conserved but is generally α-helical and is responsible for the antimicrobial specificity and temperature dependant activity of the peptide.[38-40] Based on sequence similarity (Figure 1), pediocin PA-1 (Ped, **2**),[41] mesentericin Y105 (MesY105, **3**), and piscicolin 126 (PisA, **4**) are expected to be structurally similar. Identification and characterization of the receptor for type IIa bacteriocins is on-going, but current literature suggests involvement with the mannose phosphotransferase (mpt) system.[42-44] Type IIa bacteriocins are proposed to interact with the mpt system, encoded by *mpt* genes, based on the observations that high levels of resistance result from loss of *mpt* operon expression[45] and that the level of *mpt* expression correlates to bacteriocin sensitivity.[46, 47] This class of bacteriocins is proposed to act by binding to the receptor and then permeabilizing the membrane of the target cell,

causing leakage of cellular contents and loss of the proton motive force. This non-specific depletion of protons destroys the cells ability to generate energy in the form of ATP and leads to cell death. The requirement of a receptor mediated binding by the bacteriocin (instead of a non-specific detergent effect) is supported by the synthesis of the enantiomer of LeuA[48] (D-LeuA), which is biologically inactive. This inactivity indicates that a chiral recognition event is required for antimicrobial activity and that direct insertion into the membrane is not responsible for the observed biological activity.

Given the complexity of the system, the exact nature of the receptor interaction is not yet clearly understood, but it may be possible to obtain further information on the peptide-receptor complex through the synthesis of carefully designed analogues. Based on the assumption that all type IIa bacteriocins bind to the same receptor in the same fashion, examination of similarities between bacteriocins within the highly conserved *N*-terminus is expected to contribute to understanding this interaction. LeuA (**1**) and Ped (**2**) differ by only six residues in the first 21 amino acids, four of which differ only in their relative position near the disulfide bridge. Cysteine residues in Ped (**2**) have been reported to be essential for antimicrobial activity,[49] and given the highly conserved nature of the disulfide bond throughout type IIa bacteriocins, this is expected to be general throughout all of the group members. Through the synthesis of rationally designed analogues, it is expected that further insight into the peptide-receptor complex and the requirement for the highly conserved disulfide bond will be obtained.

1.3 Induction Peptides

Many bacteria are able to communicate with each other in a cell-density-dependent manner called quorum sensing, by the secretion of signaling molecules.[50] It has been shown that the production of several type II bacteriocins by LAB are regulated by signaling molecules referred to as induction peptides (pheromones) that vary in length between 19 and 27 amino acids.[24] These peptide pheromones are produced as precursors with double-glycine leader peptides that are recognized and cleaved by the bacteriocin ABC transporter.[51, 52] Produced at a constant but low level, induction peptides are secreted from cells and diffuse into solution. When the density of cells increases, the local concentration of induction peptide increases accordingly. Once an adequate concentration of the induction peptide is reached in solution (in some examples on the order of only 10^{-11} M)[56] the peptide activates a histidine kinase on the surface of the producing organism. This kinase uses ATP to phosphorylate a signaling molecule inside the cell (response regulator) which in turn activates the genetic machinery for bacteriocin production (Figure 2).[30] This enables the cells to respond in a coordinated manner to their environment.[50, 53, 54] Induction peptides are generally highly specific for their cognate receptor[55] and production can be affected by factors such as temperature.[56] The gene encoding the peptide pheromone is often genetically linked to genes encoding the histidine kinase and the response regulator involved in bacteriocin expression.[55]

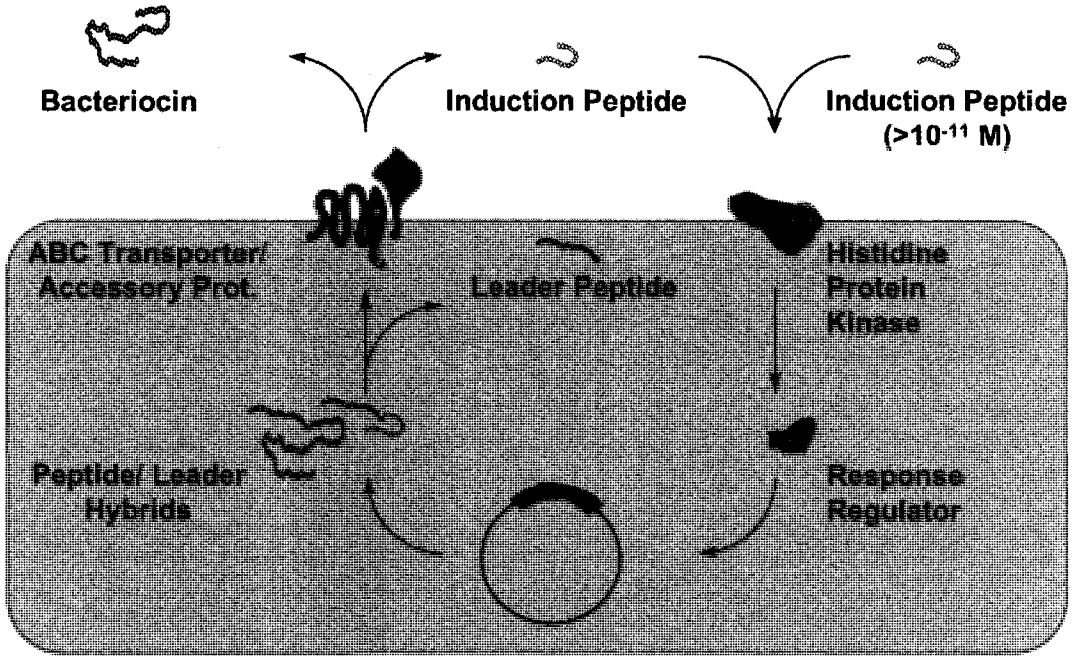

Figure 2. Bacteriocin regulation by induction peptides

Carnobacterium maltaromaticum UAL 26 produces the bacteriocin piscicolin 126 that is regulated by the induction peptide PisN (**8**, Figure 3).[56] *Carnobacterium maltaromaticum* LV17A produces the bacteriocin carnobacteriocin A[57, 58] that is regulated by the 24-mer inducer peptide CbaX[59] (**9**). Bacteriocins enterocin A and B are produced by a number of strains of *Enterococcus faecium* and are regulated by the induction peptide EntF (**10**).[60] Significant sequence homology, especially in the *C*-terminal domain, can be seen between these three peptide pheromones.

```
PisN  (8) NKSVIKGNPASNLAQCVFSFFKKC
CbaX  (9) SINSQIGKATSSISKCVFSFFKKC
EntF (10) AGTKPQGKPASNLVECVFSLFKKCN
```

Figure 3. Some relevant induction peptides involved in bacteriocin production.

1.4 Peptides on Solid Support

Solid phase peptide synthesis can be problematic for a variety of reasons. As already mentioned in Section 1.1, hydrophobic sequences are the most commonly encountered problem which can lead to a reduced yield. Secondly, as the *C*-terminal residue of a solid supported peptide is attached via an ester linkage, the acidity of the α-proton is relatively high (pKa $\leq$ 24) and susceptible to epimerization. In the case of short peptides, any epimerized product can generally be removed by HPLC purification. However, longer peptides can produce increasingly difficult separations when differing by only one residue. This problem is generally addressed by the introduction of steric bulk around the *C*-terminus by incorporating a trityl ester to hinder the attack of base onto the α-proton.[61, 62] This steric method (Figure 4) is sufficient for intermediate length peptides.

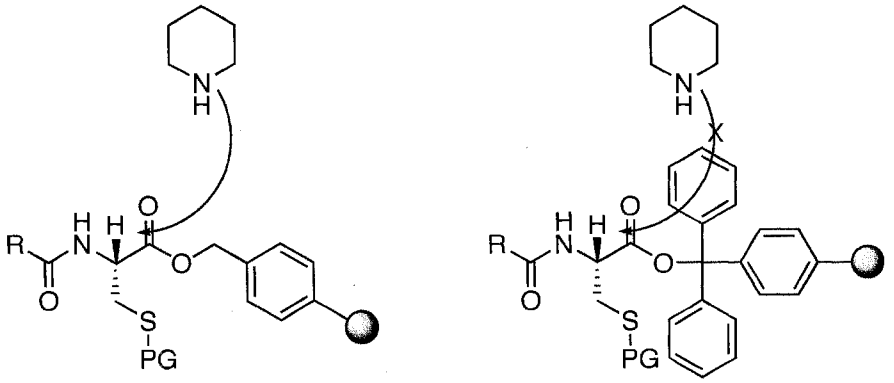

11 **12**

Figure 4. Undesired side reaction with base occurring during Fmoc deprotection. No hindrance to base using Wang resin (11) and steric hindrance using Trt resin (12)

For peptide chains greater than 30 residues, where aggregation of the growing chain interferes with residue coupling and Fmoc-deprotection, it is occasionally

necessary to use bases stronger than piperidine to remove the Fmoc group from the *N*-terminus. This leads to an increased amount of epimerization and thiol-eliminated product which can dramatically lower product yields (Scheme 2, Section 1.1).

Another logistical problem for peptide synthesis is the fact that it can be difficult to obtain large amounts of high quality piperidine due to government regulations.[63] These regulations are imposed due to the use of piperidine in the manufacture of illegal drugs. The combination of these factors indicate that it would be beneficial to develop a general method of peptide immobilization on solid support that is able to tolerate stronger bases and simultaneously reduce dependency on the use of piperidine.

1.5 Analgesic Peptides

The final section of this thesis will examine an application of a peptide as a drug candidate to treat pain. The pharmacology of pain is a multi billion dollar industry and there is tremendous demand for development of new drugs that address this problem, particularly chronic and neuropathic pain. The administration of general analgesics for extended periods of time leads to drug tolerance as well as dependence. As well, the complexity of pain makes it challenging to design drugs that target specific mechanisms.[64] Pain can be classified into four groups (Figure 5).

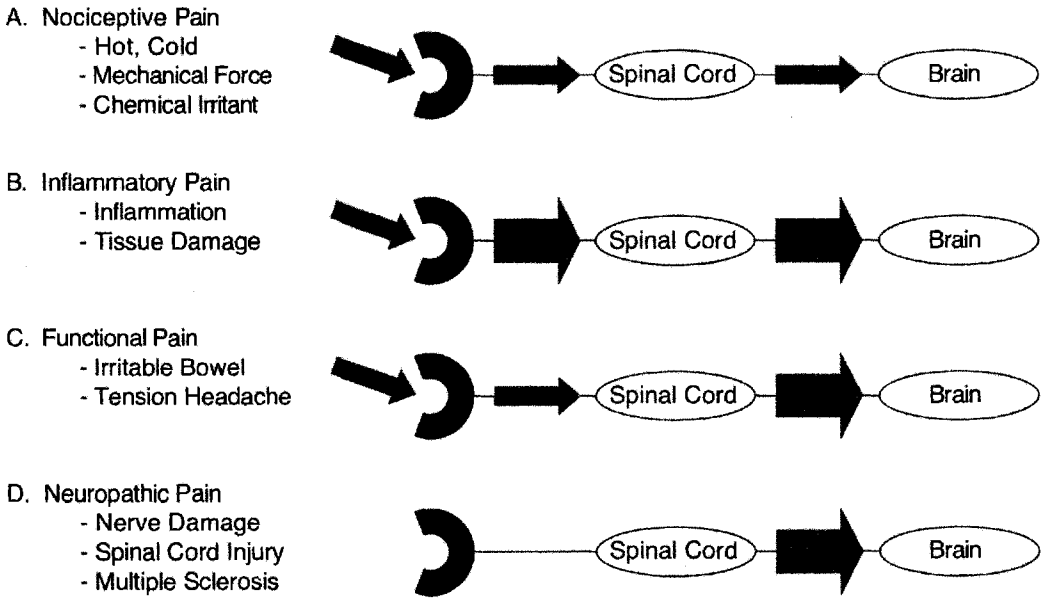

Figure 5. Four primary types of pain with examples of representative stimuli demonstrating signal transfer to brain.[64]

Nociceptive pain is important to warn against potentially damaging stimuli. Loss of nociceptive pain response leads to tissue damage, self-induced mutilation of tongue and lips and pressure ulcers. Inflammatory pain is a related phenomenon that causes increased sensitivity to an affected region. This type of pain prevents contact with an

injury and helps avoid further damage. In some cases, such as after surgery, it is necessary to moderate this type of pain while leaving sufficient nociceptive response to avoid excessive damage from external stimuli. A third type of pain is referred to as functional pain and arises due to abnormal responsiveness to an external stimulus. Examples of this type of pain include the conditions of irritable bowel syndrome and tension headaches. The fourth type of pain is neuropathic pain and is of significant pharmaceutical interest. This occurs due to a damaged nervous system or abnormal nervous system operation in which pain can occur even without external stimulus, resulting in a chronic pain sensation. Functional and neuropathic pains are the most poorly understood and represent the greatest need for selective pharmaceuticals. Most current pain medications cause an overall reduction of pain sensation with little selectivity and inevitably lead to the development of tolerance. Further complications arise from the fact that all individuals have varying responses to identical pain stimuli. Pain that is evoked from a low-intensity, normally innocuous stimulus is referred to as *allodynia.*[64] By contrast, pain that is present due to prolonged response to a noxious stimulus is referred to *hyperalgesia.*[64] Given the complexity of pain, there are numerous methods of quantifying pain in different models so that they are more amenable to analysis. It is not sufficient to ask a subject their opinion under the effect of a drug, as there is significant inconsistency between subjects based on variability of pain thresholds and different responses to identical stimuli. This is overcome by using a monitoring system that is more quantitative and not open to interpretation by the subject. For example, von Frey hairs exert a reproducible amount of force onto the skin of a subject and a withdrawal response indicates that the subject has felt the stimulus. This method is

used on new-born infants[65] and is one method of measuring *mechanical allodynia.*[66] Another method used to introduce a stimulus to a subject is referred to as the Hargreaves model and measures *thermal allodynia.*[67] This approach uses an infrared heat beam surrounded by a motion sensor to gently increase the temperature at the surface of the skin. The heating is immediately ceased after the motion detector perceives a withdrawal response and an attached timer produces a quantitative value for the thermal latency of the subject. Importantly, a cut-off threshold is always used for any pain monitoring method so that tissue damage does not occur due to the monitoring method.

The methods for generating reproducible and humane pain stimuli in animal models vary widely.[66] For acute pain models, injection of carragheenan causes inflammation at the point of injection that lasts for up to one day. Another method that is commonly used is the injection of prostaglandin PGE_2, a pain-signaling molecule. For chronic pain models, Complete Freund's Adjuvant (CFA), the chronic constriction model (CCI) and spared nerve injury (SNI) are some of the standard techniques that are used. CFA is popular as it is a simple, non-surgical method where constant allodynia begins quickly. CCI and SNI are surgical methods that involve loosely tying constrictions around or cutting nerves at the mid thigh of a rat leaving the remaining nerves in a hypersensitive state.[66] To reduce variability among subjects, the thermal and mechanic latencies are tested both before and after administration of the pain stimulus. The subjects displaying allodynia after administration of the stimulus are given the drug candidate and the latencies are repeatedly monitored at pre-set timepoints or until control subjects no longer display allodynia. To add further complexity to the concept of testing, the route of administration also has tremendous effect on drug absorbance and uptake. Taken

together, it is important to test any potential drug candidates using multiple models and testing methods to ensure that potential effects are not overlooked based on an incorrect method of testing.

One of the most extreme demonstrations of the need for pain medications is the use of venom from the South American rattlesnake *Crotalus durissus terrificus* as an analgesic. The crude venom has reportedly been administered orally to patients with chronic pain.[68] A peptide that has been named crotalphine (**13,** Figure 6) has been isolated and is reported to be the orally-active venom component as shown in mouse and rat pain models.[69] Co-administration of the peptide with selective opioid receptor antagonists (C-TOP, nor-BN1 and ICI 474864) in animal models suggests that this peptide acts via the delta and kappa opioid receptors.[69] This peptide is structurally interesting as it contains a *C*-terminal cysteine residue that is part of a disulfide bond and an *N*-terminal pyroglutamic acid that effectively caps the *N*-terminus leaving no positively charged residues on the peptide.

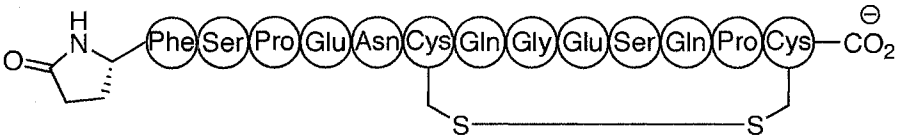

13

Figure 6. Reported structure of crotalphine (13), produced by *Crotalus durissus terrificus*. Note the absence of any basic residues.

Recently reported results in the Vederas laboratory indicate that disulfide bonds can be replaced with carbon-carbon double bonds in oxytocin to produce active structures.[70, 71] New peptide models are required to test the generality of this effect and to explore the range of systems in which this substitution is acceptable. As crotalphine (**13**) contains a disulfide ring, a *C*-terminal cysteine residue, and has intriguing biological

activity, it is an ideal candidate for SAR studies to examine disulfide bond analogues and *C*-terminal cysteine synthesis methods.

1.6 Thesis Goals and Objectives

This thesis is most conveniently discussed in four sections. The first section focuses on antimicrobial peptides named bacteriocins. The synthesis of LeuA (**1**), Ped (**2**) (Figure 1), and a number of analogues prepared to examine structure activity relationships (SAR) will be presented, with particular attention given to the disulfide ring. This work will examine the concept that disulfide bonds can be replaced with carbon-carbon double bonds and retain significant biological activity.

The second section of this thesis will examine the induction peptides PisN (**8**), CbaX (**9**), and EntF (**10**) (Figure 3, Section 1.3), which induce the production of piscicolin 126, carnobacteriocin A and enterocins A and B, respectively. Through chemical synthesis, these induction peptides will be prepared and then subjected to biological testing. Regarding the CbaX and EntF peptides, hybrid peptides and fragments will be closely examined to elucidate how these peptides function and interact with different receptors.

Difficulties in the preparation of CbaX (**9**) inspired the development of the third project. Observation of *C*-terminal epimerized product, as well as a piperidinyl-alanine residue indicated that the cysteine attached to the solid support was undergoing side reactions, potentially due to the acidity of the *C*-terminal α-proton. This study incorporates the synthesis and purification of a standard peptide by a variety of conditions to examine the effect of base on different linkers.

The final project involves a structure activity relationship study of crotalphine (**13**) (Figure 6, Section 1.5) which has been reported to be biologically active as an orally administered analgesic. Using chemical synthesis, a variety of analogues that examine

role of the disulfide bridge and the *N*-terminal pyroglutamic acid residue will be prepared and tested. This project is related to the other projects as it contains a *C*-terminal cysteine residue as well as a disulfide bond. Common themes that occur throughout the thesis are the synthesis of hydrophobic, cysteine-containing peptides and examining the effect of replacing disulfide bonds with carbon-carbon double bonds. The underlying goal of all of these projects is to develop generally applicable methods to improve peptide synthesis while simultaneously preparing compounds that address important biological questions.

2. BACTERIOCINS

2.1 Synthesis of 9,14-Substituted Analogues of Type IIa Bacteriocins

Recently reported results from the Vederas laboratory have demonstrated that replacement of the disulfide bond in oxytocin with a carbon-carbon double bond produces a biologically active oxytocin analogue.[70, 71] As the disulfide bond of a peptide is susceptible to reduction and thiol exchange, replacement of the disulfide moiety with a carbon-carbon double bond is expected to produce compounds with increased stability relative to the parent structures, while retaining similar biological activity. This moiety can arise from incorporation of allyl glycine residues in place of cysteine, followed by ring closing methathesis (RCM) to form the desired alkene. Given the identical ring sizes between residues 1-6 in oxytocin and residues 9-14 in the type IIa bacteriocins (Figure 1, Section 1.2), it was anticipated that a similar trend might be observed with the representative example LeuA (**1**) (Figure 7).

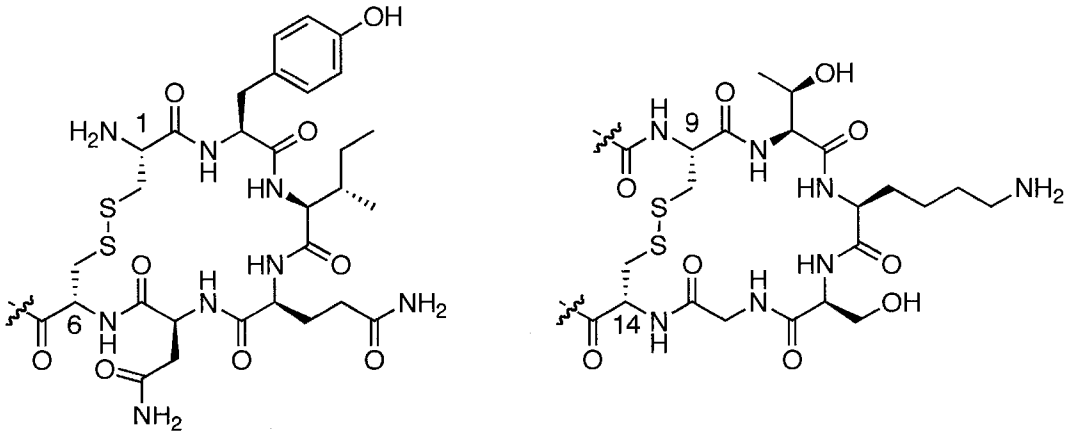

Oxytocin (1-6) LeuA (9-14)

Figure 7. Comparison of the cyclic portions of oxytocin and LeuA. Note the identical 20 membered ring size highlighted in blue.

It was also expected that the RCM reaction to form the alkene[72, 73] would occur with the similar ease as had been demonstrated with oxytocin. One obvious structural difference between oxytocin and LeuA (**1**) is the relative size of the two peptides. Oxytocin contains only nine amino acids while LeuA (**1**) consists of 37 residues. As both rings occur at or near the *N*-terminus of the respective peptides, the site of the required RCM reaction for a dicarba analogue of LeuA has much higher potential to be affected by on-resin aggregation than oxytocin. Based on this reasoning, a convergent approach was expected to allow for the convenient cyclization of the allyl glycine residues to give the respective dicarba analogue.

Our approach to the synthesis involved using native chemical ligation (NCL) followed by desulfurization to convert cysteine, at the point of ligation, into alanine as found in the native sequence (Scheme 3).

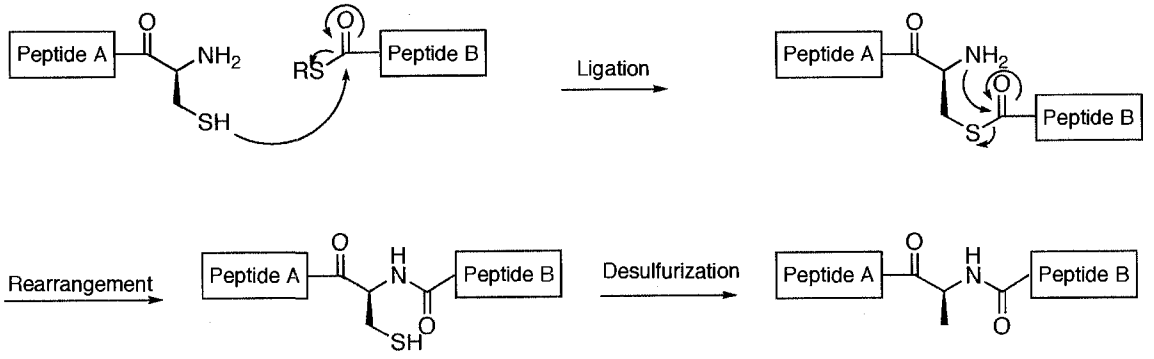

Scheme 3. Ligation methodology coupled with desulfurization to yield an alanine residue at the point of ligation.

Using SPPS methods, the 17-mer would be prepared containing a cysteine at the *N*-terminus. The 20-mer coupling partner would be synthesized on sulfamylbutyryl resin, already containing the preformed dicarba linkage, to yield a *C*-terminal thioester upon resin cleavage. The use of this shorter fragment was expected to allow the RCM

cyclization to occur more readily than using the full-length peptide. The *C*-terminal 17-mer **15** was initially prepared on Wang resin, using manual Fmoc-SPPS (Scheme 1), with a Fmoc-Cys(Acm)-OH protection strategy to assist in the purification of the peptide. It was anticipated that the synthesis and purification of the acetamidomethyl (Acm) protected precursor **14a** would allow for deprotection to the free 17-mer **15** when required without the potential of forming an unwanted disulfide dimer during storage. Unfortunately, this technique proved to be incompatible with the preparation of the desired peptide as the removal of the protecting group using $Hg(OAc)_2$ in the presence of 2-mercaptoethanol could not be completed in acceptable yield (Scheme 4). The 17-mer **15** was thus resynthesized with Fmoc-Cys(Trt)-OH protection **14b** as this allowed the complete deprotection of the desired peptide upon acid cleavage. The peptide was handled under argon whenever possible to reduce the potential for forming the disulfide dimer byproduct. Ligation of the *N*-terminal cysteine 17-mer **15** and the *C*-terminal thioester 20-mer **16** (prepared by a former graduate student, Dr. Jake Stymiest), using thiophenol and benzyl mercaptan in buffering conditions, appeared to proceed smoothly to **17** as analyzed by MALDI-MS (Scheme 4).

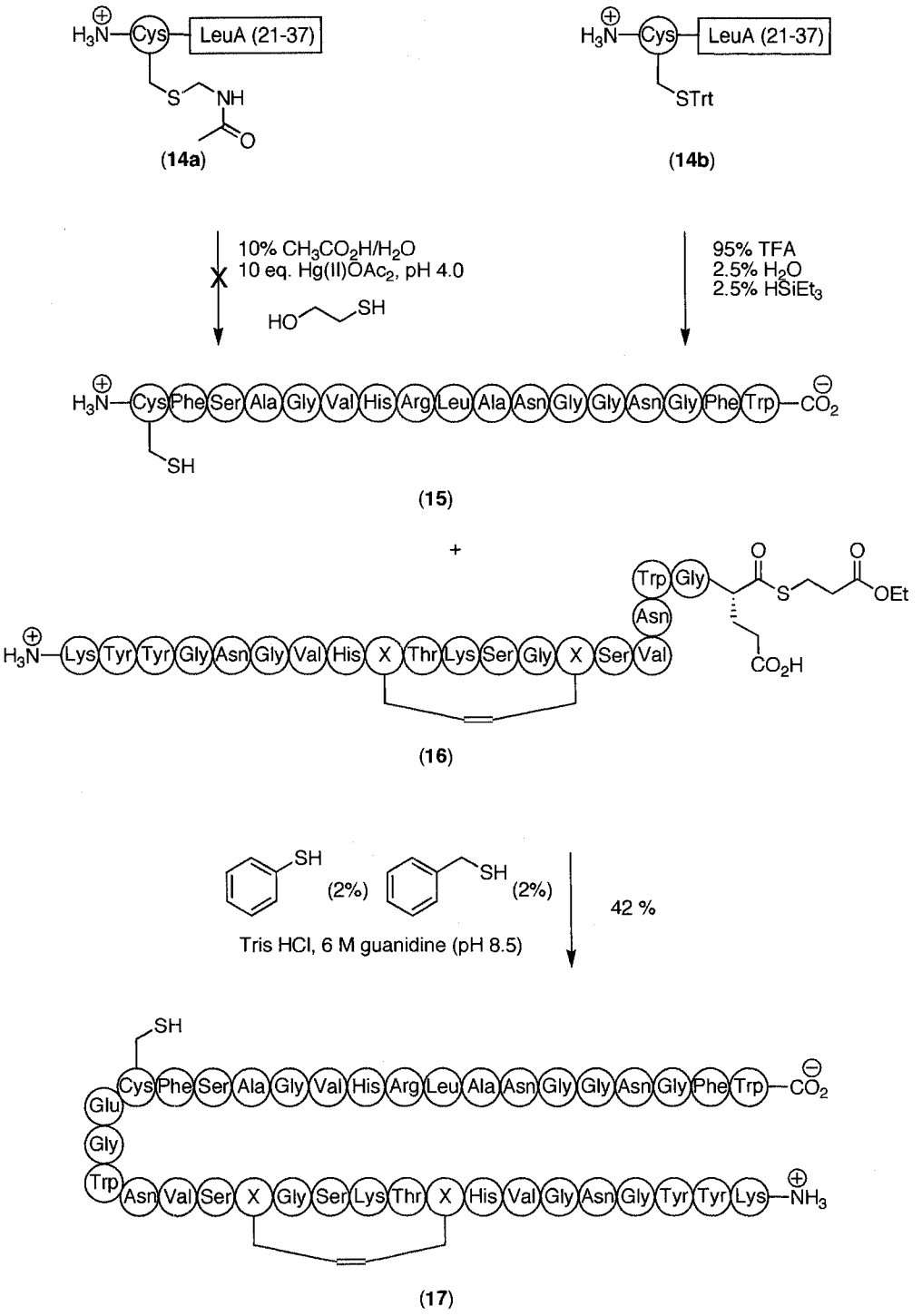

Scheme 4. Ligation of two fragments using native chemical ligation (NCL) in an attempt to form A21C precursor to [9,14]-dicarba LeuA.

Attempts to produce dicarba-LeuA **22** by desulfurization directly from **17** were unsuccessful, as no product could be isolated from the reaction using the reported method of H_2, 10% Pd/C in 20% aqueous AcOH.[11] We hypothesized that this could be because the free thiol of cysteine may be causing difficulties such as forming disulfides or forming insoluble complexes with the metal. To circumvent this problem, alkylation of the free cysteine to the acetamide derivative **18** (Scheme 5) was completed and then purified by HPLC. Unfortunately, two peaks containing the desired mass of the ligated-alkylated product were observed. This may occur by rearrangement of the thioester glutamic acid **16** to the corresponding anhydride **19** that could re-open and react to form two products, the desired product **18**, as well as side-chain linked product **20** via intermediate **21**. Further attempts at desulfurization remained unsuccessful even following alkylation of the Cys 21 with iodoacetamide.

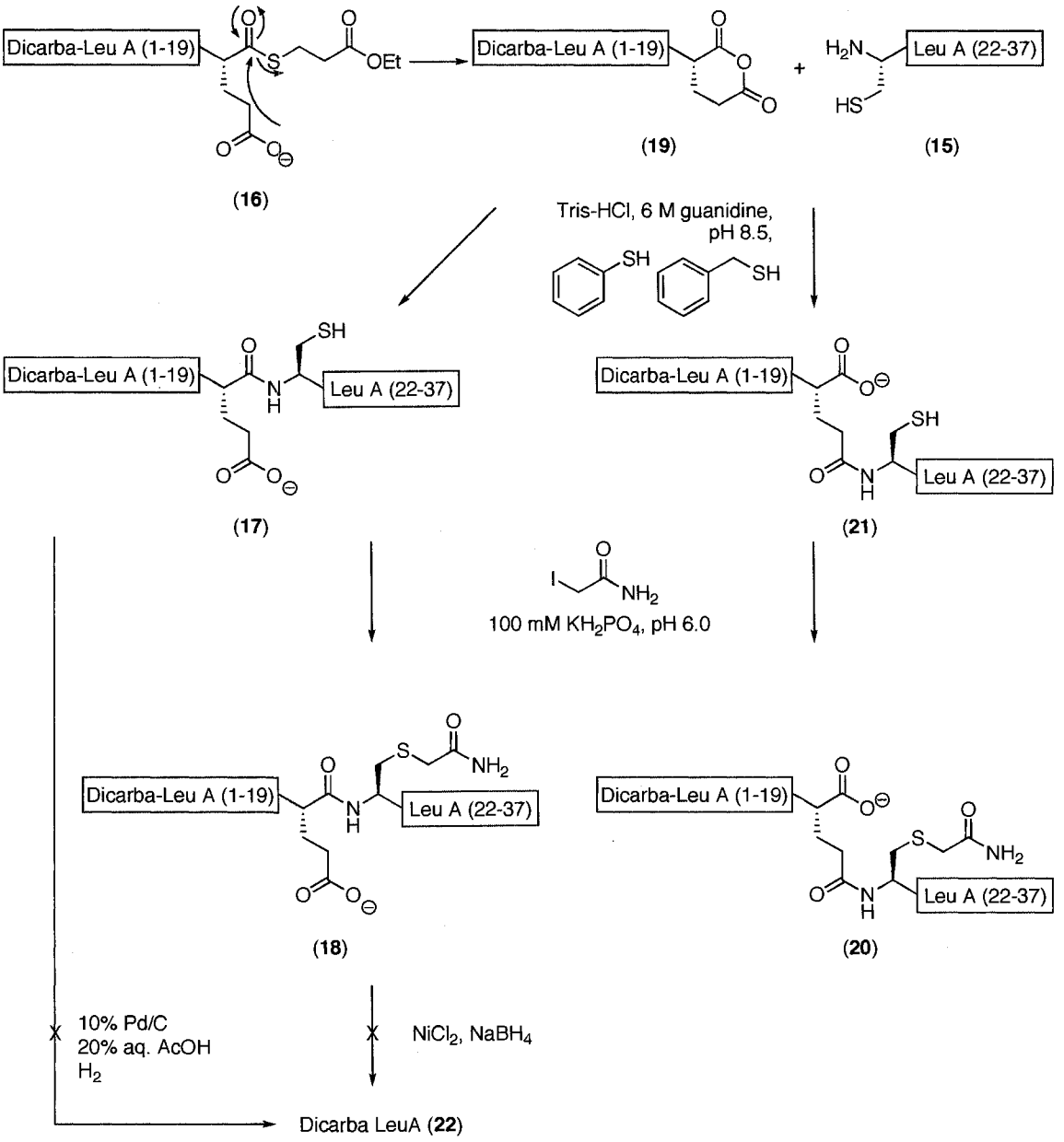

Scheme 5. Potential rearrangement to yield undesired by-product

These difficulties led us to pursue an alternative route to dicarba-LeuA (**22**). As the ligation approach was unsuccessful, the linear method via **23** (Scheme 6) was attempted to obtain the desired product. The linear precursor **22** was prepared using standard SPPS methods on low loading resin (to prevent dimerization). To prevent

aggregation of the long peptide, especially for the late stage RCM reactions, a pseudo-proline residue[12] was incorporated into the peptide sequence at positions 22-23. This is proposed to induce a "kink" in the immobilized peptide that disrupts the secondary structure.[12, 14] It was also found that heating to 45 °C and addition of a large excess of amino acid were required for the successful coupling of the last eight residues of the peptide. As anticipated, RCM of the linear peptide is unsuccessful using the conditions developed for the oxytocin analogue. We hypothesized that the reaction was not proceeding due to on-resin peptide aggregation, and thus incorporated a technique that has been applied to the synthesis of aggregated peptides.[74] Washing the resin with a solution of 0.8 M LiCl has been used to disrupt the on-resin secondary structure of the peptide. Washing **23** with this chaotropic salt followed by the addition of second generation Grubbs catalyst[72] is successful in cyclizing the 9,14-diallyl LeuA precursor **23** to yield **22**. The reaction is monitored by MALDI-MS as this method allows for the detection of much smaller amounts than HPLC methods based on UV detection. Given the similarity between the starting material and product, **22** and **23** were expected to have similar properties by MALDI-MS and this was exploited to monitor the progress of the RCM cyclization (Scheme 6).

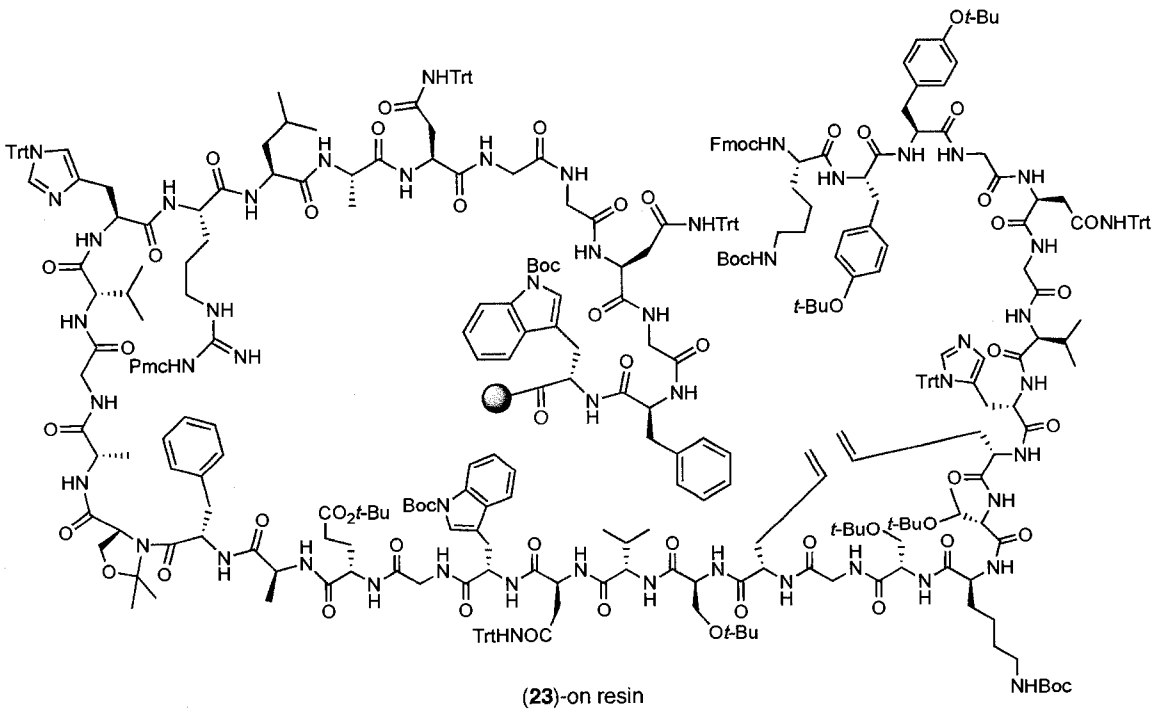

(**23**)-on resin

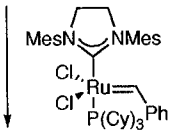

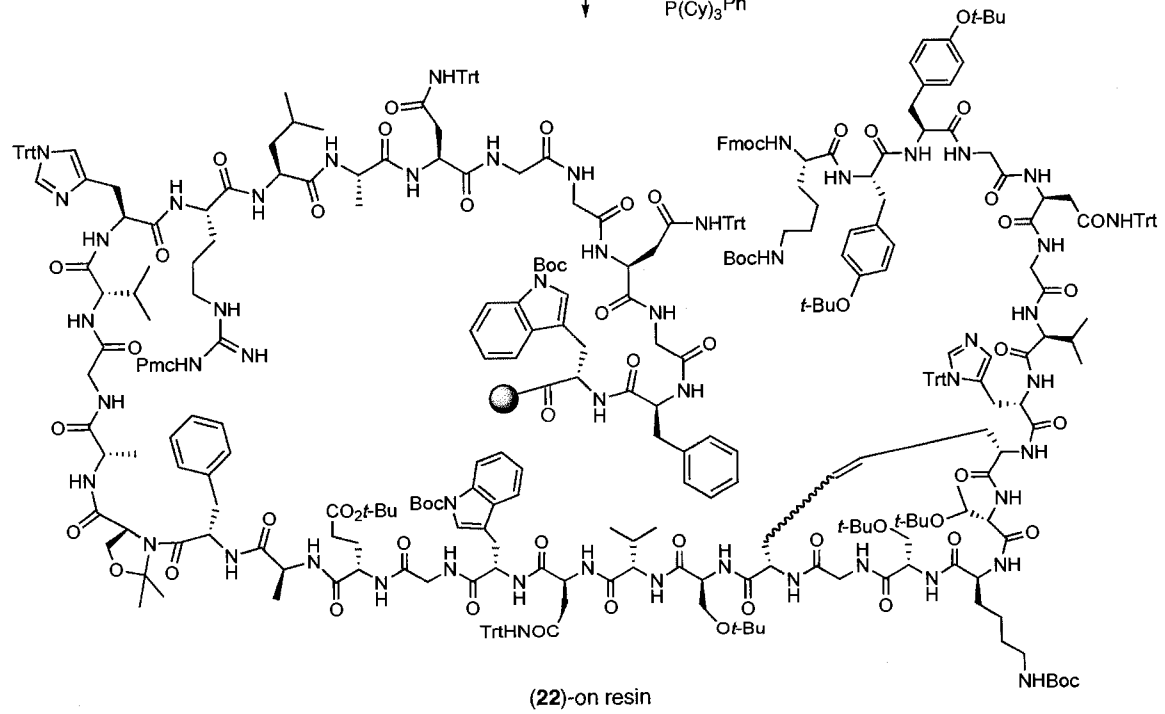

(**22**)-on resin

Solvent	Temperature (°C)	Catalyst Loading (mol%)	MALDI-MS Peak Product : S.M. ratio
Dichloromethane	40	20	No Product
Dichloromethane	40	50	No Product
Dichloromethane	40	100	No Product
1,2-Dichloroethane	50	100	No Product
1,2-Dichloroethane	50	4 x 25	No Product
1,2-Dichloroethane	83	50	Trace
1,2-Dichloroethane	83	100	5%
1,2-Dichloroethane*	83	100	50%

* Pretreated with 0.8 M LiCl in DMF

Scheme 6. Range of conditions attempted to induce RCM on diallyl LeuA precursor 23 to produce dicarba LeuA 22

After finally obtaining the target compound dicarba-LeuA (**22**), it was tested against the indicator organisms *Carnobacterium maltaromaticum* UAL26, *Carnobacterium divergens* LV13 and *Listeria monocytogenes* ATCC 43256. In all cases, dicarba-LeuA (**22**) is one order of magnitude less active than natural LeuA (**1**). In a broth assay using *C. maltaromaticum* UAL26 as the indicator organism, LeuA (**1**) achieves 50% inhibition at 35 nM while the dicarba analogue **22** requires 370 nM in the same assay for the same activity. This work supports the idea that a carbon-carbon double bond is an acceptable replacement for a disulfide bond. Employing similar synthetic techniques, the Vederas laboratory has completed an analogue study of Lacticin 3147 A2[75] (Appendix 1) to examine if a carbon-carbon double bond is an acceptable substitution for a lanthionine bridge (only one sulfur in bridge). This does not appear to be acceptable, likely due to an increase in ring size between lanthionine and the dicarba analogue. Other groups have attempted similar syntheses to replace lanthionines with carbon-carbon double and triple bonds on fragments of Nisin, but the synthesis of the completed analogues has not yet been reported.[76-78]

2.2 Acyclic Analogues of 9,14-Substituted Type IIa Bacteriocins

As the 9,14-disulfide bond is highly conserved throughout type IIa bacteriocins, it was anticipated that the cyclic structure was a requirement for biological activity. As a control compound, 9,14-diallyl LeuA (**23**) was cleaved from the solid support and purified by HPLC. Surprisingly, **23** is equally active to the parent compound **1**. This was very intriguing as the acyclic compound **23** is an order of magnitude more active than its cyclic counterpart **22**. This unexpected data prompted further investigation to identify how this activity occurs and the generality of this result in other type IIa bacteriocins.

Previous studies have shown that Acm protection of the cysteine residues in MesY105[79] (**3**, Figure 1) produces a biologically inactive compound, although it was also reported that iodoacetic acid derivatized LeuA (**1**) retains activity.[80] These results can be rationalized as LeuA (1) may not have reacted quantitatively with the iodoacetic acid and residual LeuA (**1**) was in fact responsible for the biological activity. Analogous to a previously reported study on MesY105 (**3**),[79] preparation of the [C9S, C14S]-LeuA (**24**, Figure 9) yields a compound that is completely inactive against the indicator organisms. These results suggest that the diallyl structure is inherently responsible for this unexpected activity. Looking back at previous work in the Vederas group, we explored the possibility that a "diallyl effect" had been overlooked in the case of oxytocin. Dr. Marc Boudreau, a former graduate student in the Vederas group, had previously prepared this peptide for an unrelated investigation and was able to supply some of the required diallyl oxytocin peptide. With the assistance of Dr. Bryan Mitchell in the Department of Obstetrics and Gynecology at the University of Alberta, the diallyl oxytocin analogue was tested (Figure 8) under identical conditions to those previously reported.[70, 71]

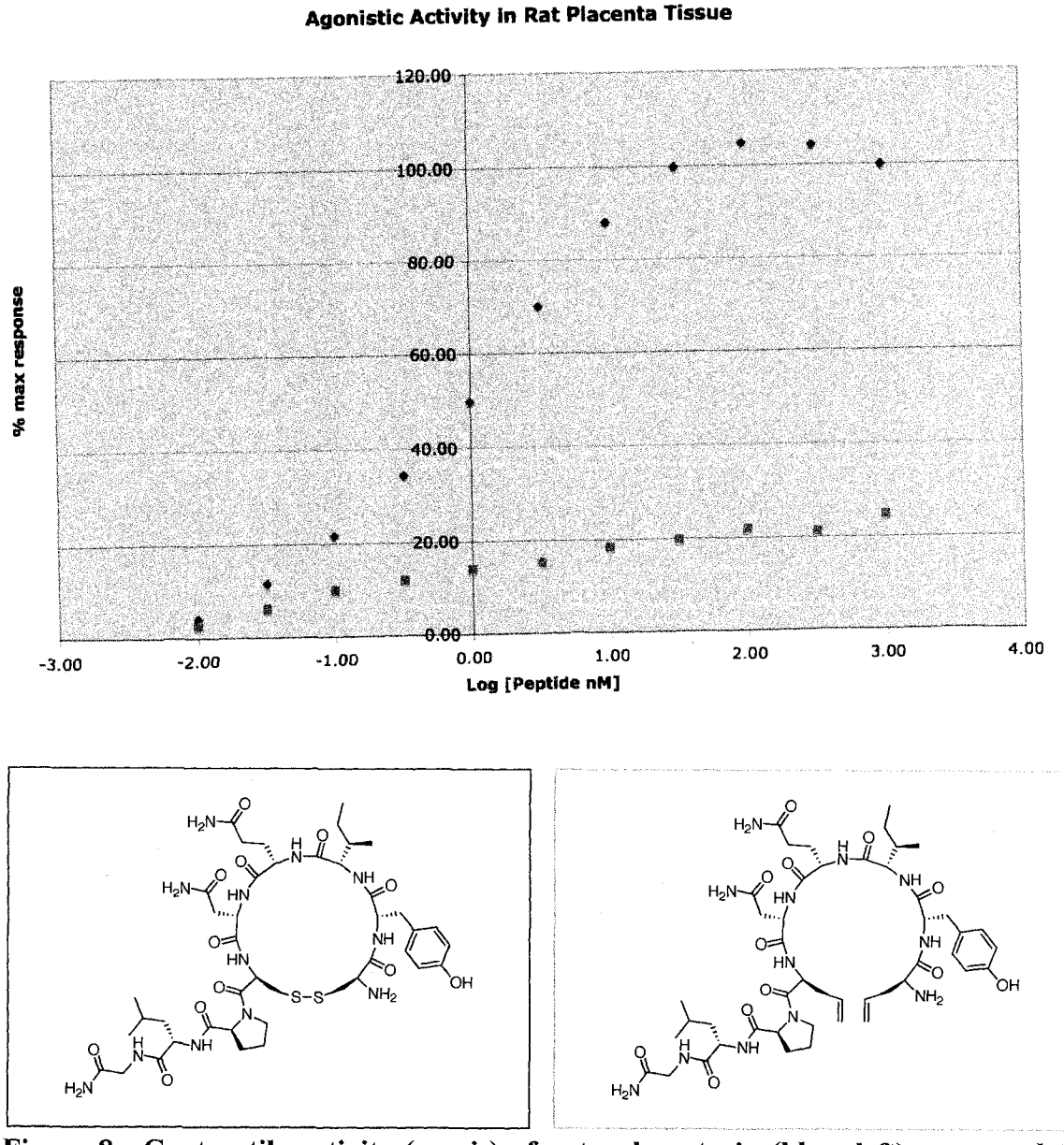

Figure 8. Contractile activity (y-axis) of natural oxytocin (blue, left) compared to diallyl oxytocin analogue (pink, right)

Using freshly excised rat uterine tissue from mature, non-pregnant Sprague-Dawley rats, small uteri strips were mounted on a Myobath™ apparatus that measures tissue contractions versus increasing amounts of oxytocin. Upon testing, it is evident that the diallyl oxytocin derivative does not possess the same trend as found with diallyl LeuA **23**. As shown in Figure 8, the response of uterine tissue to the parent oxytocin

(containing disulfide bridge) is significantly higher than diallyl oxytocin, which displays essentially no significant activity. This result implies that the diallyl oxytocin analogue does not assume that same 3-dimensional arrangement as natural oxytocin and, by extension, implies that the allyl glycine residues are not solely responsible for the retention of biological activity in LeuA (**1**).

The unexpected results with diallyl LeuA (**23**) prompted further investigation as it remained unclear how the acyclic analogue could be as potent as the parent compound when studies with other type IIa bacteriocins, MesY105 (**3**) [79] and Ped (**2**),[49] have shown that cysteine substitution leads to loss of activity. As cysteine substitution of LeuA (**1**) with allyl glycine produces a compound that retains biological activity[81] but substitution with serine abolishes all detectable activity, it was evident that a new interaction, or lack of a negative interaction, was being observed.

A variety of analogues were prepared to examine different modes of interaction (Figure 9). Given the potential of the allyl moiety to produce π-stacking or hydrophobic

```
                          1   5    10    15    20    25    30    35    40
(1)  Leucocin A (LeuA)    KYYGN GVHCT KSGCS VNWGE AFSAG VHRLA NGGNG FW
(2)  Pediocin PA-1 (Ped)  KYYGN GVTCG KHSCS VDWGK ATTCI INNGA MAWAT GGHQG NHKC
(22) [C9b, C14b]-LeuA     KYYGN GVHbT KSGbS VNWGE AFSAG VHRLA NGGNG FW
(23) [C9a, C14a]-LeuA     KYYGN GVHaT KSGaS VNWGE AFSAG VHRLA NGGNG FW
(24) [C9S, C14S]-LeuA     KYYGN GVHST KSGSS VNWGE AFSAG VHRLA NGGNG FW
(25) [C9n, C14n]-LeuA     KYYGN GVHnT KSGnS VNWGE AFSAG VHRLA NGGNG FW
(26) [C9F, C14F]-LeuA     KYYGN GVHFT KSGFS VNWGE AFSAG VHRLA NGGNG FW
(27) [M31Nle]Ped(NlePed)  KYYGN GVTCG KHSCS VDWGK ATTCI INNGA xAWAT GGHQG NHKC
(28) [C9a, C14a]-NlePed   KYYGN GVTaG KHSaS VDWGK ATTCI INNGA xAWAT GGHQG NHKC
(29) [C9F, C14F]-NlePed   KYYGN GVTFG KHSFS VDWGK ATTCI INNGA xAWAT GGHQG NHKC
(30) [C22a,C44a]-NlePed   KYYGN GVTCG KHSCS VDWGK ATTaI INNGA xAWAT GGHQG NHKa
(31) [T8H, C9F,
     G10T, C14F]-NlePed   KYYGN GVHFT KHSFS VDWGK ATTCI INNGA xAWAT GGHQG NHKC
(32) LeuLoopPed           KYYGN GVTFT KSGFS VDWGK ATTCI INNGA xAWAT GGHQG NHKC
(33) Leu-Ped              KYYGN GVHFT KSGFS VNWGK ATTCI INNGA xAWAT GGHQG NHKC
```

Figure 9. Hybrids of LeuA and pediocin PA-1 compared to explore structure activity relationship (SAR) of type IIa bacteriocins. a= allylglycine, b= cyclic carbon-carbon double bond- dicarba, n= norvaline, x= norleucine.

interactions in (C9a, C14a)-LeuA (**23**), it was necessary to prepare new derivatives that would discriminate between these respective properties. Substitution of allyl glycine by its saturated counterpart norvaline gives the analogue (C9n, C14n)-LeuA (**25**), which should be capable of hydrophobic interactions but not of π-stacking. Similarly, substitution of allyl glycine with phenylalanine residues to produce (C9F, C14F)-LeuA (**26**) could potentially enhance a π-stacking interaction. As the *N*-terminus of type IIa bacteriocins is highly conserved, the concept of cysteine substitution was extended to Ped (**2**) to examine if the unexpected activity of the acyclic analogue **23** is specific to LeuA (**1**) or is a general phenomenon in type IIa bacteriocins.

It has previously been shown that replacement of the methionine with norleucine in Ped (**2**), gives an analogue NlePed (**27**) that retains all of the biological activity of the parent compound without the potential for sulfur oxidation.[40] Hence, this substitution was incorporated into all of the pediocin analogues. This culminated in the synthesis of both the (C9a, C14a)-NlePed (**28**) and (C9F, C14F)-NlePed (**29**) to identify the generality of interaction observed for diallyl LeuA (**23**). To see if the interaction was a function of ring size, the corresponding (C24a, C44a)-NlePed (**30**) was also prepared (**28** and **30** were prepared by Dr. Marc Boudreau). The peptide sequence between residues 8 and 14 of LeuA (**1**) and Ped (**2**) was compared as this region is composed of the same constituent amino acids, differing only in relative arrangement (Figure 1, Section 1.2). Analysis of the 3-D NMR structure of LeuA[33, 48] suggests that Tyr 2, His 8 and Thr 10 (Figure 10) may interact to form a hydrophobic cluster.[35]

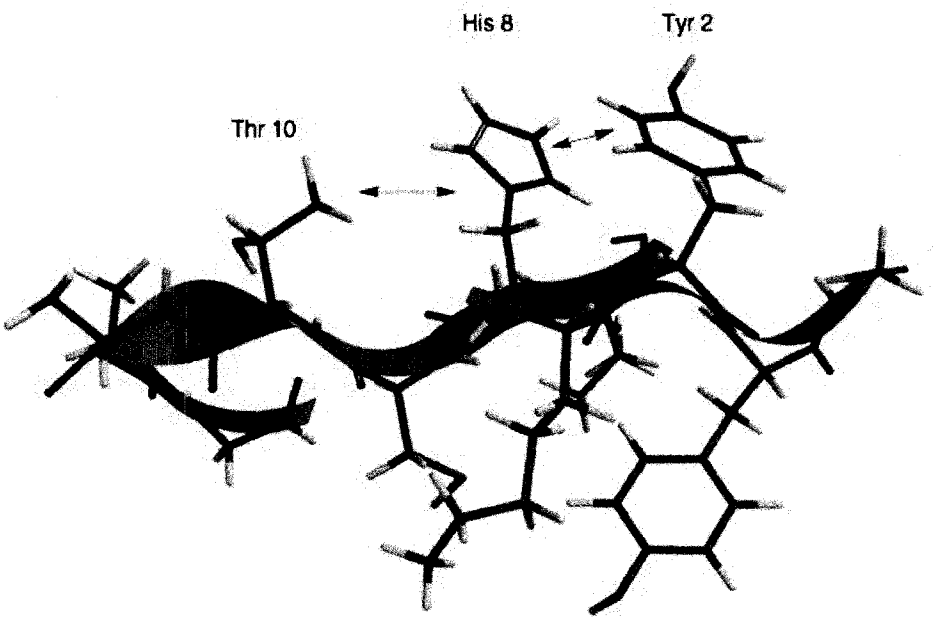

Figure 10. Basis of proposed interation between Tyr 2, His 8 and Thr 10[35] (Above plane of the ribbon). Picture directly from NMR solution structure highlighting relevant residues and deletion of extraneous peptide fragments.

Based on this analysis, pediocin analogue **31** was prepared that incorporated these respective substitutions with phenylalanine at position 9 and 14 (for comparison to the DiPhe-LeuA analogue **26**). The possibility that the intra-ring residues may be responsible for the activity of the acyclic analogue was explored via preparation of a pediocin analogue that substituted residues 10-13 from LeuA into the Ped sequence as well as substituting residues 9 and 14 with the hydrophobic amino acid phenylalanine (LeuLoopPed (**32**)). To complete the structure activity relationship study, a hybrid peptide LeuA (1-18)-Ped (19-44) (**33**) was synthesized to elucidate the role of the entire *N*-terminus on the biological activity.

The results of this study (Table 2) strongly support the idea that the biological activity of the acyclic-diallyl Leu A analogue **23** is derived from hydrophobic interactions at positions 9 and 14 combined with structural contributions from the intra-ring residues 10-13. The results clearly indicate that the activity is not influenced by the presence of the side chain double bond. The retention of biological activity in the norvaline analogue (C9n, C14n)-LeuA, **25** clearly demonstrates that the alkene, and hence π-stacking, is not required for antimicrobial activity. The activity of the phenylalanine analogue ((C9F, C14F)-LeuA, **26**) can be rationalized using hydrophobic interactions as for the norvaline analogue. Consistent with previously reported results,[49] substitution of cysteines 9 and 14 in Ped (**2**) is undesirable for bioactivity as both (C9a, C14a)-NlePed (**28**) and (C9F, C14F)-NlePed (**29**) are inactive against indicator strains. Similarly, (C24a, C44a)-NlePed (**30**) is unable to inhibit bacterial growth in the indicator organisms. As already mentioned, the (C9S, C14S)-LeuA analogue **24** is also inactive, likely due to the formation of unfavorable hydrogen bonds or interactions with a hydrophobic receptor.

Extension of these concepts to Ped (**2**) is insightful as it becomes obvious that the ring portion of the peptide reinforces the effect of the hydrophobic side chains. One possibility to explain this enhancement is that the intra-ring loop (residues 10-13) is responsible for inducing the conformation required for activity. This may occur through a β-turn inducing sequence in the ring portion of the peptide.[82, 83] The pediocin analogue containing the LeuA loop (LeuLoopPed, **32**) supports this analysis. As **32** is the only pediocin analogue containing cysteine substitutions that retains any activity, it can be concluded that the LeuA loop influences the secondary structure of the peptide. Interestingly, when the first 18 residues of Ped (**2**) are replaced by (C9F, C14F)-LeuA (1-18) **27**, biological activity is not observed.

	Listeria monocytogenes EGDe	*Carnobacterium maltaromaticum* UAL 26	*Carnobacterium divergens* LV13
(**1**) Leucocin A (LeuA)	3 μM, 2 μM*	3 μM	3 μM
(**2**) Pediocin PA-1 (Ped)	- - -**	- - -**	- - -**
(**22**) [C9b, C14b]-LeuA	50 μM*	50 μM	50 μM
(**23**) [C9a, C14a]-LeuA	3 μM, 8 μM*	3 μM	3 μM
(**24**) [C9S, C14S]-LeuA	N.A.	N.A.	N.A.
(**25**) [C9n, C14n]-LeuA	6 μM	3 μM	6 μM
(**26**) [C9F, C14F]-LeuA	6 μM	3 μM	6 μM
(**27**) NlePed	6 μM	6 μM	6 μM
(**28**) [C9a, C14a]-NlePed	N.A.	- - -	N.A.
(**29**) [C9F, C14F]-NlePed	N.A.	N.A.	N.A.
(**30**) [C22a, C44a]-NlePed	N.A.	N.A.	N.A.
(**31**) [T8H, C9F, G10T, C14F]- NlePed	N.A.	N.A.	N.A.
(**32**) LeuLoopPed	N.A.	50 μM	100 μM
(**33**) Leu-Ped	N.A.	N.A.	N.A.

*Results from *L. monocytogenes* ATCC 43256,
**Shown to have same activity as NlePed so expected value is 6 μM,
- - - = not tested due to lack of pure material
N. A.= no activity observed up to 100 μM

Table 2. Minimum inhibitory concentration (MIC) of LeuA and Ped analogues against indicator organisms

This may be rationalized by the absence of an additional interaction to the *N*-terminus of the peptide or to the receptor that disrupts the binding required for activity. The hydrophobic cluster between Tyr 2, His 8 and Thr 10 appears to be insufficient to induce activity in the acyclic pediocin analogue (**31**). These results indicate that the loop does have an influence on the activity of the peptide, but that the *C*-terminus has an effect on the receptor that also contributes to the overall activity.

When all of the data is taken together it is possible to gain insight into the structure-activity relationship of the highly conserved *N*-terminus of these type IIa bacteriocins. It is clear that a β-turn structure is required for biological activity. Whether this structure arises from a conformation enforced by a disulfide bond or is based on the inherent peptide sequence varies between peptides. In the example of Ped (**2**), the disulfide bond is a prerequisite for biological activity, but in LeuA (**1**) the disulfide bond appears to be a redundant feature that serves to reinforce the inherent β-turn inducing structure of the peptide. It is intriguing that exchanging the positions of only four amino acids between residues 8-14 from Ped (**2**) to LeuA (**1**) allows substitutions of cysteine for hydrophobic residues such as phenylalanine or allyl glycine (e.g. analogues **26** and **29**). Although the *N*-terminal ring portion of the bacteriocins is important, our results support the idea that the selectivity and activity of the peptide is dependent on its entire sequence and 3-dimensional structure.[48, 84]

2.3 Bacteriocin Summary and Future Work

In summary, the work described in this section demonstrates that allyl glycine or other hydrophobic residues may replace cysteine in LeuA (**1**) without loss of antimicrobial activity. More generally, the substitution of disulfide bridges with carbon-carbon double bonds appears to be a reasonable replacement. Although 9,14-dicarba LeuA (**22**) and 1,6-dicarba-oxytocin are biologically unrelated systems, they exhibit a similar reduction in activity (order of magnitude) when the disulfide is replaced by an alkene. This is not a large effect given the inherent potency of these peptides. However, substitution of hydrophobic residues for cysteine appears to be of much more limited application as it was found only to be acceptable for LeuA (**1**). Although the *N*-terminus of LeuA (**1**) containing the disulfide is highly conserved throughout type IIa bacteriocins, disulfide replacement could not be applied to the related bacteriocin Ped (**2**). This implies an inherent difference between these highly homologous sequences, which has been attributed to the β-turn propensity of the intra-ring residues in LeuA (**1**). This sequence appears to contribute the additional structural reinforcement to produce the required β-turn structure without a disulfide bond. From insight gained in this study, it may be possible to extend the concept of cysteine replacement with hydrophobic residues to other similar bacteriocins. Based on simple sequence analysis of representative examples,[30] potential candidates with "leucocin-like" structures that would be expected to display similar trends are MesY015 (**3**), leucocin C, plantaricin C19, sakacin 5X, PisA (**4**), curvacin A and enterocin P (Figure 11). A proposal for a thorough study of this effect would be to use the (C9F, C14F)-LeuA (**26**) sequence and systematically replace the intra-ring residues 10-13 with the corresponding sequences of different type IIa

bacteriocins. It would also be useful to incorporate the theoretically "ideal" β-turn sequences for comparison (Figure 11). Any hybrid peptides that retain activity would be reasonable candidates for cysteine substitution with hydrophobic residues. This indirect approach would be logistically much more accessible than synthesizing the C9F, C14F analogue of all type IIa bacteriocins. In the event that no further analogs would retain any activity, these negative results would still be useful as they would provide insight into how the LeuA structure provides this unusual activity.

	10	11	12	13
Leucocin A (LeuA)	T	K	S	G
Pediocin PA-1 (Ped)	G	K	H	S
Mesentericin Y105	T	K	S	G
Leucocin C	T	K	K	G
Plantaricin C19	S	K	K	G
Sakacin 5X	N	K	S	G
Piscicolin 126	N	K	N	G
Curvacin A	N	N	K	K
Enterocin P	N	N	S	K
Type I turn*	D	P	D	G
Type I' turn*	Y	N	G	K
Type II turn*	P	P	G	K
Type II' turn*	Y	G	N	T

Figure 11. Intra ring residues of type IIa bacteriocins homologous to LeuA. *Indicates representative sequences.[82]

It is relevant to mention that all the leucocin-pediocin hybrids and analogues were inactive against the LeuA (**1**) producing organism *Leuconostoc gelidum* UAL 187, implying that the immunity protein remained active against these modified peptides. Although the precise mechanism of immunity protein function is not thoroughly understood, these results suggest that: a) none of the peptides are inherently toxic to the producer cell (this is unlikely as LeuA (**1**) is toxic to the producer strain with immunity protein knockout in *L. gelidum* UAL 187-13); b) all of the analogues interact with the immunity protein in an identical fashion to LeuA (**1**); or c) the immunity protein does not directly interact with the bacteriocin. It has been proposed in the literature that the

immunity protein does not interact directly with a pediocin-like bacteriocin but its exact mode of action is not yet clearly understood.[85]

Although the application of Grubbs RCM to peptides had only been briefly introduced prior to beginning this project,[73] it has become increasingly common in recent literature. This technique has been applied to the synthesis of hydrogen bond surrogates in helices,[86] and numerous other applications as a disulfide replacement strategy.[87-89] Our work has demonstrated the utility of incorporating pseudo-proline residues in the synthesis of hydrophobic peptides. The utilization of LiCl salts to disrupt on-resin aggregation before RCM is a novel contribution as we are not aware of any reports where this has been employed to assist cyclization of aggregated substrates. Given the ability to synthesize a tremendous variety of amino acid analogues containing unsaturated side chains[90] and the increased ability to cyclize residues at the end of hydrophobic peptides using chaotropic salts,[81] the possibility of using RCM on peptides now appears to be limited only by the investigators' creativity.

3. INDUCTION PEPTIDES

3.1 Synthesis and Biological Evaluation

The investigation of structure function relationships in induction peptides was initiated with the manual Fmoc-SPPS preparation of PisN (**8**) (Figure 12). This induction peptide controls the production of the bacteriocin PisA (**4**) in *Carnobacterium maltaromaticum* UAL 26. This deceptively simple looking peptide requires special attention for chemical synthesis. Although the synthesis of residues 15-25 occurred without problems, the addition of the last 14 residues did not proceed using standard conditions. It was found to be beneficial to "double couple" the last 14 residues, effectively doubling the reaction time for each coupling. This difficulty is presumably due to on-resin aggregation of the growing, hydrophobic peptide chain. As well, during TFA cleavage of the peptide from Novasyn TGT resin (PEG based, trityl linker), some of the desired product is lost due to hydrolysis of the peptide bond between Ser 11 and Asn 12, significantly reducing the overall yield. As a side note, it is important to mention that PEG chains of the TGT resin were observed to be "leaching" from the resin according to MALDI-MS. This is demonstrated by a large number of interfering peaks in the MS spectrum differing by the mass of a PEG subunit. To further complicate matters, during exposure to the basic conditions required to form the disulfide bond (pH 8.5) more of the desired peptide product is lost due to hydrolysis between Asn 8 and Pro 9.

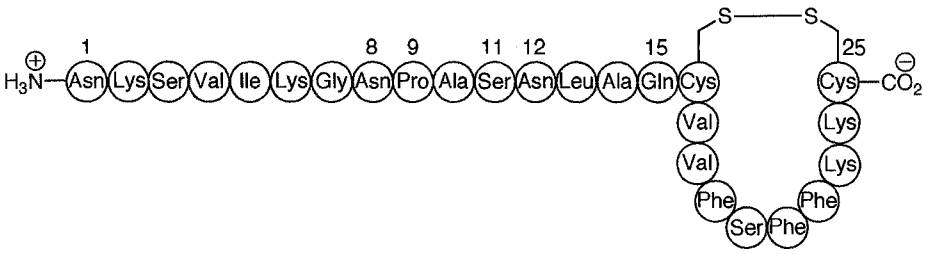

(8)

Figure 12. Induction peptide PisN (8), responsible for inducing bacteriocin production in *Carnobacterium maltaromaticum* UAL26.

This sensitivity to both acidic and basic conditions renders PisN (**8**) a challenging synthetic target. After purification by RP-HPLC, the peptide was tested for biological activity by Lucas Gursky, a graduate student in food microbiology. The regulation of the bacteriocin PisA (**4**) displays an interesting dependence on temperature. In the PisA (**4**) system, bacteriocin activity is not observable in the supernatant of cultures of UAL26 grown in liquid media at 25 °C, but at temperatures less than 19 °C, bacteriocin activity can be detected.[56] Interestingly, bacteriocin production in UAL26 grown at 15 °C can be induced by addition of 10^{-10} M chemically synthesized induction peptide (PisN, **8**) but induction of bacteriocin production in UAL26 grown at 25 °C requires 10^{-7} M of PisN (**8**).[56] Further details of the biological portion of this work are outlined in the Ph.D. thesis of Lucas Gursky. These potent biological effects illustrate the influence of induction peptides on bacteriocin production.

Structurally similar to PisN (**8**), are the induction peptides CbaX (**9**) and EntF (**10**) (Figure 3, Section 1.3) that regulate production of bacteriocins carnobacteriocin A and enterocins A and B in a similar quorum sensing dependant manner. The structure-function relationships of induction peptides were explored through the manual Fmoc SPPS preparation of CbaX (**9**) and EntF (**10**). These peptides were tested for pheromone activity by Dr. Marco van Belkum and the results are shown in Table 3. As part of the

experiment, each induction peptide was also added to the opposite organism as a negative control.

Peptide	Sequence	*Carnobacterium maltaromaticum* LV17A*	*Enterococcus faecium* CTC492*
(**9**) CbaX	SINSQIGKATSSISKCVFSFFKKC	10^{-11} M	10^{-7} M
(**10**) EntF	**AGTKPQGKPASNLVECVFSLFKKCN**	-	10^{-11} M
(**34**) CbaX:EntF	SINSQIGKAT**SNLVECVFSLFKKCN**	10^{-9} M	10^{-7} M
(**35**) EntF:CbaX	**AGTKPQGKPA**SSISKCVFSFFKKC	-	10^{-11} M

Table 3. Sequence and activities of CbaX (9), EntF (10) and hybrids (34, 35). *Minimum concentration of full length induction peptide required to induce bacteriocin production (- = No activity detected up to 10^{-5} M).

Both CbaX (**9**) and EntF (**10**) are able to induce their cognate bacteriocin production at 10^{-11} M in *C. maltaromaticum* LV17A and *E. faecium* CTC492, respectively. Unexpectedly, high concentrations of CbaX (**9**) induced bacteriocin production in *E. faecium*, but EntF (**10**) was unable to reciprocate this activity to *C. maltaromaticum*. After duplication of this result, it was intriguing that such similar peptides would have significantly different spectrums of activity. To gain further insight into how these peptides interact with their receptors, the hybrid peptides CbaX (1-10)-EntF (11-25) (CbaX:EntF, **34**) and EntF (1-10)- CbaX (11-24) (EntF:CbaX, **35**) were prepared and tested (Table 3). The biological activity demonstrated that like EntF (**10**), EntF:CbaX (**35**) was potent at only 10^{-11} M in the *E. faecium* CTC492 organism and inactive in *C. maltaromaticum* LV17A. Similarly to CbaX (**9**), CbaX:EntF (**34**) was active at 10^{-7} M in *E. faecium* CTC492. In the CbaX cognate system, there was a small decrease in the activity of the CbaX:EntF (**34**) sequence compared to the natural CbaX (**9**) sequence. These results indicate that the *N*-terminal domain is important in recognition by the cognate receptor.

To further elucidate which parts of the peptide pheromones interact with cellular receptors, various *N*- and *C*-terminal fragments derived from the sequences of CbaX (**9**) and EntF (**10**) were manually synthesized using Fmoc SPPS and purified by HPLC (Table 4). Peptides CbaX (7-24) (**36**), CbaX (11-24) (**37**), and CbaX (16-24) (**38**) consist of the *C*-terminal 18, 14 and 9 amino acids of CbaX (**9**), respectively. EntF (7-25) (**39**), EntF (11-25) (**40**) and EntF (16-25) (**41**) consist of the *C*-terminal 19, 15 and 10 amino acids of EntF (**10**), respectively. In addition, CbaX (1-11) (**42**) and EntF (1-11) (**43**) were prepared based on the *N*-terminal sequences of CbaX (**9**) and EntF (**10**). The fragment lengths were carefully chosen so that a conserved residue was situated at the *N*-terminus of the corresponding peptides.

Peptide	Sequence	*Carnobacterium maltaromaticum* LV17A*	*Enterococcus faecium* CTC492*
(**9**) CbaX	SINSQIGKATSSISKCVFSFFKKC	10^{-11} M	10^{-7} M
(**10**) EntF	**AGTKPQGKPASNLVECVFSLFKKCN**	-	10^{-11} M
(**34**) CbaX:EntF	SINSQIGKAT**SNLVECVFSLFKKCN**	10^{-9} M	10^{-7} M
(**35**) EntF:CbaX	**AGTKPQGKPA**SSISKCVFSFFKKC	-	10^{-11} M
(**36**) CbaX(7-24)	GKATSSISKCVFSFFKKC	10^{-6} M	-
(**37**) CbaX(11-24)	SSISKCVFSFFKKC	-	-
(**38**) CbaX(16-24)	CVFSFFKKC	-	-
(**42**) CbaX(1-11)	SINSQIGKATS	-	-
(**39**) EntF(7-25)	**GKPASNLVECVFSLFKKCN**	10^{-5} M	10^{-6} M
(**40**) EntF(11-25)	**SNLVECVFSLFKKCN**	10^{-5} M	-
(**41**) EntF(16-25)	**CVFSLFKKCN**	10^{-6} M	-
(**43**) EntF(1-11)	**AGTKPQGKPAS**	-	-

Table 4. Induction peptides and fragments prepared for pheromone study. *Minimum concentrations of induction peptides and fragments required to initiate bacteriocin production (- = No activity detected up to 10^{-5} M).

Peptides **36** and **39** both have Gly at the *N*-terminus, **37** and **40** both have Ser at the *N*-terminus, **38** and **41** both have Cys at the *N*-terminus and **42** and **43** both have Ser at the *C*-terminus. All of these peptides were prepared by manual Fmoc-SPPS and purified by

RP-HPLC. The peptides were screened for pheromone activity by Dr. Marco van Belkum against *C. maltaromaticum* LV17A and *E. faecium* CTC492 at concentrations up to 10^{-5} M. All induction peptides described were tested at a concentration of 10^{-3} M for antimicrobial activity towards *C. maltaromaticum* LV17A and *E. faecium* CTC492 using the spot-on-lawn technique and did not show inhibition of growth. The activity of the peptide fragments and hybrids gives insight into the sequence responsible for binding to their receptors (Table 4). CbaX (7-24) (**36**) and EntF (7-25) (**39**) induce their own cognate bacteriocin systems at concentrations up to 10^{-6} M in *C. maltaromaticum* LV17A and *E. faecium* CTC492, respectively. None of the other CbaX fragments show any pheromone activity in *C. maltaromaticum* LV17A or *E. faecium* CTC492. The *C*-terminal 19-, 15- and 10-mers of EntF show pheromone activity in *C. maltaromaticum* LV17A. Neither of the *N*-terminal 11-mers **42** or **43** were able to induce bacteriocin production in either system. It is interesting to note that in the EntF series of fragments, EntF (7-25) (**39**) shows some induction in both test organisms. As the length of the fragment shortens, EntF (11-25) (**40**) becomes less able to induce its cognate system (*E. faecium* CTC492) but retains the ability to induce *C. maltaromaticum* LV17A. Further abbreviation of the EntF sequence to EntF (16-25) (**41**) actually leads to an increase in its ability to induce bacteriocin production in *C. maltaromaticum* LV17A. These results indicate that the *C*-terminal portion of the induction peptides is able to bind non-specifically with the receptor at high concentrations while the *N*-terminal domain facilitates this interaction. As CbaX (16-24) (**38**) and EntF (16-25) (**41**) differ by only two amino acids (**41** has an additional asparagine residue at its *C*-terminus and a phenylalanine residue instead of a leucine at position 20) but have different biological

activity in *C. maltaromaticum* LV17A, two intermediate peptides, CbaX (16-24+N) (**44**) and EntF (16-25-N) (**45**), were manually prepared and tested. These two peptides did not demonstrate bacteriocin induction in either system, indicating that these single amino acid substitutions are sufficient to abolish activity.

Peptides that did not previously show induction were then tested for antagonistic activity of the parent induction peptides. Both *C. maltaromaticum* LV17A and *E. faecium* CTC492 were induced using a concentration of 2 x 10^{-11} M CbaX and EntF, respectively (the minimum required for induction of each cognate system, Table 4), and the potential antagonistic peptide fragments were added at concentrations ranging from 10^{-5} M to 10^{-7} M. None of the longer CbaX or EntF fragments, or the intermediate peptides **44** or **45,** displayed any activity as antagonists for bacteriocin production (Table 5).

Peptide	Sequence	*Carnobacterium maltaromaticum* LV17A*	*Enterococcus faecium* CTC492*
(**37**) CbaX (11-24)	SSISKCVFSFFKKC	-	N.A.
(**38**) CbaX (16-24)	CVFSFFKKC	10^{-5} M	10^{-6} M
(**44**) CbaX (16-24+N)	CVFSFFKKC**N**	-	-
(**42**) CbaX (1-11)	SINSQIGKATS	-	N.A.
(**40**) EntF (11-25)	**SNLVECVFSLFKKCN**	N.A.	-
(**41**) EntF (16-25)	**CVFSLFKKCN**	N.A.	-
(**45**) EntF (16-25-N)	**CVFSLFKKC**	-	-
(**43**) EntF (1-11)	**AGTKPQGKPAS**	N.A.	-

Table 5. List of peptides that were tested for antagonistic activity of parent bacteriocins. *Minimum concentration of peptide necessary to antagonize bacteriocin production (- = No activity detected up to 10^{-5} M, N. A. = not tested).

CbaX (16-24) (**38**) was the only peptide that demonstrated antagonistic activity to bacteriocin production. At 10^{-5} M, CbaX (16-24) (**38**) reduces bacteriocin production in its cognate system *C. maltaromaticum* LV17A, and at up to 10^{-6} M, **38** also reduces or completely inhibits, bacteriocin production in *E. faecium* CTC492. This data supports

the concept that the *C*-terminal part of the induction peptide interacts relatively non-specifically with the receptor. Furthermore, these combined results indicate that single amino acid mutations (addition of Asn, or Phe to Leu substitution) are sufficient to abolish induction.

It is worth mentioning that MALDI-MS experiments were performed in an attempt to develop a quick method to detect bacteriocin production after induction. Conceptually, this technique would provide a direct and rapid method to verify the product of an induction event. In cultures that had lost their ability to produce bacteriocin (by dilution) the minimum amount of full-length induction peptides CbaX (**9**) and EntF (**10**) was added to each of *C. maltaromaticum* LV17A and *E. faecium* CTC492 in separate experiments. In a similar manner, the cross induction experiments were also completed. After being allowed to grow overnight to a fully grown culture, an aliquot was removed, mixed with sinapinic acid, and placed onto a MALDI-MS plate. Unfortunately, the product bacteriocins are not detected by MALDI-TOF MS. Aliquots of these reactions were also tested by LC-MS, but the expected products are also not detected by this technique. Although it may be possible to purify the product from the bacterial culture and identify its constituents, this method takes significantly more time than a standard spot-on-lawn assay, rendering is unsuitable as a rapid method of detection. However, these results emphasize the potent activity of bacteriocins. In ideal conditions, MALDI TOF-MS instruments are reportedly able to detect between picomol (10^{-12}) and femtomol (10^{-15}) levels. Although a bacterial culture is clearly not an ideal system for MALDI-MS, the level of bacteriocin that is produced can easily be detected by biological assays, but is insufficient for current mass spectrometry techniques.

3.2 Structural Information and Insight into the Receptor Active Site

Circular dichroism (CD) spectroscopy of the induction peptides gives perspective into the structure of the active peptides (Table 6). The full-length peptides **9**, **10**, **34** and **35** were dissolved at a concentration of 50 μM in a variety of solvent mixtures of trifluoroethanol (TFE) and 10 mM potassium phosphate buffer (pH 7.4), varying the TFE concentration from 0-80%. At concentrations of 0% and 20% TFE, the samples did not appear to assume any secondary structure.

Peptide (50 μM)	%TFE: Phosphate buffer (pH 7.4)	Molar ellipticity at 222 nm	% α-helix (Calculated)[a]
CbaX (**9**)	40	-9320.36	32
	60	-12033.78	39
	80	-14014.60	44
CbaX:EntF (**34**)	40	-17421.24	52
	60	-7700.73	27
	80	-12476.15	40
EntF:CbaX (**35**)	40	-3444.39	17
	60	-7974.83	28
	80	-643.17	9
Ent F (**10**)	40	-3271.62	16
	60	-2965.30	15
	80	-3960.83	18

Table 6. Percent α-helical content of CbaX, EntF and hybrid peptides at varying trifluoroethanol concentrations. [a]Calculated using:

% α-helix = [(-[θ] 222nm) + 3000) / 39000] x 100%[91]

At concentrations of 40, 60 and 80% TFE, the CD spectra indicate that the parent peptides CbaX (**9**) and EntF (**10**) display relatively constant secondary structure ranging from 32-44% and 15-18% α-helical content, respectively. It is interesting to note that the CD spectra of the hybrid peptides respond much more to TFE concentration than the parent compounds. There is a much wider range of α-helical content in the hybrids, 27-52% for the CbaX:EntF (**34**) hybrid and 9-28% for the EntF:CbaX (**35**) peptide as

compared to the parent peptides **9** and **10** (Table 6). In the general sense, the secondary structure of CbaX (**9**) and CbaX:EntF (**34**) show higher α-helical content in membrane-mimicking environments (such as TFE) compared to EntF (**10**) and EntF:CbaX (**35**).

This structural data appears to exhibit an interesting correlation to peptide activity as the CbaX (**9**) and CbaX:EntF (**34**) peptides have similar CD spectra (Figure 13) and both are able to induce and cross-induce bacteriocin production at similar levels. Similarly, the CD spectra of EntF (**10**) and EntF:CbaX (**35**) are very similar as is their pheromone activity profile. To our knowledge, this is the first example of cross-talk between different bacteriocin expression systems. It is important to note that it is not likely that this type of cross-talk takes place under normal circumstances as the amount of CbaX (**9**) required to induce enterocin production in *E. faecium* CTC492 is four orders of magnitude higher than is required with EntF (**10**). When the spent supernatant (remaining after the culture has grown in broth) of *C. maltaromaticum* LV17A is used, no bacteriocin induction in *E. faecium* CTC492 is observed, indicating that the amount of CbaX (**9**) produced by *C. maltaromaticum* LV17A in the supernatant is not enough to activate enterocin production in *E. faecium* CTC492.

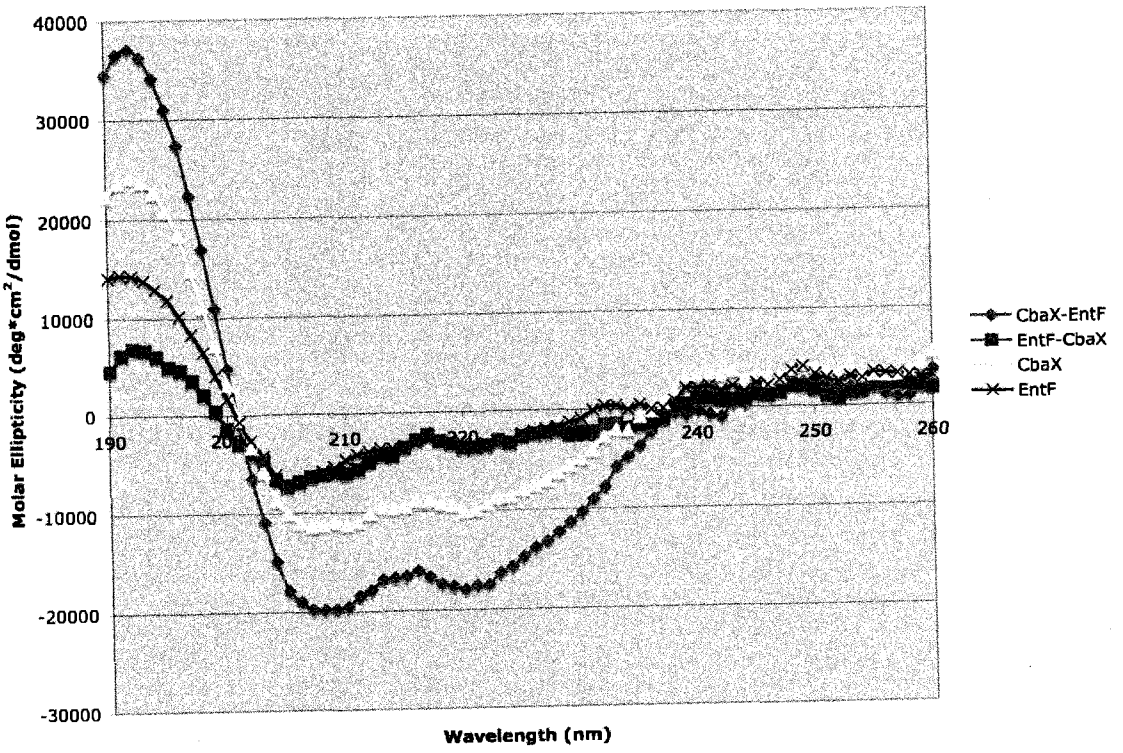

Figure 13. CD spectra of peptide pheromones CbaX (9), EntF (10) and hybrids (34, 35) at a concentration of 50 μM in 40 % TFE/ 60% 10 mM potassium phosphate (pH 7.4)

Although there is some indication of peptide secondary structure from the CD spectra, it is possible that the peptides could adopt a slightly different conformation in the presence of the receptor. To help obtain a picture of what the receptor-induction peptide complex looks like *in vivo*, it would be ideal to obtain a crystal structure of the receptor with the substrate bound in the active site. In order to achieve this goal, it is necessary to have both pure receptor protein and the induction peptide. To this end, the expression of the histidine kinase receptor with a histidine tag is presently underway in the Vederas laboratory by Dr. Marco van Belkum. As all of the induction peptides and fragments have already been prepared, they could theoretically be incorporated into a crystal structure once this protein has been purified. It is possible that the induction peptides will

not incorporate into a preformed crystal or co-crystallize with the receptor protein. In that case, analogues of the induction peptides could be prepared that would bind into the protein active site by formation of a covalent bond to the receptor protein. One method of accomplishing this task is through the use of photoaffinity labels (Figure 14).[92] Typically, a photoaffinity label mimics a naturally occurring amino acid and can be activated by irradiation with light to form a covalent bond with the receptor.[92]

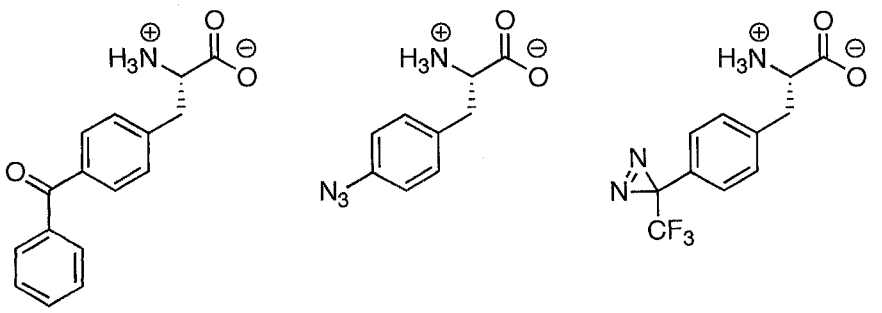

46 **47** **48**

Figure 14. Photoaffinity labels commonly used for binding to receptor active sites 4-Benzoylphenylalanine (Bpa, 46), 4-Azidophenylalanine (Apa, 47) and 4-[3-(Trifluoromethyl)-3*H*-diazirin-3-yl]-phenylalanine (H-Phe(4-Tmd)-OH, 48).

Photoaffinity labels **46-48** are analogues of the aromatic residues of phenylalanine and tyrosine (Figure 14). The use of photoaffinity label **46** is ideal based on chemical properties while **47** and **48** are appropriate when the respective amino acid is required to bind into a tight binding pocket with little flexibility. Analogues **47** and **48** have been shown to be difficult to handle based on their high reactivity as irreversible decompostion to the nitrene or carbene occurs at around 260 nm and 360 nm, respectively (near UV - visible light region).[93, 94] As a solution to this problem, the aromatic portions of these labels have been introduced after peptide synthesis by acylation onto serine or lysine residues.[95, 96] By comparison to **47** and **48**, 4-benzoylphenylalanine (Bpa, **46**) is

significantly more stable, but its larger structure and increased hydrophobicity limits its incorporation into peptides. The Bpa (**46**) residue reacts when exposed to light at 360 nm by formation of a diradical species (Scheme 7). The major advantage of this label is the fact that this activation process is reversible and if no suitable reactive site is present within a 3.1 Å reactive sphere around the carbonyl oxygen, the triplet state readily relaxes to the ground state.[92] The reactivity order of the diradical for C-H bonds is $-NCH_x$ > $-SCH_x$ > $-C{=}CCH_2$ > $-CH_2$ > $-CH_3$, but ultimately the bond insertion is dependant on proximity to a reactive site.[97] Another advantage of the Bpa (**46**) photoaffinity label is that it reacts poorly with water. This is ideal for labeling studies of proteins. As with any structural modifications, it is necessary to test the activity of the photoaffinity labeled peptide before activation to ensure that the underlying biological activity is retained.

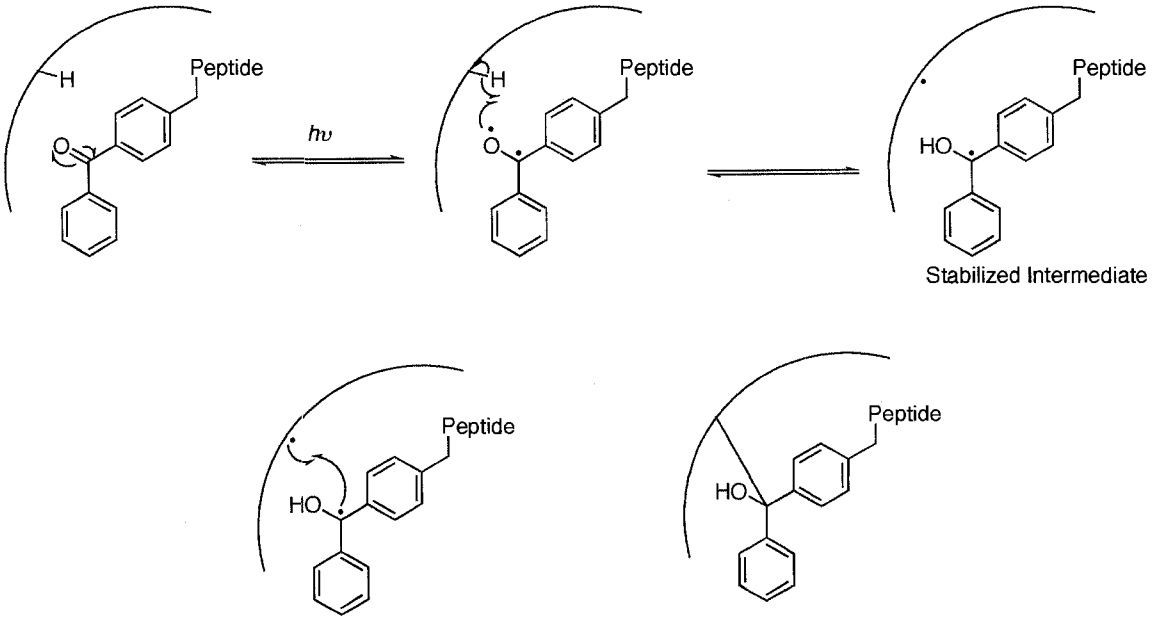

Scheme 7. Conceptual approach to photoaffinity labeling of induction peptide into receptor active site.

An attractive approach to elucidating the receptor-induction peptide complex is to initially prepare the desired histidine kinase receptor with a handle to assist in

purification. Upon verification that the modified receptor is active with the natural substrate, the organism containing the altered receptor would then be tested with the modified substrate containing the photoaffinity label. Once activity of the modified receptor and substrate has been verified, the solution could then be irradiated under appropriate conditions containing radical scavengers to reduce the amount of non-specific binding.[98] The induction peptide would then theoretically be covalently bound in the active site, in the natural state of the receptor protein (Scheme 7). Subsequent purification and characterization x-ray crystallography would then give a clear picture of the receptor active site. Given the fact that the shortest fragment of CbaX (**9**), CbaX (16-24) (**38**), was active as an antagonist to the full-length induction peptides, this peptide offered an ideal test substrate to produce analogues containing photoaffinity labels. By systematic replacement of the three phenylalanine residues in the CbaX (16-24) (**38**) sequence (Scheme 9), it would be possible to determine which position would most likely tolerate incorporation of the large benzoyl phenylalanine (Bpa) residue (Figure 15). These Bpa containing fragments **49-51** were synthesized by a first year summer student, Ms. Emma Heydari, under my supervision. Synthesis of the Bpa containing analogues was completed on 2-ClTrt resin on a 0.9 mmol scale using manual Fmoc-SPPS (1.6 mmol/g loading). After loading of Fmoc-Cys(Trt)-OH and subsequent addition of the next two residues, Fmoc-Lys(Boc)-OH and Fmoc-Lys(Boc)-OH, the resin was split into three portions of 0.3 mmol and elongated to compounds **49-51** by manual SPPS and purified by RP-HPLC.

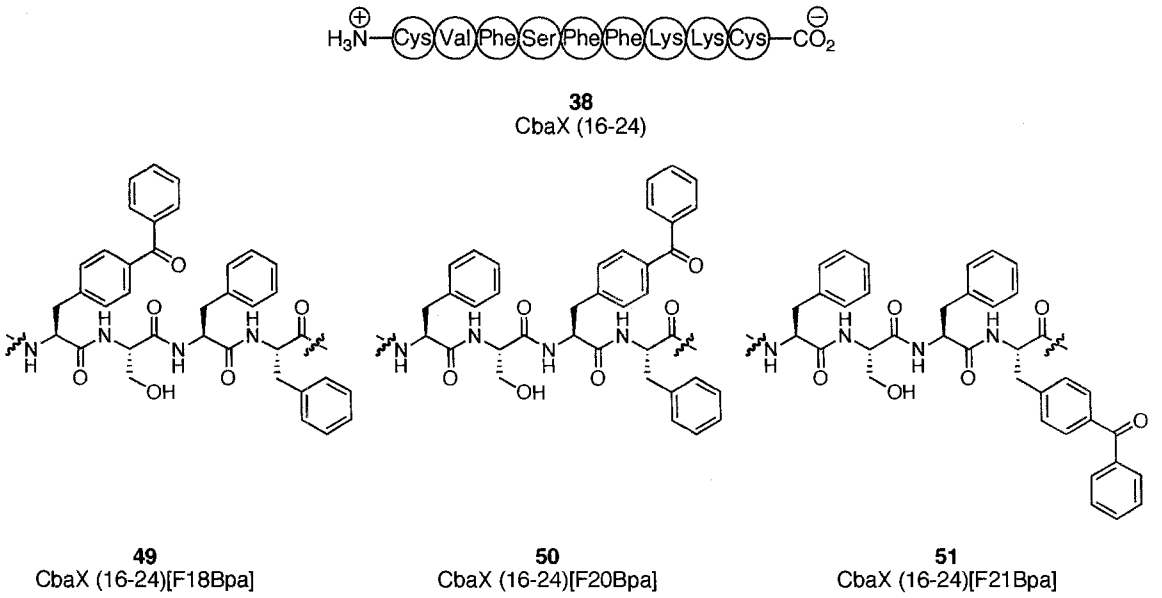

Figure 15. Systematic substitution of phenylalanine residues to determine the appropriate position for substitution.

From the results of antagonist studies with the fragment peptides (Table 7), CbaX (16-24)[F18Bpa] (**49**) and CbaX (16-24)[F21Bpa] (**51**) retained biological activity whereas CbaX (16-24)[F20Bpa] (**50**) lost almost all detectable activity. These results could be interpreted in two different ways. In one analysis, the fact that analogue F18Bpa **49** retains essentially the same activity as **38** could imply that the benzoyl substituent projects into solvent and would thus not be useful for analysis of the active site. However, it may be that the active site is closed to solvent and that the benzoyl susbtituent projects into a cavity in the active site in an unobtrusive manner, in which case this would be an ideal substrate for photoaffinity labeling. The modest reduction in the activity of analogue F21Bpa **51** indicates that the Bpa side chain does slightly interfere with binding to the active site. As the peptide does still retain activity, it would likely be a useful substrate for photoaffinity labeling.

Induction Peptide	Concentration of Antagonist Induction Peptide			
	10^{-5} M	10^{-6} M	10^{-7} M	10^{-5} M (No EntF)
(38) CbaX (16-24)	0 AU	0 AU	400 AU	0 AU
(49) CbaX (16-24) [F18Bpa]	0 AU	200 AU	400 AU	0 AU
(50) CbaX (16-24) [F20Bpa]	100 AU	400 AU	400 AU	0 AU
(51) CbaX (16-24) [F21Bpa]	0 AU	400 AU	400 AU	0 AU

Table 7. Antagonistic activity of CbaX analogues containing photoaffinity labels against EntF induction peptide (10).

The final analogue, F20Bpa **50,** appears not to be suitable as a position for a photoaffinity label as this leads to nearly a complete loss of antagonistic activity. However, this data is helpful as it indicates that phenylalanine 20 may bind more tightly into the receptor active site so substitution of phenylalanine 20 with a smaller photaffinity label may be an effective alternative. Based on this data, the synthesis of the full-length peptide analogues of CbaX (**9**), CbaX [F18Bpa] (**52**) (but not CbaX[F20Bpa] **53**) and CbaX [F21Bpa] (**54**) were similarly completed with the assistance of Ms. Emma Heydari and await biological testing. The synthesis of another analogue using a smaller photoaffinity label, 4-azido phenylalanine (Fmoc-Apa-OH), was attempted in place of Phe 20. The preparation of CbaX (16-24)[F20Apa] (**55**) was attempted by Ms. Emma Heydari but the product was not observed by HPLC or MALDI, potentially due to the high reactivity the azido substituent during peptide synthesis, resulting in decomposition or side reactions. After testing of the full-length analogues to ensure they retain the expected activity, these peptides await reaction with the purified histidine kinase receptor.

It is important to mention that some optimization was required to develop an efficient synthetic route for the induction peptides, particularly for the derivatives of CbaX. Based on difficulties with PEG leaching[99] in the synthesis of PisN (**8**) with PEG-containing trityl resins, the synthesis of the CbaX peptide series was initially attempted on the robust Wang resin. This proved to be a poor choice as approximately 50% of the desired product was lost at the 9-mer (CbaX 16-24, **38**) stage and none of the desired product remained upon elongation to the 14-mer (CbaX 11-24, **37**). Moreover, repeated exposure of the peptide to piperidine used for Fmoc-deprotection led to epimerization and elimination of the side chain thiol of cysteine to produce piperidine adducts (Scheme 8). To circumvent this problem, the peptides were prepared using a trityl based resin, but this served to inspire a new approach to solve the underlying problem of α-proton acidity. It was envisioned that replacement of the adjacent ester moiety, potentially by an orthoester, would reduce the acidity of the α-proton and improve the efficiency of syntheses containing *C*-terminal cysteine residues.

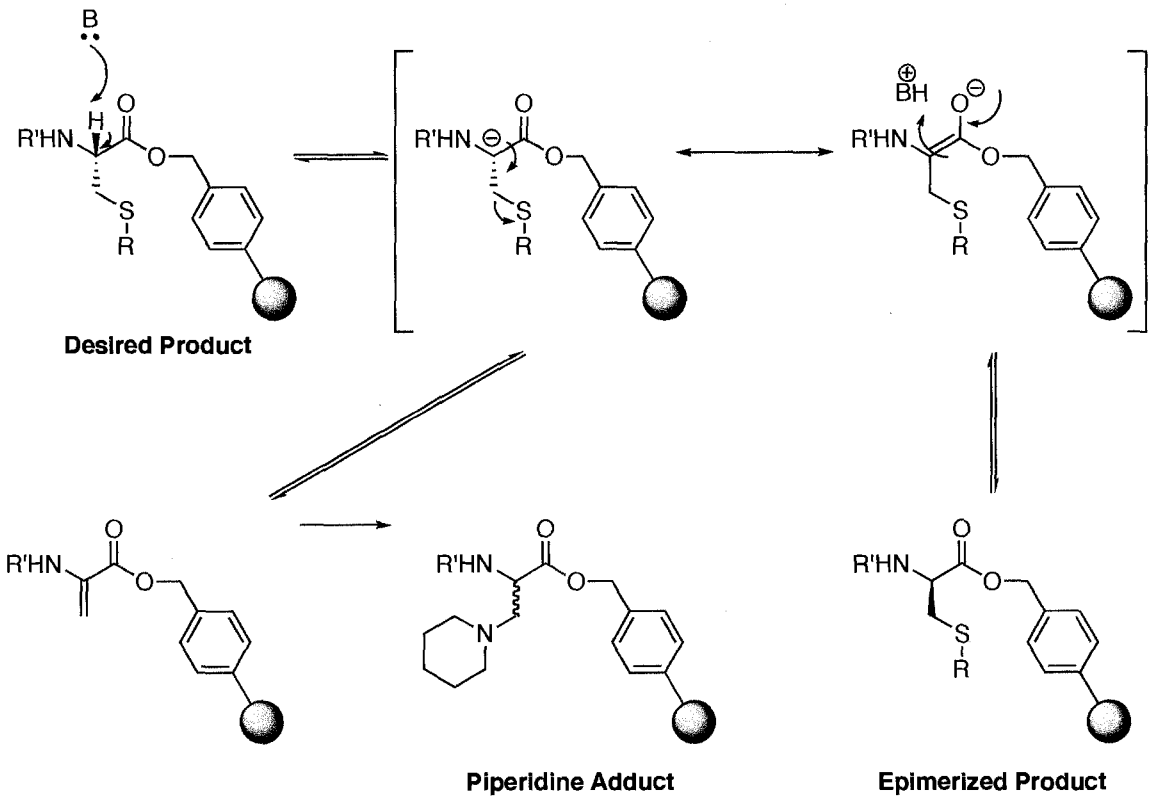

Scheme 8. Synthesis of *C*-terminal cysteine containing peptides on Wang resin leading to undesired side products.

3.3 Summary and Future Work – Induction Peptides

Experiments with the *N*- and *C*-terminal fragments of CbaX and EntF show that the *C*-terminal 18-mer of CbaX (**36**) and 19-mer of EntF (**39**) are able to induce their cognate bacteriocin system in *C. maltaromaticum* LV17A and *E. faecium* CTC492, but the *N*-terminal 11-mer fragments of CbaX **42** and EntF **43** do not show any activity. When shorter versions of the *C*-terminal 18- and 19-mer of CbaX and EntF are used, the peptides lose the ability to induce their cognate bacteriocin systems.

Unexpectedly, the *C*-terminal 19, 15 and 10-mers of EntF (**39**, **40** and **41**) cross-induce bacteriocin production in *C. maltaromaticum* LV17A. The 10-mer has even more pheromone activity than the 19- or 15-mer peptides as the concentration of EntF (16-25) (**41**) needed to cross-induce carnobacteriocin A production in *C. maltaromaticum* LV17A is 10-fold lower than that of EntF (11-25) (**40**) and EntF (7-25) (**39**). This indicates that the interaction of the *C*-terminal domain of these peptide pheromones is not necessarily specific towards its own cognate receptor. This seems to be confirmed by the result that the *C*-terminal fragment CbaX (16-24) (**38**) is able to inhibit pheromone activity of CbaX (**9**) as well as EntF (**10**) in their cognate systems. The interaction of CbaX (16-24) (**38**) with the receptor appears to be insufficient to initiate induction but adequate to interfere with pheromone activity of the full-length peptides. However, the results with CbaX (16-24+N) (**44**) and EntF (16-25-N) (**45**) show that a single amino acid substitution can inhibit interaction of the *C*-terminal induction peptide with the receptor.

The circular dichroism (CD) spectra of CbaX (**9**) and CbaX:EntF (**34**) show considerable α-helical content in the presence of structure-inducing solvents and

demonstrate an interesting correlation to their activity profiles. Similarly, EntF (**10**) and EntF:CbaX (**35**) display comparable CD and biological activity profiles.

The induction experiments with the full-length peptide pheromones and their hybrids reveal that the *N*-terminal domain plays a major role in the recognition of the peptide pheromone to its cognate receptor. The results with EntF (**10**) and CbaX:EntF (**34**) demonstrate that substitution of the *N*-terminal domain of Ent F (**10**) with the corresponding sequence in CbaX (**9**) leads to a significant reduction of activity in the EntF natural system (*E. faecium* CTC492). This is consistent with the result in the *C. maltaromaticum* LV17A system where the *N*-terminus of CbaX (**9**) is exchanged with the *N*-terminus of EntF (**10**) in the analogue EntF:CbaX (**35**) and activity is completely abolished in the CbaX cognate system. An important observation from these results is that the selectivity of inducer peptides seems to correlate to the *N*-terminal domain of the peptide, but the *N*-terminal fragment alone is inadequate for induction. This indicates that the *C*-terminal portion of the induction peptide interacts weakly with the histidine protein kinase in a relatively non-specific fashion. This small interaction is then enhanced by the *N*-terminal domain responsible for conferring the increased specificity and biological activity demonstrated in the full-length induction peptide pheremones.

The structure of the induction peptide-receptor complex will be tremendously valuable to better understand the features of the histidine protein kinase. With some insight into the requirements for induction, the door would be opened to small molecules that could potentially activate bacteriocin production. In the event that reactions of the photoaffinity labels are problematic, the preparation of the Phe-(4-Tmd) photoaffinity label at Phe 20 of CbaX (**9**) may be beneficial. The smaller size of the diazirine moiety

in **48** combined with the information that the Phe 20 position may be in a tight fitting portion of the receptor, suggests that this combination may give the required interaction necessary to produce a representative receptor-ligand complex.

The alternative possibility of photoaffinity labeling by acylation onto Ser 19, Lys 22 or Lys 23 make the *C*-termini of CbaX and EntF ideal substrates for photoaffinity labeling studies. As many bacteriocin producing organisms are already present in food that is used for human consumption, it appears reasonable that addition of a very small amount of induction peptide could induce many foods to produce "natural" preservation agents. Based on high sequence homology in the *C*-terminal (non-specific binding) portion of the induction peptides (Figure 3, Section 1.3) it seems reasonable to test the ability of PisN (**8**), for cross induction in the CbaX (**9**) and EntF (**10**) cognate systems *C. maltaromaticum* LV17A and *E. faecium* CTC492, respectively. Aside from the direct testing of the parent peptides in all of the organisms, it would be logical to extend a study to the synthesis of similarly designed hybrids such as PisN (1-10)-CbaX (11-24), PisN (1-10)-EntF (11-25), EntF (1-10)-PisN (11-24) and CbaX (1-10)-PisN (11-24). It would be very interesting to see if correlations between CD spectra and induction activity are observed. If promising results are observed in the full length hybrids, small fragments of PisN could be prepared analogous to the CbaX and EntF fragments.

4. ORTHOESTER PROTECTED PEPTIDES

4.1 Model Studies Using Established Methods

As previously encountered in the synthesis of the CbaX induction peptides, difficulty can arise in the synthesis of long peptides containing a *C*-terminal cysteine residue (Scheme 8, Section 3.2). The Fmoc protecting group is routinely employed in peptide synthesis for the *N*-terminal protection of the growing peptide chain. Due to the acidity of the proton in position 9 of the fluorene ring, removal of the Fmoc protecting group can be completed using mild bases. The standard method employed for this task uses a solution of 20% piperidine in dimethylformamide (DMF). However, in the synthesis of long, aggregated peptides, this mixture is often inadequate and it becomes necessary to wash the resin numerous times to achieve sufficient levels of deprotection (Figure 16).

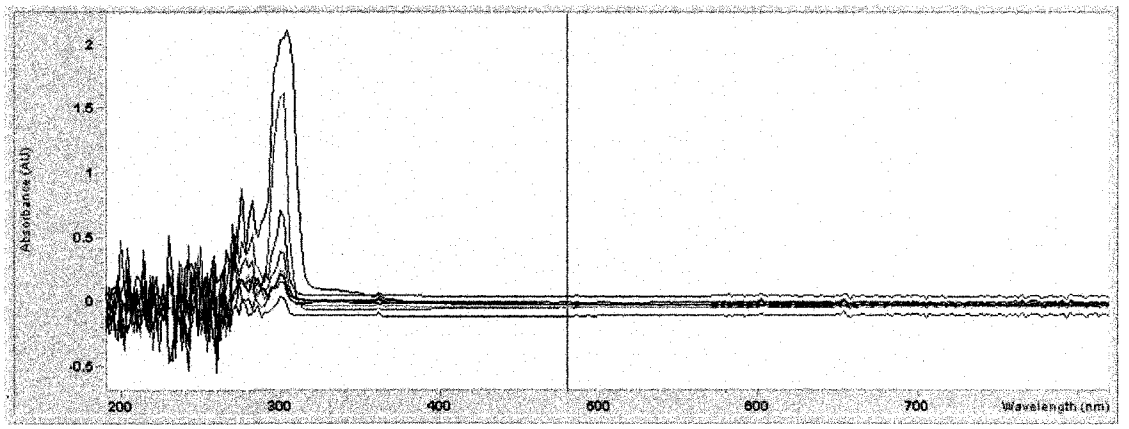

Figure 16. Fmoc deprotection using 20% piperidine/DMF on an aggregated peptide. Sequential washes demonstrate decreasing absorbance of fulvene adduct at 301 nm. The tallest peak is the initial piperidine wash and the smallest peak is the final deprotection.

Although the repeated washing with 20% piperidine eventually removes most of the *N*-terminal Fmoc group, repeated washes amplify the problem of *C*-terminal epimerization and elimination, particularly when cysteine is the first residue.[100, 101] Alternatively, stronger bases must often be employed to ensure complete removal of the Fmoc protecting group. One commonly used solution to facilitate Fmoc removal in difficult cases consists of 2% piperidine, 2% 8-diazobicyclo[5.4.0]undec-7-ene (DBU) and 96% DMF (Figure 17). Although these methods facilitate removal of the Fmoc group, *C*-terminal cysteine containing peptides remain difficult to synthesize in adequate yields as even the standard piperidine washes repeated over long peptides erode yields to an unacceptable level due to epimerization and elimination. Although the steric bulk of the trityl based resins (**12,** Figure 18) helps to reduce these unwanted side reactions as compared to Wang resin (**11,** Figure 18), epimerization and elimination still occur.

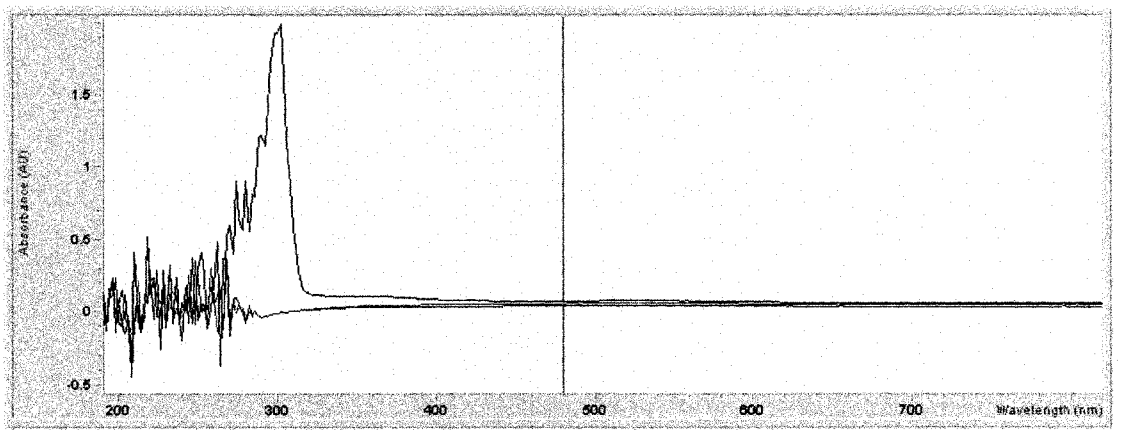

Figure 17. Fmoc deprotection using 2% DBU/2% piperidine/96% DMF on identical aggregated peptide shown in Figure 16. Sequential washes show that complete deprotection occurs in only one cycle. Tallest peak is the initial Fmoc deprotection with no Fmoc-piperidine adduct detected in subsequent washes.

We hypothesize that this problem can be addressed by reducing the acidity of the α-proton. One method of reducing the acidity of the α-proton is to replace the adjacent carbonyl moiety with an orthoesther. This methodology has previously been employed to

prepare serine and threonine derivatives.[102] By linking the cysteine amino acid to the resin via the side chain sulfur atom, combined with appropriate *C*-terminal protection, the cysteine residue should no longer be prone to these deleterious side reactions (**56,** Figure 18). Side chain immobilization strategies have previously been employed, but protection of the *C*-terminus as an ester limited its utility as the α-proton remained equally acidic.[101]

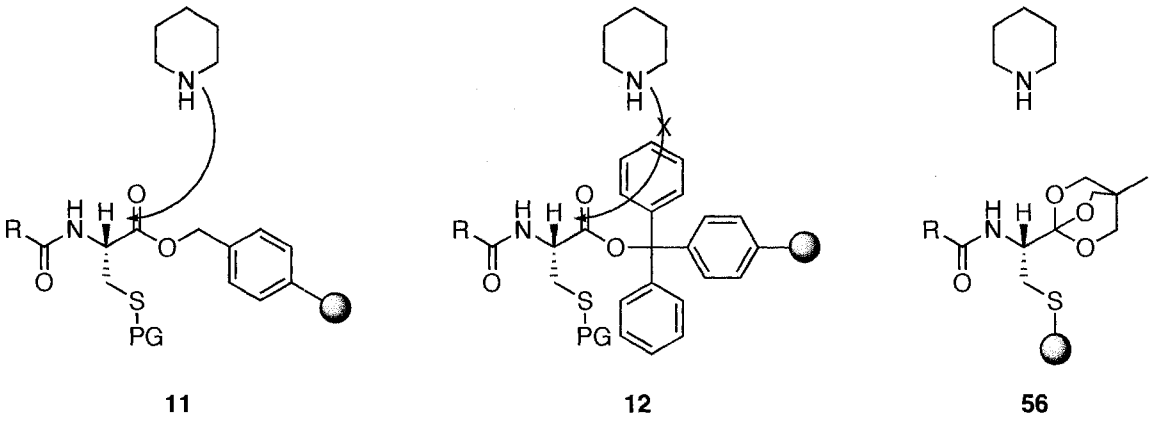

Figure 18. Comparison of Wang resin (11), trityl resin (12) and proposed orthoester protected resin (56).

The only benefit of the ester protection method is that any product that eliminates to form the dehydroalanine intermediate is eliminated from the resin and is washed into the waste in the same step. This is also the major disadvantage of the methodology as this results in a direct loss of product. The shortfall of the side chain method incorporating a methyl ester is that not only has there been no reduction in the acidity of the α-proton but there is no steric bulk to prevent deprotonation of the α-proton. To the best of our knowledge, no methods to date utilize an orthoester-protecting group for reduction of the acidity of the α-proton in *C*-terminal cysteine residues. To complete a thorough study of synthetic methodology it was necessary to compare any new methods against existing techniques. The model tripeptide used in this study consists of H-Gly-Phe-Cys-OH, and was selected

based on its simplicity and the fact that the D and L cysteine epimers are known to be separable by HPLC.[101] This allows the percentages of epimerized cysteine product and piperidine adduct side product to be easily calculated by integration of the HPLC trace. The basic steps towards the synthesis of the model tripeptide are illustrated in Scheme 9.

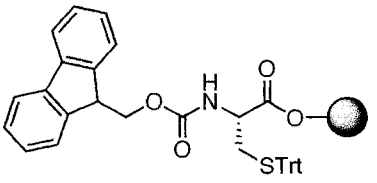

1) Fmoc Deprotection
2) Fmoc-Phe-OH, PyBOP, NMM
3) Fmoc Deprotection
4) Fmoc-Gly-OH, PyBOP, NMM
5) Fmoc Deprotection
6) Cleavage from resin

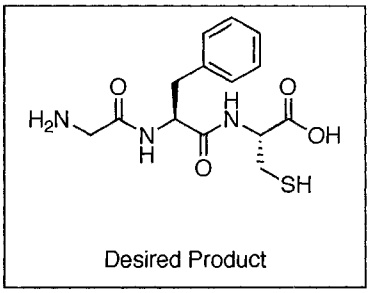

57

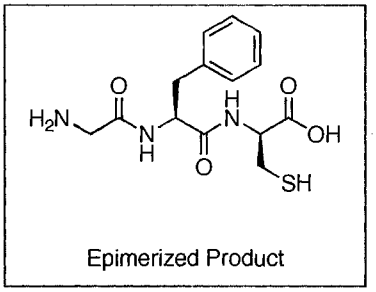

58

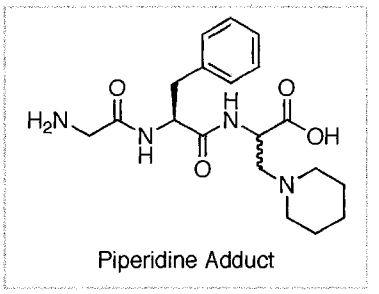

59

Scheme 9. Synthesis of the model tripeptides by varying methods of Fmoc deprotection and cleavage conditions

All resins used in this study were obtained preloaded with Fmoc-Cys(Trt) unless otherwise indicated. The model tripeptides were synthesized and purified by an undergraduate, Ms. Landon Reid, as part of her fourth year honors project under my supervision. The peptide was prepared on Wang and 2-ClTrt resins using the two types of Fmoc deprotection methods previously discussed (20% piperidine or 2% DBU: 2% piperidine in DMF) and four different cleavage conditions consisting of:

A) 96% trifloroacetic acid (TFA): 2% water : 2% Triisopropylsilane (TIPSH)

B) 5% TFA: 90% DCM: 5% TIPSH

C) 95% TFA: 2% ethanedithiol (EDT): 2% water: 1% TIPSH

D) 70% TFA: 5% EDT: 14% bromotrimethylsilane: 10% thioanisole : 1% m-cresol

These cleavage conditions were selected based on their potential ability to cleave an orthoester with minimum epimerization. Solution A is the standard cocktail used for cleavage of Wang type resins. Solution B is the standard solution employed for cleavage of trityl based resins. Solution C is a standard solution for the cleavage of *C*-terminal cysteines, and solution D was the only previously reported method used to cleave peptides that used a TMS halogen. It has been reported that TMS-protected halogens (e.g. TMS-I) react with orthoesters to produce the corresponding carboxylic acid in one step.[102] Multiple cleavage conditions were employed in this study to also expose any epimerization that was occurring during the resin cleavage step. The results are summarized in the following charts (Figure 19-20).

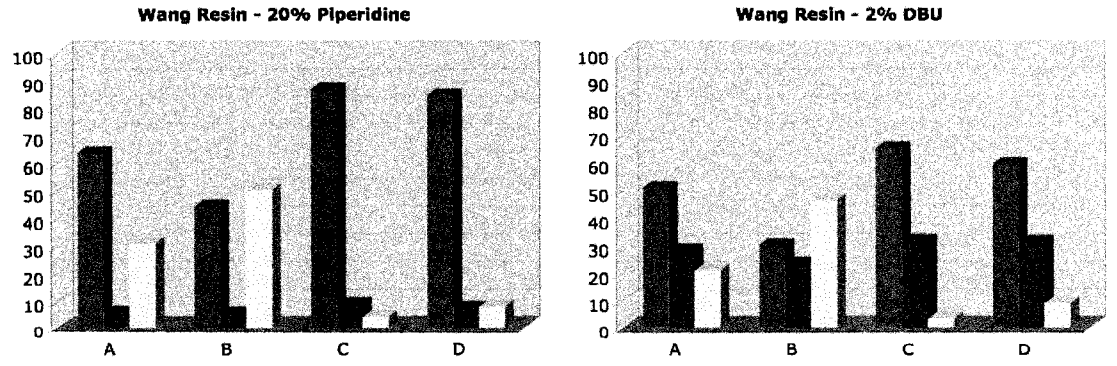

Figure 19. Tripeptides synthesized using Wang resin and 20% piperidine (left) and 2% piperidine/ 2% DBU (right) using cleavage conditions show on previous page. Blue = desired tripeptide 57, red = epimerized tripeptide 58 and yellow = piperidine adduct 59.

After manual preparation and HPLC analysis of the tripeptides, some clear trends are demonstrated in the resulting data. It was found that utilization of the stronger base, DBU, results in a decrease of the desired product in both resins compared to using only piperidine for Fmoc deprotection. The types of conditions employed for resin cleavage also affect the percentages of epimerization and elimination products that are obtained. Cleavage conditions employing thiol scavengers (conditions C and D) tend to produce smaller percentages of epimerization and elimination products. The cleavage condition using smaller concentrations of TFA (condition B) results in the largest percentage of epimerization and elimination products being obtained. The low yield of desired product obtained from using a low TFA concentration is likely due to only partial hydrolysis from resin as less than 50% TFA is generally insufficient for cleavage of Wang type resins (Figure 19, Condition B). When 2-Chloro trityl resin is employed in the synthesis, variation in the type of cleavage conditions does not noticeably affect the percentage of epimerization and elimination products that are observed (Figure 20).

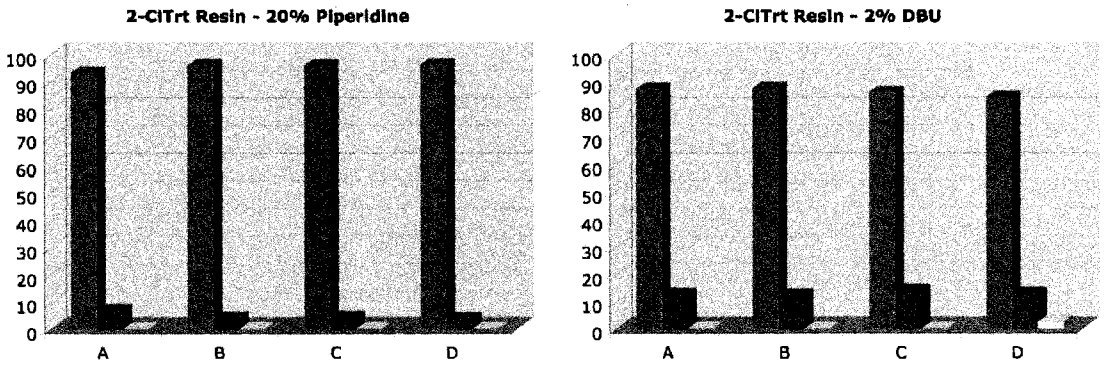

Figure 20. Tripeptides synthesized using 2-Cl-Trt resin and 20% piperidine (left) and 2% piperidine/ 2% DBU (right) using the same cleavage conditions as Figure 13. Blue = desired tripeptide 57, red = epimerized tripeptide 58 and yellow = piperidine adduct 59.

Very little piperidine adduct **59** or epimerized product **58** are formed with the use of 2-Chloro trityl resin and piperidine deprotection. It is important to note that use of 2% DBU results in an increase in the amount of epimerized product that is observed using both resins in the model tripeptide. Although this study displays the superiority of 2-ClTrt over Wang resin for the synthesis of *C*-terminal cysteine peptides, extrapolation of these results to much longer peptides clearly demonstrates the underlying problem of using an ester linkage in peptide synthesis and the need for a more robust resin linkage.

4.2 Attempts to Prepare an Orthoester Protected Cysteine

In an effort to reduce the amount of product lost due to side reactions caused by the acidity of the α-proton in *C*-terminal cysteine peptides, an attempt was made to synthesize the proposed side chain immobilized resin containing the orthoester **56** (Figure 18). The initial method of preparation was based on the published method of incorporating orthoesters onto serine.[103] The requisite oxetane esters **62** and **63** were prepared via reaction of the protected cysteine derivatives **60** and **61** with DIPCDI, HOBt and the required oxetane alcohol (Scheme 10). Reaction with boron trifluoride etherate (BF_3-OEt_2), as reported for the preparation of the serine orthoester, and a variety of other Lewis acids such as $TiCl_4$, $MgBr_2$, $SnCl_4$, $La(OTf)_3$, $Gd(OTf)_3$, $Ho(OTf)_3$ and $Lu(OTf)_3$ were attempted.

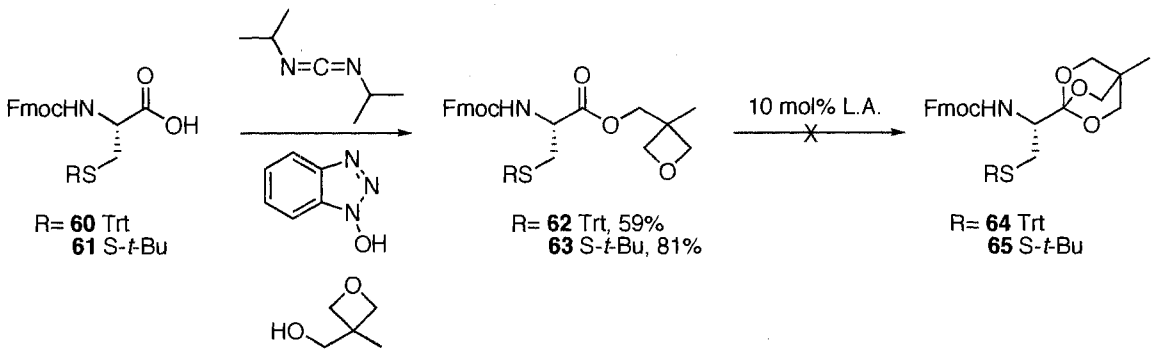

Scheme 10. Attempted rearrangement of cysteine oxetane esters to corresponding orthoesters.

Unfortunately, the orthoester rearrangement did not proceed to the desired products **64** or **65** under any of the conditions attempted. This was likely due to preferential coordination of the Lewis acid to the sulfur atom instead of the oxetane oxygen. This hypothesis is supported by the observation that upon addition of boron trifluoride etherate to the trityl protected cysteine derivative **60**, the reaction mixture instantly turns bright

yellow, implying that the relatively stable trityl cation had been liberated as the boron bound to the sulfur atom. None of the other Lewis acids employed displayed any detectable reaction after 24 h. With the direct approach proving unsuccessful, it was envisioned that an indirect method could lead to the desired cysteine orthoester (Scheme 11).

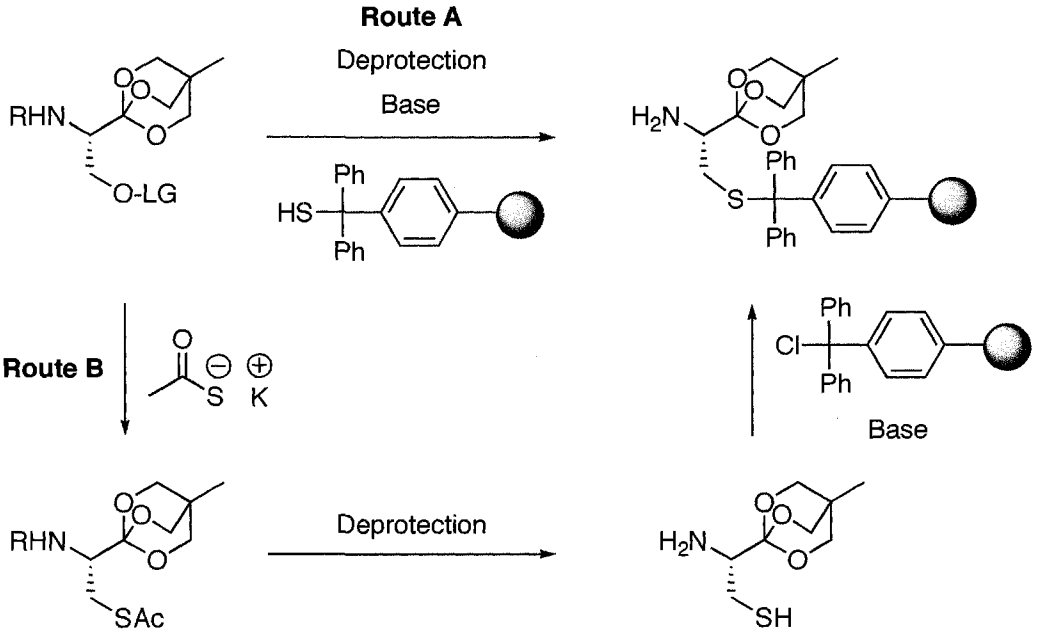

Scheme 11. Proposed scheme to indirectly access the orthoester of cysteine without exposing sulfur to a Lewis acid. Route A- Direct approach using thiol containing resin, Route B- Indirect approach forming cysteine before immobilization.

It was expected that displacement of the activated serine side chain with a thiol containing resin would produce the desired cysteine residue protection while achieving immobilization onto a solid support. Alternatively, displacement of the activated side chain with a protected thiol allowed another approach to prepared the desired resin.

Installation of an ortho ester in place of the carboxylic acid group is the first step toward the synthesis of the side chain immobilized resin. Following literature procedure,[102] Cbz-L-serine (**66**) initially reacts with cesium carbonate to afford a

nucleophile that is lyophilized to a dry white powder. This then reacts with oxetane tosylate **67** and sodium iodide to produce the desired oxetane ester **68** (Scheme 12). Rearrangement of the oxetane ester with boron trifluoride etherate affords the orthoester **69** as a protected carboxylic acid functionality. This reaction is favorable in part due to the reduction of ring strain that occurs during formation of the ortho ester from the oxetane substituent.[103] Conversion of the serine alcohol into the mesylate **70** and tosylate **71** proceeds smoothly in 68% and 71% yields, respectively.

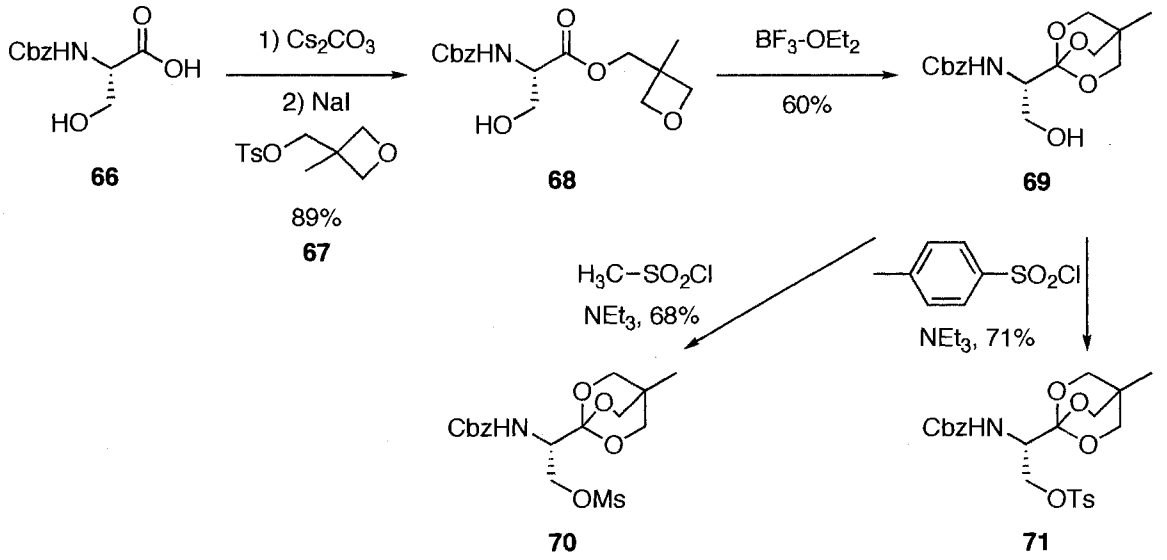

Scheme 12. Synthesis of the serine derived orthoester with the side chain converted to a leaving group.

The tosylated intermediate **71** is then subjected to hydrogenation conditions to remove the Cbz protecting group and filtered and concentrated *in vacuo* (Scheme 14). The H-Ser(OTs)-OBO residue **72** is then dissolved in DMF, added to 4-methoxy thiol trityl resin and reacted for 2 h. The resin is then acylated with acetic anhydride and the steps to form the model tripeptide **57** are completed as previously shown in the model systems (Scheme 13).

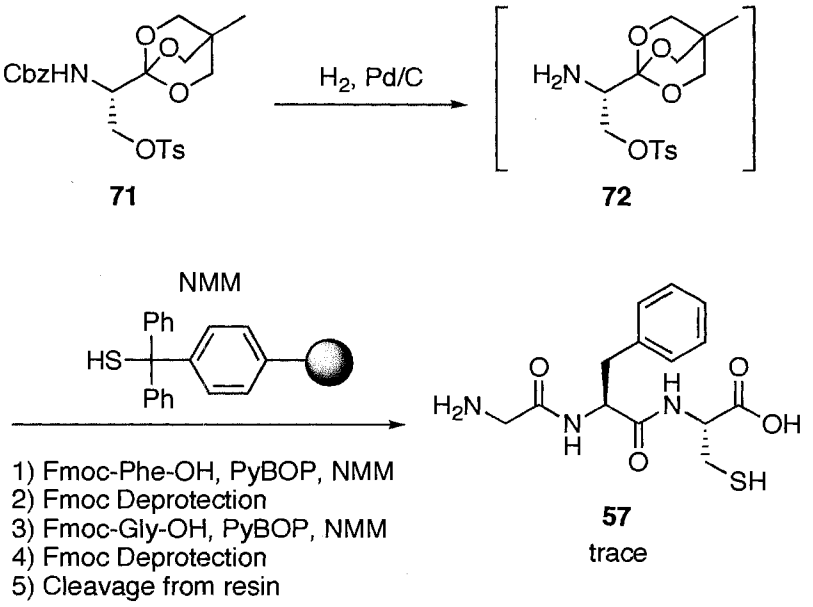

Scheme 13. Attempted reaction to prepare desired L-tripeptide using orthoester protected cysteine.

After cleavage of the peptide from the solid support, the product containing the appropriate mass for peptide **57** was collected at the expected retention time. Although the mass of the desired peptide was obtained, integration of the HPLC trace was insufficient to determine the amount of product that was produced. To examine more closely what was happening in this reaction, H-Ser(OTs)-OBO (**72**), N-methylmorpholine (NMM) and trityl thiol were combined in an NMR tube with deuterated-DMF and an identical experiment was prepared without the NMM. Over a period of 24 h, the ^{1}H-NMR spectra of both experiments indicated that the tosylate was being displaced and intramolecular aziridine formation to **73** was occurring rather than intermolecular displacement by the thiol. We suspect that this result may be due primarily to steric encumbrance around the reactive site with the large trityl thiol nucleophile. Unfortunately, Route B suffered from similar difficulties (Scheme 14). Although displacement of the tosylate from **71** with thioacetic acid proceeds readily to

produce **74**, further manipulation of this compound proves problematic. Attempted removal of the acetate functionality with nucleophiles (sodium methoxide, potassium hydroxide, ammonia or sodium amide) to yield **75** required prohibitively long reaction times (greater than 3 days) with more than 50% of the starting material remaining.

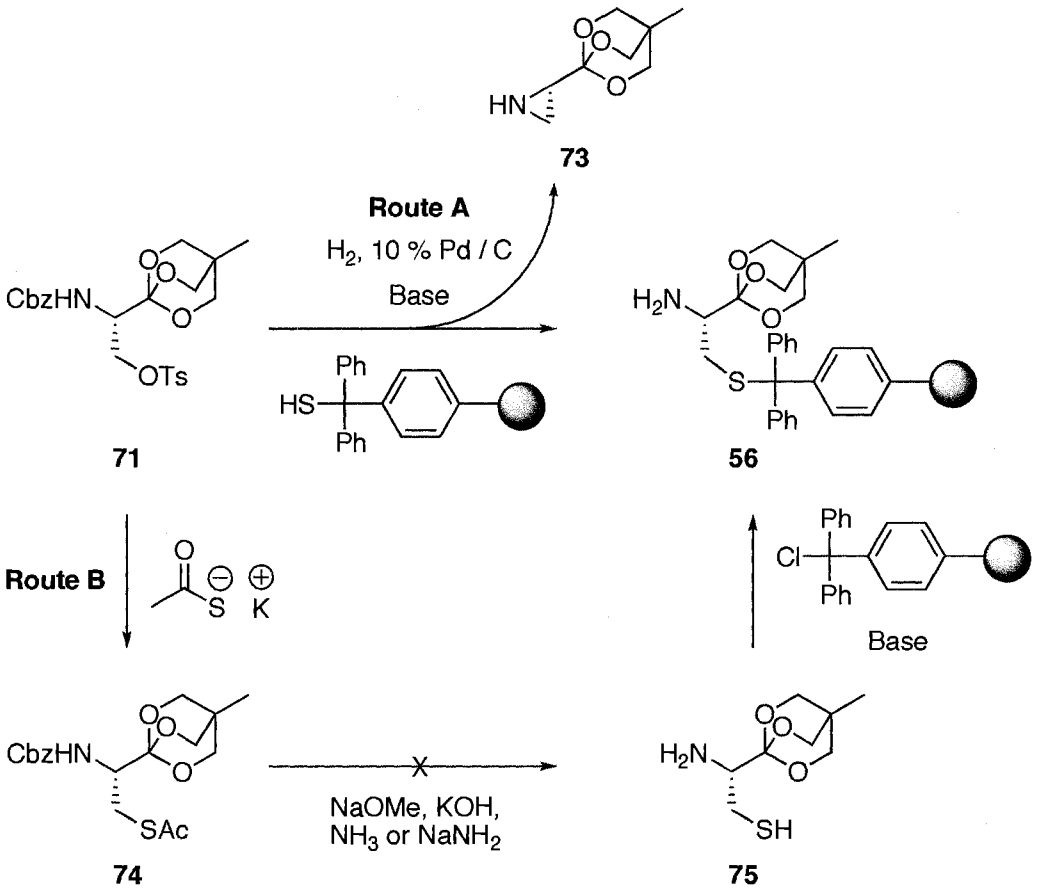

Scheme 14. Attempts to produce desired side chain immobilized cysteine resin.

At this point it was clear that the Cbz protecting group for nitrogen was inappropriate for these purposes. Unfortunately, the dense functionalization of the molecule restricts potential substitutes. As the desired product was ultimately to be used for Fmoc SPPS, the ideal substituent would need to incorporate an Fmoc or other base labile group for nitrogen protection. Under standard conditions, the Fmoc group is also unsuitable as this group can be cleaved by thiolates. The use of Bronsted or Lewis acid labile protecting

groups is similarly unacceptable due to lability of the orthoester to these reagents. Attempts were made to prepare the pthalyl (Pth) derivative via Pth-Ser-OAllyl (**76**, Figure 21), but further reaction to produce the required Pth-Ser-oxetane ester did not yield the desired product under standard conditions.

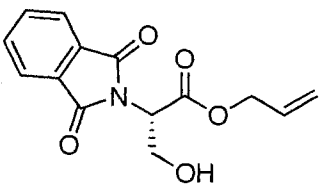

76

Figure 21. Structure of Pth-Ser-OAllyl.

4.3 Summary and Future Work - Orthoester Protected Peptides

The basis has been established for the development of an orthoester containing cysteine derivative to be used in SPPS. Although the preparation of a sidechain immobilized, orthoester protected cysteine resin (**56**) has proved particularly difficult, future work that that may potentially lead to the desired product are:

1) Employment of different thiol equivalents to introduce sulfur. NaSH may be possible, but safety concerns limit the practicality of its routine use.

2) The use of different protecting groups on nitrogen, ideally stable to thiol addition and removable under mild, orthogonal conditions. As Fmoc has been used to prepare serine orthoesters,[102, 104] it could possibly be used in conjunction with base labile sulfur-protecting groups under buffering conditions.

Although the preparation of this molecule may prove possible with subsequent optimization, it is important not to lose sight of the original goal of reducing α-proton acidity of the residue attached to the solid support. An alternative approach to solve this

problem is to immobilize an orthoester protected cysteine equivalent via the orthoester functionality. Conceptually, this would not only solve the problem of *C*-terminal cysteine epimerization, but more importantly could be extended to use with any *C*-terminal amino acid. One proposal (Scheme 15) utilizes Grubbs catalyst to complete a cross-metathesis forming a linkage to vinyl benzene resin.

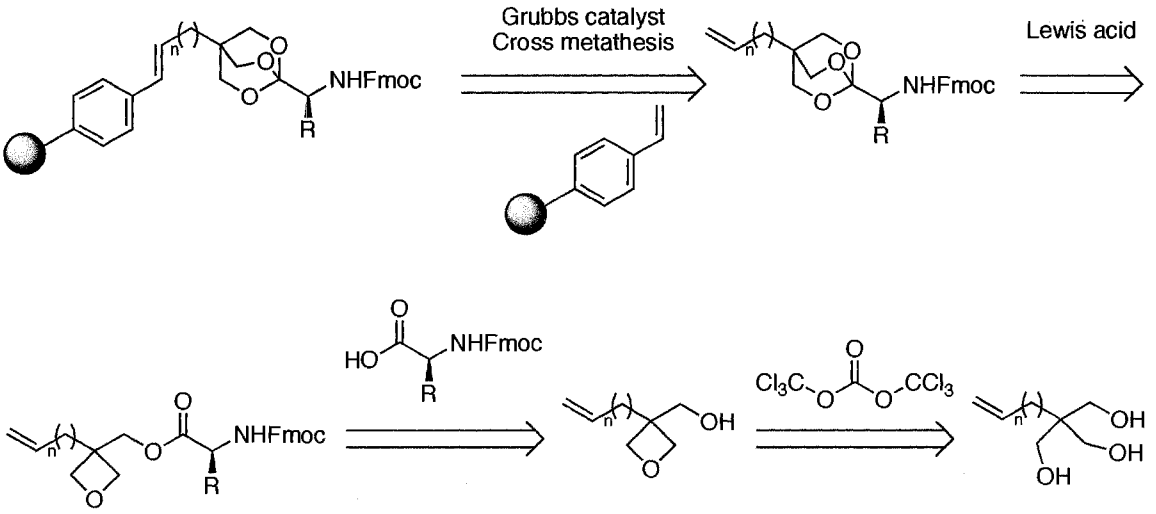

Scheme 15. Potential route to formation of an amino acid linked via an orthoester protecting group.

Once the synthesis of an orthoester containing resin is completed, the synthesis of the model Gly-Phe-Cys tripeptide[101] using both piperidine and DBU deprotection methods would complete this study and validate the underlying hypothesis that orthoesters can be used in Fmoc SPPS. Ideally, any new methodology that is developed would also be applied to the total synthesis of a small natural product containing a *C*-terminal cysteine and then to larger targets such as CbaX (**9**).

5. ANALGESIC PEPTIDES

5.1 Preparation and Testing of Analgesic Peptides

The oral activity as an analgesic and relatively simple peptide structure make crotalphine (**13**) an ideal candidate for structure activity relationship (SAR) studies. Inspection of the crotalphine (**13**) structure indicates two features that lend themselves well to SAR studies: the disulfide bond and *N*-terminal pyroglutamic acid. Replacement of the disulfide is interesting based on our previous results where disulfide replacement in oxytocin and LeuA (**1**) produces structures with similar biological activity to the parent compounds. Replacement of the *N*-terminal pyroglutamic acid is based on the logistical preparation of the peptide analogue. If this unusual residue could be replaced by proline, the peptide would consist of completely natural amino acids and allow the possibility that the peptide could eventually be produced by biological methods. Through Fmoc SPPS methods, analogues were compiled to begin an SAR study of these variables (Table 8).

Modification	Sequence
(13) Synthetic Crotalphine	**q**FSPEN**C**QGESQP**C**
(77) Natural Venom	**---***
(78) [C7a,C14a]- Crotalphine	qFSPEN**a**QGESQP**a**
(79) [C7F,C14F]- Crotalphine	qFSPEN**F**QGESQP**F**
(80) [C7S,C14S]- Crotalphine	qFSPEN**S**QGESQP**S**
(81) [C7b,C14b]- Crotalphine	qFSPEN**b**QGESQP**b**
(82) [q1P]-Crotalphine	**P**FSPENCQGESQPC
(83) [q1(Ac)P]-Crotalphine	**(Ac) P**FSPENCQGESQPC

Table 8. Crotalphine and analogues prepared to examine structure activity relationships of disulfide bond and pyroglutamic acid. q = pyroglutamic acid, a = allylglycine, b= allylglycine after RCM reaction. *Expected to be identical to 13.

Continuing on our previous work with LeuA (**1**), Ped (**2**) and oxytocin,[70, 71] crotalphine analogues containing cysteine substituted with allyl glycine (**78**), phenylalanine (**79**),

serine (**80**) and ring closed allyl glycines (**81**) were prepared to examine the role of the disulfide bridge on biological activity. Synthesis of **13, 79, 80** was assisted by another graduate student in the Vederas group, Ms. Avena Ross. Cysteine containing peptides were prepared on preloaded 2-ClTrt resin with a loading of 0.25 mmol/g. All other peptides were prepared on Wang resin with a loading of 0.8 mmol/g. As it was expected that further pyroglutamic acid analogues would be required, resin from all syntheses was split at Phe 2 so that more peptides could be readily prepared by coupling of the final residue. To analyze the effect of substitutions for the pyroglutamic acid moiety, the proline analogue **82** and acylated proline analogue **83** were also prepared. Before any of the analogues were tested, it was important to verify the parent crotalphine results as reported by the Butantan Institute in Brazil.[69]

As the reported data indicated that crotalphine interacts with opioid receptors, samples were taken to the laboratory of Prof. Peter Smith in the Deparment of Pharmacology at the University of Alberta to determine the peptides affinity to opioid receptors. Unfortunately, experiments completed by the Smith laboratory monitoring electrophysiological changes on slices from rat spinal cord did not demonstrate any results consistent with opioid binding. To ensure that an effect had not been overlooked, crotalphine (**13**) was then tested in the laboratory of Prof. Alan Hudson in the Department of Pharmacology using an opioid binding assay to determine if the peptide binds directly to opioid receptors. Conceptually, this method determines whether a test ligand is able to displace known ligands that are specific to delta, kappa and mu opioid receptors (Figure 22).[105, 106] The assay employs tissue from guinea pig brains as the source of opioid receptors. Incubation of the tissue with the varying concentrations of the proposed drug

candidate and a constant concentration of opioid selective radiolabeled ligands, gives direct information about the compounds ability to bind with opioid receptors. After one hour of incubation, the mixture of ligands and tissue is filtered and the respective pieces of the filter are placed into scintillation vials for counting. High radioactivity indicates that the test compound is unable to displace the radioactive ligands from the opioid receptors in the tissue while low radioactivity indicates that the test compound has a high affinity for opioid receptors.

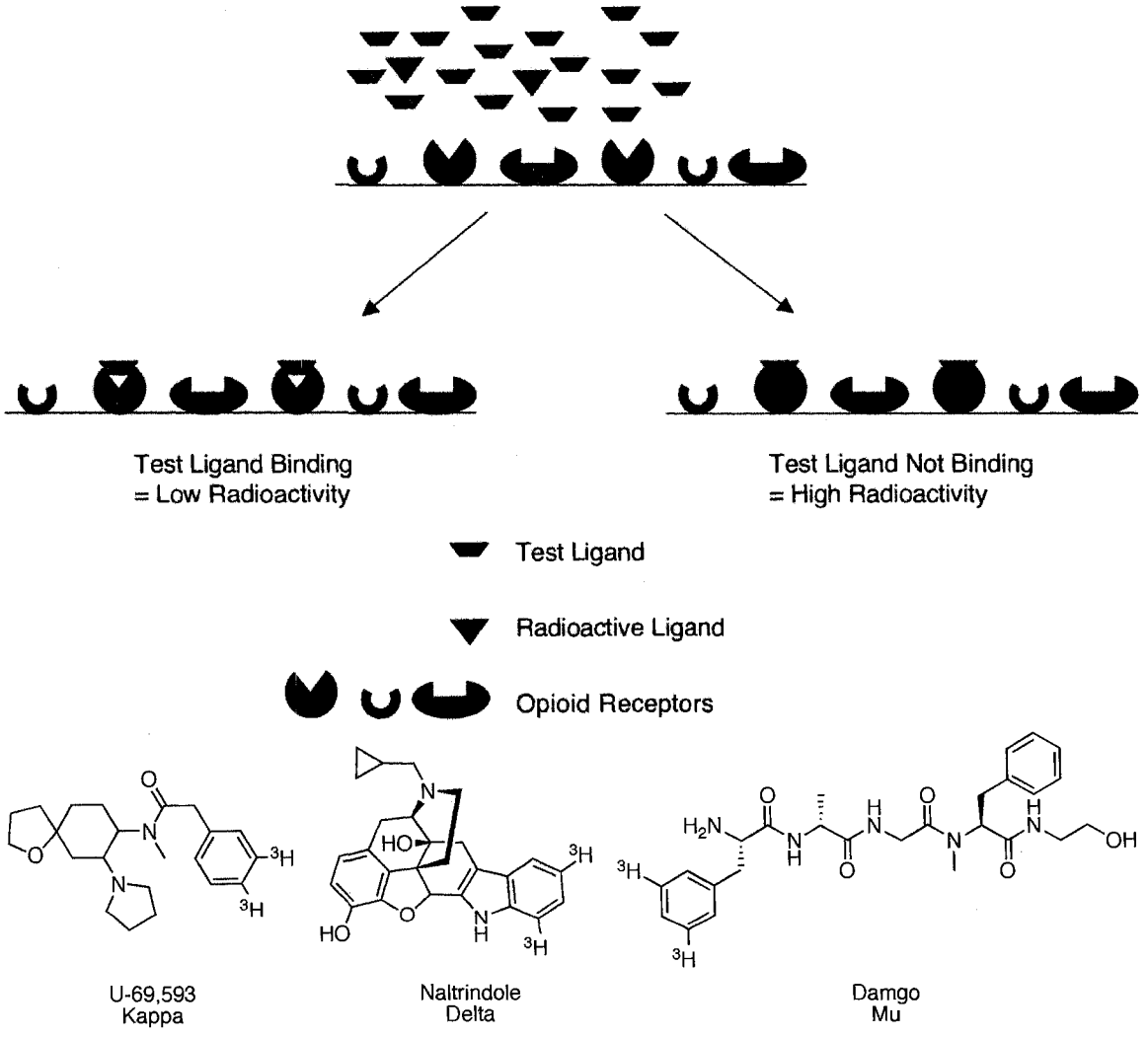

Figure 22. Overview of the assay to determine binding to opioid ligands using competitive binding with radiolabeled ligands.[105, 106]

As a positive control, d-propoxyphene (a drug known to bind with all opioid receptors[107]) is used to give the expected range able to be detected in the experiment. As the crotalphine experiment did not show any displacement of the radioactive ligand up to 100 mM, these results are not consistent with crotalphine binding to opioid receptors. Given that the peptide has been reported to display its effects for 3-5 days with a remarkable ED_{50} of 4.1 ng/kg based on interactions with opioid receptors, there was a clear discrepancy between the our data and reported values.[69] It is probable that the activity of crotalphine (**13**) is not based on direct interaction with opioid receptors.

As crotalphine is expected to be of broad general interest and remained ideal for our model studies (disulfide bond replacements, *C*-terminal cysteine synthesis methods and pyroglutamic acid substitutions) further testing was pursued in animal models in the laboratory of Professor Brad Taylor at Tulane University, New Orleans, in an attempt to repeat the reported data. Based on availability of materials and cost of testing, all tests were completed on CD1 mice instead of Wistar rats as originally reported.[69] This change was regarded as acceptable because, the response of mice and rats is generally very similar after accounting for differences in mass. The goal of the initial test was to obtain a positive result at the reported concentration.

As an aside, all of the experiments in the following section were completed following a similar timeline (Figure 23). Naive animals are initially placed onto an elevated platform (made of glass for thermal experiments and steel mesh for mechanical experiments) and are habituated for at least 30 minutes. The baseline values of the test subjects are acquired to ensure that all participants in a study display similar responsiveness to thermal or mechanical stimuli. At this point, the pain stimulus is

introduced in the identical paw to all of the study participants. After the appropriate amount of time (dependent on mode of testing), the subjects are re-habituated and tested to ensure the onset of allodynia. It is important to note that the un-injected (contralateral) paw acts as an internal control for each animal as latencies for the contralateral paw should not change as much as the injected (ipsilateral) paw. Once allodynia has been quantified, a co-worker who is blind to the experiment, matches baseline values of the animals so that representative levels of allodynia are present in each test or control group. This same co-worker then administers the drug and control groups in a manner that is blind to the researcher completing the latency measurements. This is particularly important in mice as their high activity and frequent movement can leave some measurements open to interpretation. For example, a subject may jump for no apparent reason stopping the automatic timer of a thermal test. This value needs to be rejected, as the response did not arise from the intended stimulus. This subjective nature of behavioral testing is a prime example of the requirement of blind testing, as a vested interest in the outcome of an experiment can unintentionally influence results. After drug administration, latencies are then measured at pre-determined intervals (Figure 23).

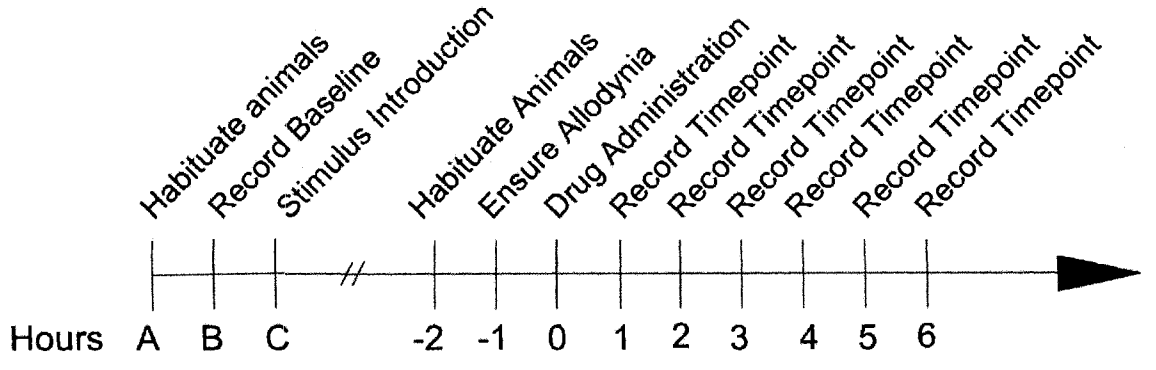

Figure 23. Timeline of biological testing. Introduction of stimulus is dependant on pain model, Carrageenin - 1 h, CFA - 3 days, SNI - 2 weeks.

Experimentally, the reported *oral* dose[69] was administered by intraperitoneal (IP) *injection* (4.1 ng/ kg). This was done simultaneously at other concentrations of one order of magnitude on either side of the reported ED_{50} in anticipation of a dose response curve. IP administration was used based on the fact that injected doses have much less variability than oral doses and require less material. This test can also give an indication about potential toxicity issues of the drug candidate. Drugs were administered into mice that had been injected with Complete Freund's Adjuvant (CFA)[66] two days prior to testing and clearly showed allodynia based on the reduction of thermal latencies in the Hargreaves model[67] (e.g. take less time to respond to thermal stimulus after CFA administration). The CFA model is a chronic pain model based on swelling at the point of adjuvant administration. The negative control for this test, as with all other tests where the drug is administered by injection, was saline. The results showed that there was no distinguishable difference from the saline control in any of the test subjects (Figure 24). Instead, it was important to note that the subjects actually appeared more stressed than animals in the control group. The thermal latencies were indistinguishable (within error limits) and some of the test group animals were observed to be writhing (visually appear to be stretching hind paws), a clear sign of stress.[66] The averaged latencies are summarized in the graph CFA-IP (Figure 24).

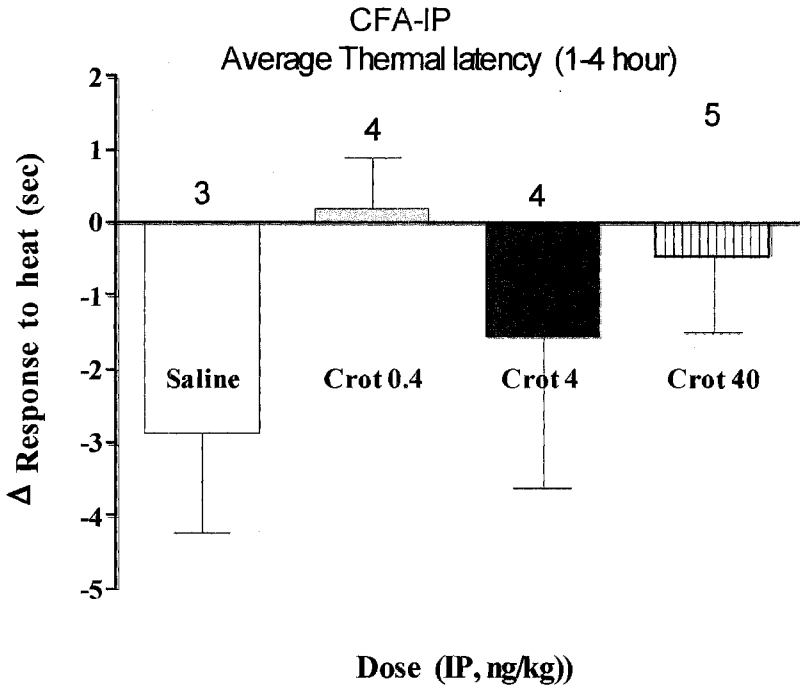

Figure 24. Comparison of crotalphine activity by interperitineal (IP) injection using CFA as the acute pain model. (Effective oral dose reported to be near 4 ng/kg). Number above bar indicates number of subjects in test group.

After this experiment, it was thought that only the oral mode of delivery was effective for biological activity. Repeating the mode of testing from the initial crotalphine (**13**) reports as close as possible, crotalphine was given by oral administration to animals that had been fasting overnight and were then assessed using the carrageenin model, monitoring mechanical allodynia[66] (von Frey hairs) (Figure 25).

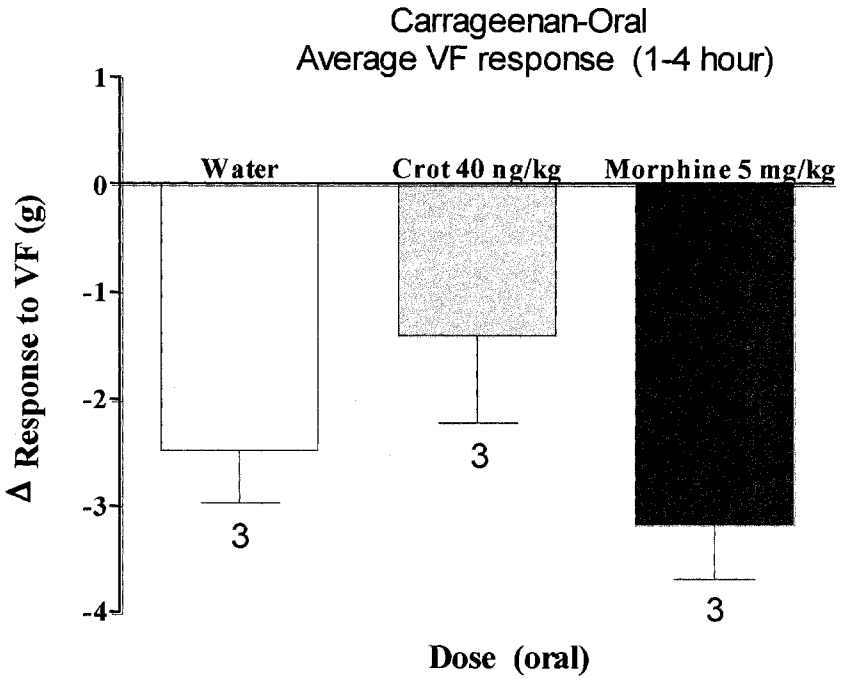

Figure 25. Test of crotalphine at 10 fold of the reported oral ED_{50} dose. Carrageenin model of acute pain, using mechanical response and oral mode of drug administration. Numbers below bars indicate number of subjects in test group.

The difference between the reported model and the test experiment is that the report uses a paw-pressure test to monitor mechanical allodynia while the test experiment employed von Frey hairs. This substitution was made based on the unavailability of a paw pressure testing instrument. The negative control for this experiment is water. Unfortunately, the selection of morphine positive control was at too low of a dose to be effective via oral administration.[108] However, the results clearly show that even at 10 fold higher dose than the reported ED_{50}, crotalphine (**13**) does not show activity that is distinguishable from the negative control group.

After incrementally increasing the crotalphine dose up to 5 mg/kg (approx 1,000,000 times the reported dose[69]) tests were completed using a range of pain models,

including complete Freund's adjuvant (CFA) and spared nerve injury (SNI) using thermal and mechanical responsiveness, respectively.[66] The SNI model provides insight into the potential use of drug candidates for the treatment of neuropathic pain as it employs the use of a dysfunctional nervous system. Crotalphine is reported to be active in the chronic constriction (CCI) model,[69] also used to test chronic pain, at 4 ng/kg by oral administration. The difference between the CCI and SNI models is that the CCI model involves loosely tying a string around a nerve while the SNI model actually cuts some nerves leaving the remaining ones in a hypersensitive state.[66] Although these testing methods are similar, our results clearly show (Figure 26) that there is very little difference between the test and negative control groups in the SNI system.

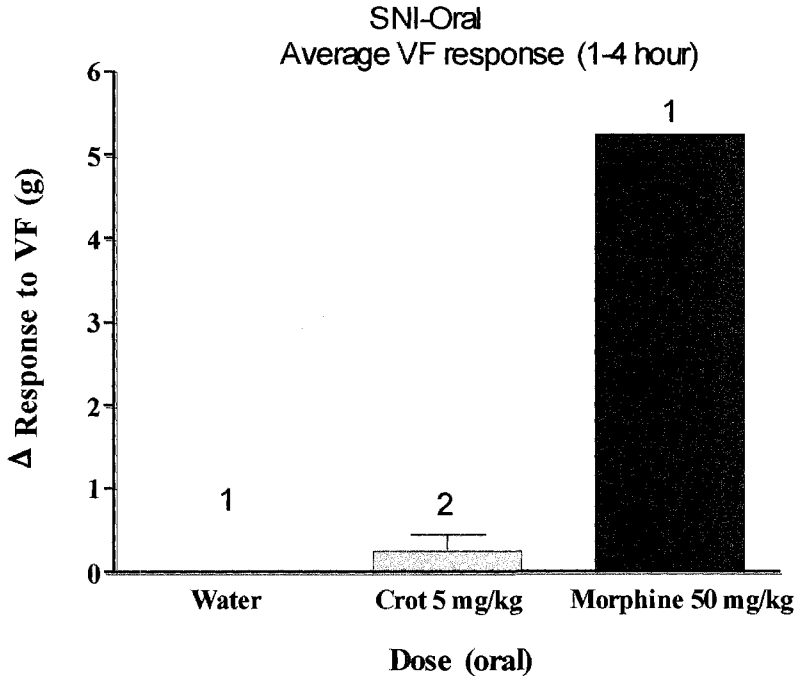

Figure 26. Test of crotalphine via oral administration in Spared Nerve Injury Model (Note concentration of crotalphine is over 1,000,000 fold the reported ED_{50} in CCI model). Numbers above bars indicate number of subjects in group.

The CFA model monitoring thermal latency provided the promising data, but again fell well short of the expected 3-5 day activity. At 24 hours after administration there was no clear effect of crotalphine. No effects of the crotalphine peptide were detected past 48 hours. As the largest responses were obtained from the CFA-thermal model, this system was used for the remaining tests.

There are a few important things to consider when interpreting the following graphs of thermal latencies. The first graph (Figure 27) is the average of timepoints for the first 4 hours subtracted from the baseline response after administration of CFA.

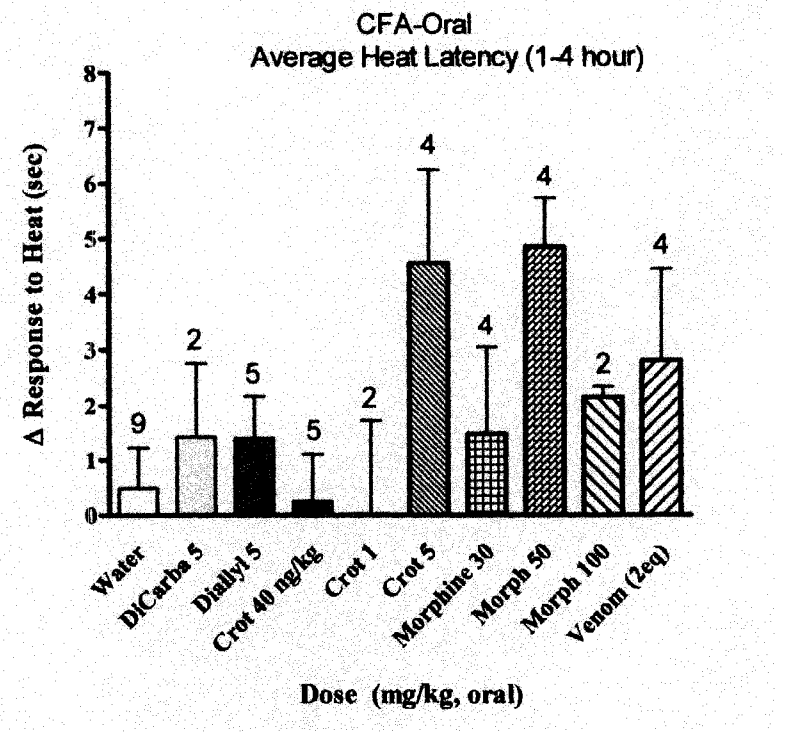

Figure 27. Average of first 4 h of testing (average minus baseline after CFA administration) displaying range of observed values and number of subjects per group.

This subtraction is used to remove the variability from subjects that do not respond equally to pain stimuli. The second plot (Figure 28) is the data averaged from the 4-5 hour timepoint (subtracting baseline) and this data clearly exhibits different trends from

the earlier plot indicating longer-term effects. It is also important to note that the group referred to as "Morph 100" (Morphine 100 mg/kg) shows a decrease in thermal latency versus the "Morph 50" (Morphine 50 mg/kg) group. This is not a real reduction but is an artifact of the experimental method. When subjects are given high doses of morphine, they respond by marching in circles until the drug wears off. During this time, they do not respond to pain stimuli, but do not remain motionless long enough to obtain a valid measure of the thermal latency. For completeness, this data has been included, but should not be interpreted as a reduction in the activity of morphine at high doses. The columns listed as "Dicarba" and "Diallyl" are the synthetically prepared crotalphine analogues **81** and **78**, respectively.

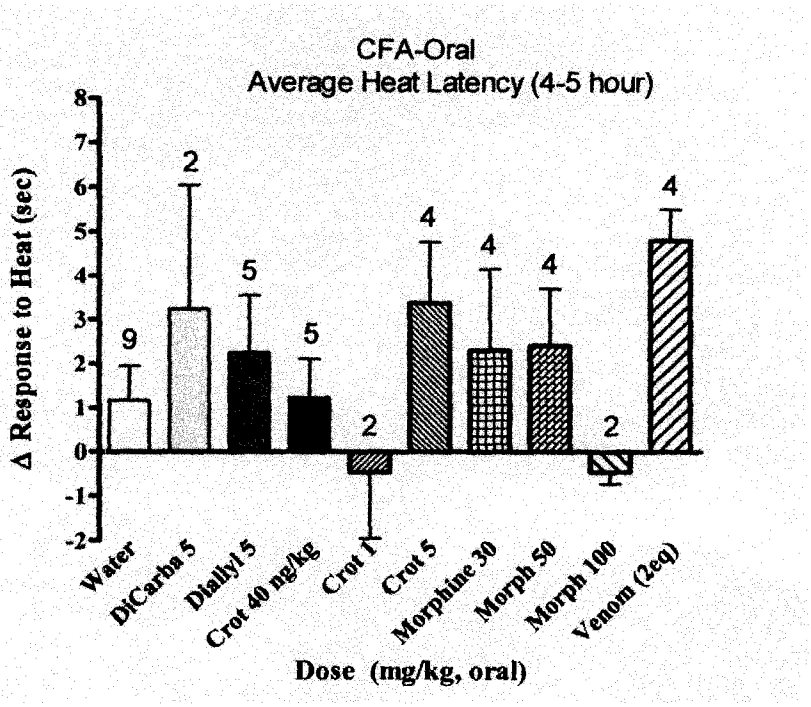

Figure 28. Average of hours 4-5 of testing (average minus baseline after CFA administration) displaying range of observed values and number of subjects per group.

There are a few interesting conclusions that can be drawn from this data. The venom extract (prepared by removal of high molecular weight compounds using a 5000 MWCO centrifugal spin filter) does show activity in both time frames and appears to be increasing relative to both morphine and water controls by the 4-5 hour timepoint. It is very important to also note, that even in the cases of the natural venom extract **77**, no activity remains (relative to water) after 24 hours. This implies that either the natural venom does not contain crotalphine (**13**) (unlikely based on supplier assurance that it has been unmodified from the natural source) or that there are no components in the venom extract, with a molecular weight less than 5000 Da, that display activity for periods greater than 24 hours in the mouse model. The possibility of variation between snakes was reduced as the sample was prepared by combining 600 mg of lyophilized venom, the equivalent of 30 rattlesnakes. There is no activity in the synthetic crotalphine (**13**) sample at 10 times (40 ng/kg), and even 500,000 times (1 mg/kg) the reported ED_{50} but there does appear to be an effect at doses of 5 mg/kg.

Although we are currently unable to reproduce the data given in the initial report,[69] the fact that a peptide structure is orally active at all is interesting from the standpoint of mode of action. To ensure that no errors had been made in obtaining **77** or producing crotalphine **13**, samples were exchanged with the group of Dr. Yara Cury at the Butantan Institute in Brazil. Reports from the laboratory of Dr. Cury reported that the peptide prepared in our group had identical biological activity to the samples used in their studies. These troubling results indicate that an effect has been overlooked, potentially by the mode of testing.

At the time of preparation of this document, the synthetically prepared crotalphine sample **13** and a sample prepared on behalf of the Brazilian research group of Dr. Yara Cury, have been tested using the initially reported methods[69] in the laboratory of Prof. Brad Taylor. Using male Wistar rats and the paw pressure test[66] to measure mechanical allodynia, preliminary results with the crotalphine peptides indicate that they are equally active at the reported values, contrary to the results described in the previous tests involving CD1 mice. All of this combined data produces many new interesting questions. It is possible that the peptide is not active in CD-1 mice but is active in rats and that the Hargreaves and von Frey methods are unable to detect the induced analgesic effect of crotalphine (**13**). Although this is academically interesting, it is problematic for further development of crotalphine as a drug candidate.

The observation of writhing in the mouse subjects suggests that injection of the crotalphine containing solution is producing stress. According to our skilled collaborators at the Tulane University, this suggests that crotalphine may be inducing production of natural opiates in the body, producing an effect referred to as stress induced analgesia.[109] Stresses to the body are known to cause natural bodily production of endorphins that interact with opioid receptors.[109] This may explain the observation that the opioid receptor antagonists inhibited the analgesic effect of the venom in animal models.[69] Another important factor that must be considered is the possibility that the peptide is interfering with the ability of the animal to move (e.g. temporary paralysis or sedation). These factors could potentially be examined by using a rota-rod apparatus to ensure the animal is able to function at a normal level and that the increase in latency is not due to the inability to move. This simple apparatus is essentially an animal treadmill

in which the subject will be unable to remain on top of the apparatus if its motor skills are impaired. There is no reason to believe that the compound does cause temporary paralysis or sedation, but as these testing methods are indirectly measuring drug effects by animal movement, similar results would be observed with these conditions. With respect to chemistry, the most important question that arises out of this project is whether crotalphine (**13**) acts via a receptor mediated process or via a non-selective mode. If this is a receptor mediated process, then the testing of analogues may produce results that are useful for SAR studies and direct synthesis toward new analogues. If this is not a receptor mediated process, it is possible that the analogues may not contribute to furthering understanding of the crotalphine mode of action.

5.2 Summary and Future Work – Analgesic Peptides

In summary, the crotalphine project has been a brief tour through modern pain pharmacology. After the synthesis of analogues to be used for SAR studies of the parent structure, tests on opioid receptors and animal models indicate that the mechanism of action is likely not via opioid receptors as initially reported. Once it has been established that crotalphine (**13**) is active in a standard reproducible pain model, there are some new directions for this project. The first approach is to complete the SAR study with prepared analogues **78-83**. Results of this testing will give some insight into the requirement for the *C*-terminal disulfide bond and the *N*-terminal pyroglutamic acid. Combined with the previous projects described in this thesis, this peptide remains an interesting model compound to be produced using any new synthetic methods for incorporation of *C*-terminal cysteine residues while the analogues may demonstrate the generality of

disulfide replacement with carbon-carbon double bonds. If crotalphine (**13**) does show promising results as an analgesic, it may prove to be a useful target to be produced by biological expression.[110] Ideally, activity in the *N*-terminal proline analogues **82** or **83** would allow preparation of the peptide by either direct expression or by simple acylation, respectively. In the event that only the parent peptide retains appropriate activity, another alternative route to access crotalphine is via semi-synthesis (Scheme 16). As crotalphine is composed of standard amino acids except for the *N*-terminal residue, residues 2-14 could conceptually be prepared by expression[110] followed by coupling of an appropriately activated[111] pyroglutamic moiety. This proposed scheme benefits tremendously from the unusual lack of basic residues in the sequence. As the *N*-terminus is the only basic site on crotalphine 2-14, appropriate adjustment of the pH should render the free amine to be the most reactive position on the molecule and allow for selective reactivity with the appropriate coupling partner.

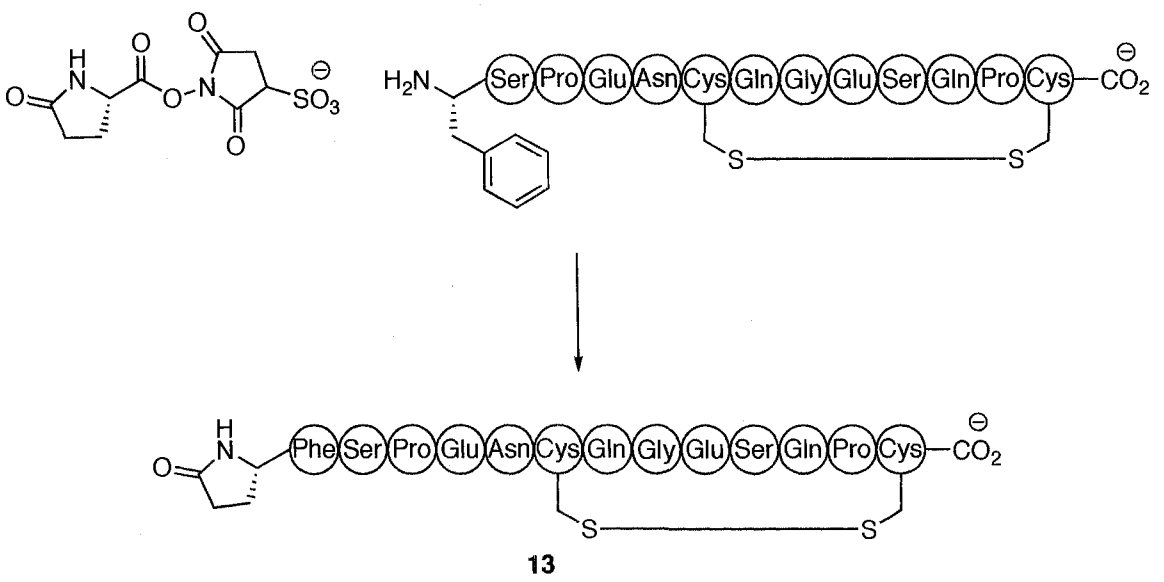

Scheme 16. Potential method of preparing crotalphine (13) by semi-synthesis onto a biologically produced precursor.

6. CONCLUSIONS AND SUMMARY

This thesis has demonstrated the preparation and biological activity of three main groups of peptides. The first study on antimicrobial peptides included the successful synthesis, purification and testing of eleven peptides ranging in length from 37-44 amino acids. It was observed that the incorporation of pseudoproline dipeptides had a significant effect in obtaining the desired products due to a decrease in on-resin aggregation. New data on the preparation of [9,14]-dicarba-LeuA (**22**) also verified the hypothesis that disulfide bonds can be replaced by carbon-carbon double bonds with minimal reduction in activity. Insight has also been gained into the structure activity relationships in type IIa bacteriocins. Aside from the carbon-carbon double bond, it was found that acyclic analogues of LeuA with cysteine replaced by hydrophobic resides such as allyl glycine (**23**), norvaline (**25**) or phenylalanine (**26**) retained similar biological activity to the parent LeuA (**1**). Although type IIa bacteriocins are highly conserved, this trend was not observed in the related peptide Ped (**2**). This presents some interesting implications for the LeuA (**1**) peptide as this implies that there is an inherent difference between these two related peptides, which is surprising as they differ by only seven residues of the 20 *N*-terminal amino acids. Evidence suggests that the intra ring residues 10-13 contribute to this unexpected result, potentially via a turn inducing sequence that helps the peptide assume the required conformation in the receptor active site. These results support the idea that, although the highly conserved ring portion of the type IIa bacteriocins is important for biological activity, the 3-dimensional structure and sequence of the entire molecule is responsible for its potent biological activity.

The method of interaction between bacteriocin induction peptides and their receptors was also investigated. Through the manual preparation and purification of 14 induction peptides and fragments, it was demonstrated that the *C*-terminal portion of these induction peptides interacts non-specifically with the receptor while the *N*-terminal portion facilitates the affinity and selectivity of this interaction. Three peptide fragments homologous to CbaX (16-24) (**38**) have been prepared indicating that substitution of phenylalanines 18 and 21 with benzoylphenylalanine is tolerated by the receptor while substitution at Phe 20 appears to be the least acceptable. Based on this data, two full length peptides were prepared that contain benzoyl-phenylalanine at positions 18 or 21. It is anticipated that the expression and purification of the histidine protein kinase (the proposed induction peptide receptor) will allow for binding studies with either the natural induction peptides or those containing the photoaffinity label to identify the receptor active site. In the course of preparing the CbaX induction peptides, the problem of preparing *C*-terminal cysteine containing peptides was observed. In an effort to solve this problem, the preparation of a side-chain linked, orthoester-protected cysteine was attempted. Unfortunately, the direct approach analogous to known serine methodology was unsuccessful, but an indirect approach, whereby the sulfur is introduced after orthoester formation was able to produce a protected, orthoester-containing cysteine derivative. It is expected that future modification of this indirect method using alternative protecting groups will yield the desired precursor.

The final project involved the preparation and testing of an analgesic peptide named crotalphine (**13**), derived from the South American rattlesnake *Crotalus durissus terrificus*, and six analogues in an attempt to produce an active analogue. This involved

not only the peptide synthesis and purification but also the biological testing of these peptides. Although the initial results from tests in mice did not appear promising, new studies in rat models and a different mode of testing have led to a re-examination of the peptide. Once the activity of the parent compound has been verified, the analogues are prepared and ready for further testing to explore any potential receptor mediated processes that may exist.

There are many exciting new developments in peptide chemistry. The results reported in this thesis display the tremendous variety of applications for peptide structures and exhibit some of the strategies that can be generally applied to peptide synthesis. Future work will determine the scope of the concepts that have been discussed in this thesis, including the activity of the acyclic LeuA analogues, the interactions responsible for bacteriocin induction, the applications of orthoesters in peptide synthesis, and elucidation of the crotalphine mode of action. Regardless of future results, this thesis has demonstrated that peptide chemistry crosses many of the conventional divisions between chemistry and biology and that the ability to succinctly prepare complex peptide structures can be utilized in a diverse array of applications.

7. EXPERIMENTAL PROCEDURES

7.1 General Experimental Methods

7.1.1 Reagents, solvents and solutions

All chemicals and solvents were purchased from the Aldrich Chemical Company Inc. (Madison, WI), Fisher Scientific Ltd (Ottawa, ON) or Caledon (Georgetown, ON) and used without further purification unless otherwise stated. Dichloromethane was distilled over CaH_2 and then degassed with argon. All protected amino acids, derivatives and solid phase peptide synthesis (SPPS) solid supports were purchased from Calbiochem-Novabiochem Corporation (San Diego CA) in > 98% purity and were used as received. Water, for RP-HPLC, was obtained from a Milli-Q reagent water system. All other solvents were of reagent or HPLC grade and used without further purification.

7.1.2 Purification techniques

HPLC purification was completed using Gilson, Varian, Beckman or Rainin HPLC insturments. Purification methods are outlined in the Synthesis and Characterization Section 7.2.1. Preparatory scale purifications were completed with Waters Prep LC modules using radial compression reverse phase columns using μ-Bondpak, Delta-Pak or Prep-Pak C18 columns (15 μm, 100 Å, 25 x 100 mm) and matching guard columns (25 x 10 mm). Analytical purifications were completed using Varian HPLC Microsorb MV columns (250 X 4.6 mm, 100-5, C_8 or C_{18})

The Gilson HPLC instrument is equipped with a model 322 pump, manual injection system and a single wavelength Gilson 151/152 UV/VIS detector. It is

equipped with Unipoint System software and was used to record and analyze all data from the Gilson instrument.

The Varian HPLC's are two identical instruments equipped with a model 210 pump and dual wavelength detectors set to observe at 220 and 280 nm for routine peptide purifications. The instruments differed only in the size of the pump head. For analytical purifications or analysis, the analytical Varian with 10 mL pump heads was used. For preparatory scale purifications, the preparatory Varian equipped with 25 mL pump heads was used.

The Beckman-Coulter System Gold HPLC instrument is equipped with programmable solvent module 126 pumps using 32 Karat software.

The Rainin HPLC instrument uses Varian software and is equipped with an external argon lamp detector (Dynamax pumpheads Model SD-200, 50 mL pumpheads and Dynamax-Rainin Absorbance Detector UV-1).

Flash column chromatography was completed according to the method outlined by Still *et al.*[112] using silica gel grade 60 (Rose Scientific 230-400 mesh). TLC was performed on glass-backed plates (2 x 5 cm) pre-coated with silica gel (Merck, Silica Gel 60 F_{254}). Visualization was achieved using UV light, iodine, or one of the following dipping solutions:

Ninhydrin: 1.5 g ninhydrin, 100 mL *n*-butanol, 3 mL acetic acid

Permanganate: 1.5 g $KMnO_4$, 10 g K_2CO_3, 1.25 mL 10 % NaOH, 200 mL H_2O

Cerium Ammonium Molybdate: 0.5 g $Ce(NH_4)_2(NO_3)_6$, $(NH_4)_6Mo_7O_{24}$-4 H_2O and 28 mL H_2SO_4.

7.1.3 Instrumentation for compound characterization

NMR spectra were recorded on a Varian Inova 600, Inova 500, Inova 400, Inova 300, or Unity 500 spectrometers. For all spectra, δ values were referenced to the corresponding deuterated solvent: H_2O (^1H- 4.79 ppm), CH_2Cl_2 (^1H- 5.32 ppm, ^{13}C- 53.1), $CHCl_3$ (^1H- 7.24 ppm, ^{13}C- 77.0 ppm), DMF (^1H- 8.03 ppm, ^{13}C- 29.8 ppm, 34.9 ppm) or DMSO (^1H- 3.53 ppm, 39.5 ppm). Reported splitting patterns are abbreviated as d = doublet, t = triplet, q = quartet, m = multiplet and ap. = apparent. Dr. Ryan McKay at NANUC performed experiments and assisted in interpretation of spectra acquired at 800 MHz.

All MALDI-TOF mass spectral data was performed on a Perspective Biosystems Voyager™ Elite MALDI-TOF with delayed extraction in reflectron mode. A two layer method using 3,5-dimethoxy-4-hydroxycinnamic acid (sinapinic acid, SA; Sigma Aldrich) as the matrix for all MALDI-MS samples. A typical sample preparation is as follows: solutions containing the sample peptides (1 μL directly from HPLC fraction) are mixed in a 1:1 ratio (v/v) with a stock solution of sinapinic acid (10 mg/mL) in 60% acetonitrile containing 0.1% TFA before depositing them on the plate. To prepare the sample plate, sinapinic acid layer one (0.7 μL; 4 mg/mL SA in a 1:1 acetone: methanol) is pipetted onto a gold target plate. The solvent is allowed to evaporate, leaving a thin layer of sinapinic acid on the surface of the plate. The sample-matrix solution (Solution two, 0.4 μL) is then spotted onto the previous layer and allowed to dry. Mass spectra are then recorded using a single-stage reflectron MALDI-TOF mass spectrometer equipped with delayed extraction technology (Voyager Elite; Applied BioSystems, Foster City, CA). Spectra were generally acquired in positive ion reflectron mode with a nitrogen

laser (λ = 337 nm) for desorption/ionization, and an acceleration voltage of 20 kV (crotalphine peptides were found to produce better results in negative mode). Spectra consist of compiled data from 100 laser shots. Insulin chain B (Sigma-Aldrich) and angiotensin (Sigma-Aldrich) were used as external mass calibrants.

7.1.4 General method for loading the first amino acid using hydroxymethyl resins (Wang or Novasyn TGA resins)

The resin to be loaded is placed into the reaction vessel, washed with DMF and DCM and is left to swell in DCM during preparation of the symmetrical anhydride.[113] The Fmoc amino acid (10 eq. relative to resin) is dissolved in a minimum amount of dry DCM and cooled to 0 °C under argon. Diisopropylcarbodiimide (5 eq. relative to resin) is then added, and the solution is left to stir. After 20 min, the flask is warmed to room temperature and DCM is removed *in vacuo*. The reaction vessel is then drained and rinsed again with DCM. The remaining residue is then dissolved in a minimum amount of DMF and added to the reaction vessel. DMAP (0.1 eq. relative to resin loading) is then added to the reaction mixture and left under argon agitation for 2 h. The vessel is then drained, washed with DMF and then reacted with 20% acetic anhydride in DMF (15 min). After capping, the resin is washed repeatedly (5-6 times) with DMF and DCM before use in manual or automated synthesis.

7.1.5 General method for loading the first amino acid using trityl resins (2-ClTrt or Novasyn TGT chloride resins)

The resin to be loaded is placed into the reaction vessel, washed with DMF and DCM and is left to swell in DCM for at least 1 h.[114] The amino acid (2 eq. relative to

resin) and DIPEA (4 eq. relative to resin) are dissolved in a minimum amount of dry DCM and added to the reaction vessel containing the resin. The resin is then left to agitate for 2 h and the solvent level is maintained to allow for freely moving resin throughout the reaction vessel. After 2 h, the vessel is drained and washed with DCM and then with a solution of 85% DCM: 10% MeOH: 5% DIPEA (3 x 5 min). The resin is then sequentially washed with DCM, DMF, and again with DCM before being used in manual or automated synthesis.

7.1.6 General method for manual solid phase peptide synthesis (SPPS)

All amino acids for manual synthesis were coupled using the appropriate Fmoc protected amino acid (2 eq. relative to resin), benzotriazole-1-yl-oxy-tris-pyrrolidino-phosphonium hexafluorophosphate (PyBOP®) as the activating agent (1.95 eq.) and *N*-methylmorpholine (5 eq.) in DMF (10 mL). The solution was pre-activated for 5 min and then added to the pre-swelled resin. The mixture was then reacted for 2 h. The completion of couplings was monitored by a negative result from the Kaiser test,[115] followed by end capping with a solution of 20% acetic anhydride in DMF for 15 min. If the Kaiser test yielded a positive result, the coupling step was repeated. Removal of the Fmoc group was completed using a solution of 20% piperidine in DMF for 5 min. Completion of deprotection was monitored by disappearance of the absorbance at 301 nm (dibenzofulvene-piperidine adduct) (See Figure 16 and Figure 17 in Section 4.1 for examples of typical spectra). The following side chain protecting groups were employed for synthesis: Fmoc-Cys(Trt)-OPfp , Fmoc-Asp(O-*t*Bu)-OH, Fmoc-Glu(O-*t*Bu)-OH, Fmoc-His(Trt)-OH, Fmoc-Lys(Boc)-OH, Fmoc-Asn(Trt)-OH, Fmoc-Gln(Trt)-OH, Fmoc-Arg(Pmc)-OH, Fmoc-Ser(O-*t*Bu)-OH, Fmoc-Thr(O-*t*Bu)-OH, Fmoc-Trp(Boc)-

OH, and Fmoc-Tyr(O-*t*Bu)-OH. Pseudo-prolines Fmoc-Ala-Thr($\psi^{Me,\ Me}$pro)-OH, Fmoc-Phe-Ser($\psi^{Me,\ Me}$pro)-OH and Fmoc-Val-Thr($\psi^{Me,\ Me}$pro)-OH, were incorporated in the sequence to disrupt peptide aggregation. Peptides were cleaved using standard conditions of 95% TFA: 2.5% TIPS-H: 2.5% H_2O or 94% TFA: 2.5% EDT: 2.5% H_2O: 1% TIPS-H. Peptides were then filtered through a plug of glass wool and the solvent was removed *in vacuo.* The crude peptide was then repeatedly triturated with cold ether until only a white solid remained. The remaining white solid was then dried under vacuum.

7.1.7 General method for automated solid phase peptide synthesis (SPPS) using ABI 433A

Automated synthesis was completed on an ABI 433A instrument (Applied Biosystems) with UV monitoring capability (Perkin Elmer) detecting at 301 nm using standard *Fastmoc*™ methodology from Applied Biosystems. This method employs the coupling agents 2-(1H-benzotriazole-1-yl)-1,1,3,3- tetramethyl uronium hexaflorophosphate (HBTU) and N-hydroxybenzotriazole (HOBt) to preactivate the corresponding Fmoc protected amino acid for 2.1 minutes. The pre-activated solution is then transferred to the reaction vessel and allowed to react. After completion of coupling, end capping is accomplished using a solution of acetic anhydride, HOBt and diisopropylethylamine (DIPEA). Removal of the Fmoc group is completed using piperidine in NMP and monitored by the change in absorption at 301 nm (difference of less than 3.5% from tallest peak). The standard cycle for each residue is approximately 50 minutes but can be extended by a feedback mechanism if deprotection of the previous residue is problematic as determined by UV deprotections. For syntheses using less than 0.1 mmol of resin, the 0.1 mmol *Fastmoc* protocol was modified from the standard 3.5%,

by adjusting the 301 nm feedback loop by the percentage difference from 0.1 mmol to account for the reduction in initial value of deprotection (e.g. 0.05 mmol of resin used a cut-off of 7%). The following side chain protecting groups were employed for the synthesis: Fmoc-Cys(Trt)-OH , Fmoc-Asp(O-*t*Bu)-OH, Fmoc-Glu(O-*t*Bu)-OH, Fmoc-His(Trt)-OH, Fmoc-Lys(Boc)-OH, Fmoc-Asn(Trt)-OH, Fmoc-Gln(Trt)-OH, Fmoc-Arg(Pmc)-OH, Fmoc-Ser(O-*t*Bu)-OH, Fmoc-Thr(O-*t*Bu)-OH, Fmoc-Trp(Boc)-OH, and Fmoc-Tyr(O-*t*Bu)-OH. Pseudo-prolines Fmoc-Ala-Thr($\psi^{Me,\ Me}$pro)-OH, Fmoc-Phe-Ser($\psi^{Me,\ Me}$pro)-OH and Fmoc-Val-Thr($\psi^{Me,\ Me}$pro)-OH, were incorporated in the sequence when necessary to disrupt peptide aggregation. Peptides were cleaved using standard conditions of 95% TFA: 2.5% TIPS-H: 2.5% H_2O or 94% TFA: 2.5% EDT: 2.5% H_2O: 1% TIPS-H. Peptides were then filtered through a plug of glass wool and solvent was removed *in vacuo.* The crude peptide was then repeatedly triturated with cold ether until only a white solid remained. The remaining white solid was then dried under vacuum.

7.1.8 General procedure for the ring closing metathesis (RCM) of peptides

After installation of both of the prerequisite allyl glycine residues, the resin is washed thoroughly with DMF, DCM and MeOH, and dried under a stream of argon before being placed into a dessicator. After determining the amount of resin, a portion was removed for use as a cyclization test substrate. This resin was then re-swelled in DMF and DCM. If required, the resin was washed with 0.8 M LiCl solution (3 x 3 min). The resin was then rinsed once with DMF and re-suspended in DCM. The resin was then bubbled with argon for at least 20 min in an effort to degas the solvent, followed by addition of 20 mol% Grubbs second generation catalyst.[72] The reaction vessel was then

wrapped with heat tape attached to a Variac, a thermocouple, and was fitted with a reflux condenser. The reaction was then left to proceed for at least 8 h at elevated temperature (with argon bubbling through the solution[116]) followed by a test cleavage of the peptide for MALDI-TOF analysis. If optimization was required, catalyst loading was initially increased followed by changing of the solvent and respective temperature.

7.1.9 Assay for testing antimicrobial peptides (spot-on-lawn[117])

Spot-on-Lawn Assay- APT plates and broths were prepared using the following method.

Plates: 11.5 g APT, 3.75 g agar, 250 mL milli-Q water into 500 mL Erlenmeyer flask

Soft Agar: 5.775g APT, 0.938 g agar, 125 mL milli-Q water into 250 mL Erlenmeyer flask. The solution is then heated to a gentle boil with a hot plate and then transferred to culture tubes in 8 mL aliquots.

Broth: 5.775 g APT, 125 mL milli-Q water into 250 mL Erlenmeyer flask. The solution is then divided into culture tubes as 5 mL aliquots.

The solutions prepared above are then sterilized using an autoclave. The soft agar and broth tubes are allowed to cool to room temperature on a bench while the hot solution for the plates is placed into an oven at 50 °C. Once the temperature of the plate-agar solution has cooled to 50 °C, the contents are distributed into sterile disposable plates inside a biological containment hood. After the plates have solidified for 30 min, the plate covers are replaced and the plates are stored inside a Petri dish bag and stored inverted at 4 °C.

Sensitive indicator organisms used in the bacteriocin studies were *Listeria monocytogenes* EGDe (37 °C), *Carnobacterium maltaromaticum* UAL 26 (25 °C) and *Carnobacterium divergens* LV13 (25 °C). The LeuA (**1**) producing organism, *Leuconostoc gelidum* UAL 187 (grown at 25 °C) was used as a control to ensure peptides

were inactive against the producing organism. Compounds to be tested by the spot-on-lawn technique are prepared in a dilution series using sterile milli-Q water. Each sample is then spotted on the plate (10 μL, 9 spots per plate) and allowed to dry for at least 30 minutes. As a positive control, 1 mL of the supernatant from a full grown solution of UAL 187 was boiled for 5 min and then centrifuged (1 min, 13000 rpm). A sample of the boiled supernatant (10 μL) was then spotted onto the plates. While the sample spots are drying, previously prepared soft agar tubes are placed into a solution of boiling water until the solid melts to a free flowing liquid. The soft agar tubes are then removed from the hot water bath and allowed to cool to 40 °C where they are then inoculated with the indicator organism (2% v/v inoculum from full grown culture). Values were recorded as last clearly visible inhibition zone.

7.1.10 Assay for testing antimicrobial peptides (96 well plate)

All peptide concentrations for biological tests are initially approximated by mass and then verified or corrected using the UV molar absoptivity.[118] The assays were prepared in a 96 well plate and all indicator organisms were grown overnight before testing. Stock cultures were diluted with fresh APT broth such that A_{590} (optical density) was 0.02. The dilution series of the test peptides were prepared in APT broth in a two fold dilution so that each appropriate well contained 75 μL of fresh APT broth and the desired peptide concentration. All unused wells (and the outside two rows) were filled with 150 μL of sterile milli-Q water. Finally, 75 μL of the 0.02 OD indicator organism solution was added to each well and allowed to grow for 16 hours at 25 °C with the plate lid in place to reduce evaporation. After the elapsed time, the sample was placed into a plate reader to record the end point growth values.

7.1.11 Testing of induction peptides for pheromone activity

Fully grown cultures of *Carnobacterium maltaromaticum* LV17A and *Enterococcus faecium* CTC492 were diluted by 10^6 in 5 mL APT broth to lose bacteriocin production and then allowed to re-grow until turbid.[119] Peptides to be tested for pheromone activity were serially diluted from 10^{-5} M to 10^{-13} M in 2.5 mL APT broth. A 1% inoculum of the non-bacteriocin producing culture *C. maltaromaticum* LV17A or *E. faecium* CTC492 was then added to the broth containing the synthetic peptides and allowed to grow for 24 h. No induction peptides were added to the negative controls. The supernatant of the cultures were then tested for bacteriocin activity using the spot-on-lawn assay using *Carnobacterium maltaromaticum* LV17C or *Lactobacillus sakei* DSM20017 as the indicator organism (for carnobacteriocin A or enterocin A and B, respectively). Assignment of AU values was determined according to literature method.[120]

7.1.12 Testing for antagonistic activity in induction peptides

Peptides to be tested for inhibition of pheromone activity of CbaX or EntF were added to 2.5 mL of APT broth in concentrations from 10^{-5} M to 10^{-7} M.[119] The broth was then inoculated with 1% v/v of a non-bacteriocin producing culture of *C. maltaromaticum* LV17A or *E. faecium* CTC492 and $5x10^{-11}$ M CbaX or EntF, respectively. Assignment of AU values was determined according to literature method.[120]

7.1.13 Testing analgesic properties of peptides

7.1.13.1 Guinea Pig Brain Tissue Models

The following model was used according to standard procedure in the laboratory of Prof. Alan Hudson in the Department of Pharmacology at the University of Alberta.[105, 106]

Tissue preparation- Guinea pig brains (Rockland Immunochemicals, typical scale 30 g, approx. 8 brains) were suspended in a solution of Tris-HCl (50 mM, pH 7.4) with glucose (11 g / 100 mL). The mixture was cooled to 4 °C and then blended with a polytron at 5000 rpm. The solution was divided into equal portions and transferred to centrifuge tubes before being spun at 1500 rpm (1000 *g*) for 10 min. The supernatant was transferred to a clean flask and the remaining solid was disposed. The supernatant was returned to centrifuge tubes and spun on the centrfuge at 16500 rpm (31000 *g*) for 20 min. The remaining supernatant was disposed and the remaining pellets were collected and re-suspended in Tris-HCl (50 mM, pH 7.4, without glucose), vortexed, and centrifuged at 16500 rpm (31000 *g*) for 20 min. The supernatant was again removed and the pellets were stored at -80 °C until required.

Opioid Ligand Displacement Assay - The previously prepared pellets were suspended in a solution of Tris-HCl buffer (50 mM, pH 7.4) and vortexed. The suspension was then centrifuged at 16500 rpm (31000 *g*) for 20 min. This re-suspension, wash cycle was then repeated. (Extensive washing is required to remove any natural opiates that are present in the tissue and would lead to interference in the assay.) After washing, the pellet was placed in a fresh Tris-HCl buffer solution and placed into a homogenizer to remove any clumps of tissue. The assay is then prepared in a large series of test tubes so that each test reaction may be done in triplicate. The test ligand (50 μL of each sample in log dilution series) is first added to each corresponding tube, followed by the radioactive opioid binding ligand (50 μl of 10 nM solution). Radioligands (Perkin Elmer) used were [^{3}H]-DAMGO (specific mu opioid receptor ligand), [^{3}H]-Naltrindole (specific delta opioid receptor ligand), and [^{3}H]-U69,593 (specific kappa opioid receptor

ligand) at 1 μCi/μL. Finally, the brain tissue (400 μL) is added to the mixtures and incubated for 1 h at room temperature. D-Propoxyphene-HCl (10 μM) was used as a positive control and a blank buffer solution was used as the negative control to determine the effective testing window of the assay. After 1 h, the tubes were filtered using a cell harvester and a filter (presoaked in 0.5% aqueous polyethylene amine) and rinsed twice with the Tris-HCl buffer. The respective filter from each experiment was placed into a scintillation vial with 10 mL of scintillation fluid and counted for 3 minutes per sample.

7.1.13.2 Live Animal Models

All animals were cared for in accordance to the guidelines set forth by the National Institutes of Health regarding the proper treatment and use of laboratory animals. All experiments involving animals were approved by the Tulane University Animal Care and Use committees. The biological testing of crotalphine was tested on CD1 mice monitoring either thermal or mechanical allodynia. The thermal model is based on the Hargreaves[67] method using an apparatus obtained from Ugo Bassile. The animals were acclimated in plexiglass tubes on top of the glass table for 20-40 minutes. After habituation, the manually controlled mechanism beneath the animals is selectively activated beneath the subjects paw until there is a movement response detected by the instrument. A motion detector contained within the UV heating mechanism detects the movement and heating of the apparatus immediately stops. Heating was ceased after 20 seconds without response to ensure that tissue damage was avoided. A variety of pain models were employed including CFA, carrageenin and SNI. The subjects were administered with the pain stimulus and drugs with the qualified assistance of members

from the laboratory of Prof. Brad Taylor at the University of Tulane. This also ensured that the monitoring of latencies was blind with respect to drug administration.

7.2 Synthesis and Characterization of Compounds

7.2.1 HPLC purification methods

All peptides were purified until represented as a single peak in an HPLC chromatogram after repeated injections. Purification of LeuA (**1**) or Ped (**2**) analogues was completed using on the Gilson HPLC using one of the following HPLC methods. After each run, the method was ramped to 90% MeCN for 5 min and then re-equilibrated at the starting value for 5 min.

System A: 0-5 min - 20% MeCN/ 80% H_2O (0.1% TFA)

5-25 min - 20-50% MeCN over 20 min

Flow rate: 10 mL/min.

System B: 0-5 min - 10% MeCN / 90% H_2O (0.1 % TFA)

5-25 min - ramp to 90% MeCN

Flow rate: 15 mL/min.

System C: 0-5 min 25% MeCN/ 75% H_2O (0.1% TFA)

5-35 min - 25-95% MeCN

Flow rate: 10 mL/min.

System D: 0-5 min - 20% MeCN/ 80% H_2O (0.1% TFA)

5-35 min - 20-40% MeCN

Flow rate: 10 mL/min.

System E: 0-5 min - 10% MeCN/ 90% H_2O (0.1% TFA)

5-50 min - 10-40% MeCN

Flow rate: 10 mL/min.

Induction Peptides

The induction peptides PisN (**8**), CbaX (**9**), EntF (**10**) and fragments of these compounds were purified using the Gilson or Beckman HPLC instruments using one of the following methods:

System F: 0-5 min: 20% MeCN/ 80% H_2O (0.1% TFA)

5-25 min: 20%- 50% MeCN ramp

Flow rate: 10 mL/min.

System G: 0-5 min: 20% MeCN/ 80% H_2O (0.1% TFA)

5-55 min: 20%- 90% MeCN ramp

55-60 min: 90% MeCN/ 10% H_2O (0.1% TFA)

60-61 min: 90%- 20% MeCN ramp

61-65 min: 20% MeCN/ 80% H_2O (0.1% TFA)

Flow rate: 10 mL/min.

System H: 0-5 min: 20% MeCN/ 80% H_2O (0.1% TFA)

5-30 min: 20%- 50% MeCN ramp

30-35 min: 50%- 90% MeCN ramp

35-40 min: 90% MeCN/ 10% H_2O (0.1% TFA)

40-41 min:90%- 20% MeCN ramp

41-45 min: 20% MeCN/ 80% H_2O (0.1% TFA)

Flow rate: 10 mL/min.

System I: 0-5 min: 5% MeCN/ 95% H_2O (0.1% TFA)

5-41 min: 5%- 95% MeCN ramp

41-46 min: 95% MeCN/ 5% H_2O (0.1% TFA)

46-47 min: 95%- 5% MeCN ramp

47-50 min: 20% MeCN/ 80% H_2O (0.1% TFA)

Flow rate: 10 mL/min.

Crotalphine Peptides

Crotalphine (**13**) and analogues were purified using the following method:

System J: 0-5 min: 5% MeCN/ 95% H_2O (0.1% TFA)

5-30 min: 5%- 40% MeCN ramp

30-35 min: 40% - 95% MeCN ramp

35-40 min:95% MeCN/ 5% H_2O (0.1% TFA)

40-41 min: 95%- 5% MeCN ramp

41-46 min: 5% MeCN/ 95% H_2O (0.1% TFA)

Flow rate: 10 mL/min.

7.2.2 Synthesis methods

Piscicolin 126 Induction Peptide, PisN (8)

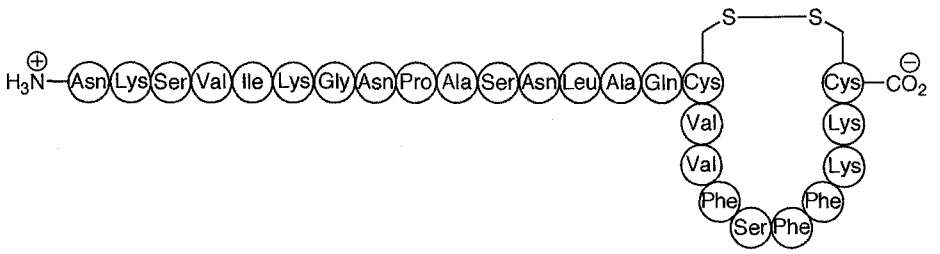

Stepwise synthesis of induction peptide (**8**) was done on a 0.3 mmol scale (1.5 g of resin with 0.2 mmol/g loading) using Novasyn TGT resin preloaded with Fmoc-Cys(Trt)-OH. Manual SPPS was completed according to the method outlined in Section 7.1.6 using NMP instead of DMF for the final 14 residues. The Fmoc protected amino acids were coupled in the following order: Fmoc-Lys(Boc)-OH, Fmoc-Lys(Boc)-OH, Fmoc-Phe-OH, Fmoc-Phe-OH, Fmoc-Ser(*t*-Bu)-OH, Fmoc-Phe-OH, Fmoc-Val-OH, Fmoc-Cys(Trt)-OH, Fmoc-Gln(Trt)-OH, Fmoc-Ala-OH, Fmoc-Leu-OH, Fmoc-Asn(Trt)-OH, Fmoc-Ser(*t*-Bu)-OH, Fmoc-Ala-OH, Fmoc-Pro-OH, Fmoc-Asn(Trt)-OH, Fmoc-Gly-OH, Fmoc-Lys(Boc)-OH, Fmoc-Ile-OH, Fmoc-Val-OH, Fmoc-Ser(*t*-Bu)-OH, Fmoc-Lys(Boc)-OH and Fmoc-Asn(Trt)-OH. The peptide was cleaved from the resin using a freshly prepared solution of 95% trifluoroacetic acid, 2.5% triethylsilane and 2.5% water under mechanical stirring for 3.5 h. The crude peptide was dissolved in a 1:1 solution of acetonitrile/water, and purified by RP-HPLC on a preparative μBondpak C_{18}-10 μm column and monitored at 220 nm using solvent system F. The purified sample containing the uncyclized product mass (2630.4, M + H) was lyophilized. The dried fraction was dissolved in 0.1 M ammonium bicarbonate buffer and stirred in an oxygen environment for 2 d. The sample was lyophilized and re-suspended in milli-Q water twice more to

assist in the removal of the volatile buffer. The sample was then purified using solvent system F at t_R =19.4 min to yield the desired product (1.41 mg, 0.2% yield). MALDI-TOF MS: calcd for $C_{118}H_{186}N_{32}O_{32}S_2$ 2627.3, found 2628.4 (M+H).

CbaX (9)

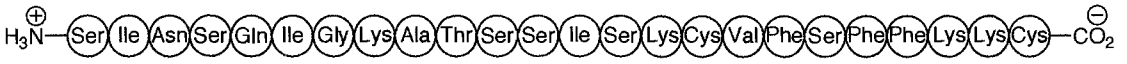

Peptide **9** was prepared on 0.05 mmol scale by elongation of resin separated from the preparation of CbaX(7-24) (**36**). Manual SPPS was completed according to the method outlined in Section 7.1.6. The Fmoc protected amino acids were coupled in the following order: Fmoc-Ile-OH, Fmoc-Gln(Trt)-OH, Fmoc-Ser(*t*-Bu)-OH, Fmoc-Asn(Trt)-OH, Fmoc-Ile-OH and Fmoc-Ser(*t*-Bu)-OH. The peptide was isolated as a single peak using solvent system G, t_R = 18.2 min to give the product **9** as a white solid (1.6 mg, 8.4% based on purification of 19.0 mg of triturated/ dried, crude product). MALDI-TOF (MS): calcd for $C_{116}H_{188}N_{30}O_{34}S_2$ 2609.3, found 2610.6 (M+H).

EntF (10)

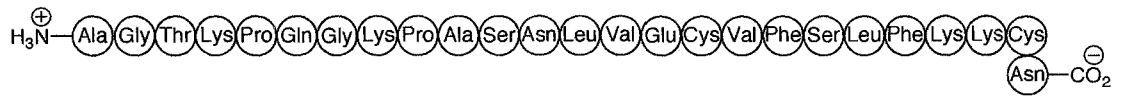

Peptide **10** was prepared on 0.05 mmol scale by elongation of resin separated from the preparation of EntF(7-25) (**39**). Manual SPPS was completed according to the method outlined in Section 7.1.6. The Fmoc protected amino acids were coupled in the following order: Fmoc-Gln(Trt)-OH, Fmoc-Pro-OH, Fmoc-Lys(Boc)-OH, Fmoc-Thr(*t*-Bu)-OH, Fmoc-Gly-OH and Fmoc-Ala-OH. The peptide was isolated as a single peak using

solvent system H, t_R = 23.7 min to give the product **10** as a white solid (2.57 mg, 1% based on purification of 18 mg of triturated/dried, crude product). MALDI-TOF MS: calcd for $C_{118}H_{192}N_{32}O_{34}S_2$ 2665.4, found 2666.4 (M+H).

Synthetic Crotalphine (13)

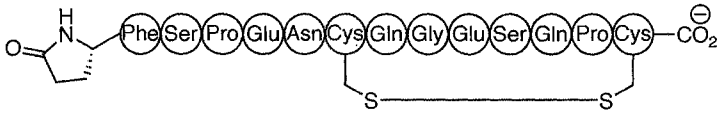

This peptide was synthesized and purified by Ms. Avena Ross with my assistance in an identical fashion to crotalphine analogue **78**.

7.2.3 Preparation of bacteriocins and corresponding analogues

Leucocin A [A21C] 21-37 (Cys-Acm) (14a)

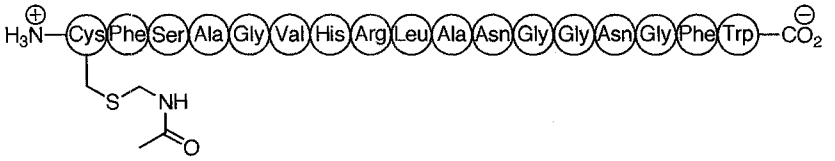

Peptide **14a** was prepared on a 0.5 mmol scale using preloaded Fmoc-Trp(Boc)-Wang resin (0.85 g, 0.5 mmol, 0.59 mmol/g loading). Manual SPPS was completed according to the method outlined in Section 7.1.6. The Fmoc protected amino acids were coupled in the following order: Fmoc-Phe-OH, Fmoc-Gly-OH, Fmoc-Asn(Trt)-OH, Fmoc-Gly-OH, Fmoc-Gly-OH, Fmoc-Asn(Trt)-OH, Fmoc-Ala-OH, Fmoc-Leu-OH, Fmoc-Arg(Pmc)-OH, Fmoc-His(Trt)-OH, Fmoc-Val-OH, Fmoc-Gly-OH, Fmoc-Ala-OH, Fmoc-Ser(*t*-Bu)-OH, Fmoc-Phe-OH and Fmoc-Cys(Acm). Deprotection of acid-labile protecting groups and HPLC purification using method A, t_R = 18.9 min, followed by

lyophilization yielded the desired peptide **14a** as a white solid (5.0 mg, 1.1% yield). MALDI-TOF (MS): calcd for $C_{83}H_{118}N_{26}O_{22}S$ 1862.9, found 1863.6 (M + H).

Leucocin A [A21C] 21-37 (15)

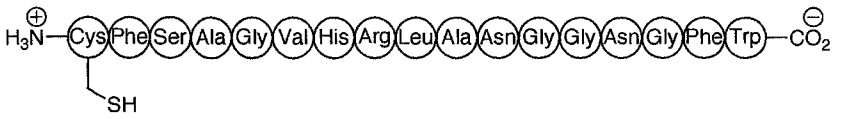

Attempted synthesis from **14a**:

The Acm protected LeuA fragment **14a** (3 mg, 1.6 μmol) was dissolved in a solution of 10% acetic acid in water (0.6 mL) that had been degassed with argon for 30 min. Mercury (II) acetate (5.1 mg, 16 μmol, 10 eq) was added to the solution and the pH of the solution was then adjusted to 4.0 using glacial acetic acid. β-Mercaptoethanol (2.3 μL, 32 μmol) was then added and the resulting mixture was shaken for 5 h. The precipitate was isolated by centrifugation and purified by HPLC. The desired product was not obtained but a side product was isolated by HPLC with a mass of SM + 17.

Repeated synthesis via **14b**:

Fmoc-Trp(Boc)-OH was loaded onto Wang resin (0.625 g, 0.5 mmol, 0.59 mmol/g loading) using the symmetrical anhydride method (Section 7.1.4). The resin was prepared in an identical fashion to **14a** with the exception of the last residue which was incorporated as Fmoc-Cys(Trt)-OPfp. The Pfp ester was dissolved in DMF (10 mL) and combined with the pre-swelled resin and left to react for 2 h (no base or further activation agents were used). Deprotection and HPLC purification using method A, t_R = 17.4 min,

followed by lyophilization yielded the desired peptide **15** as a white solid (4.5 mg, 1% yield). MALDI-TOF (MS): calcd for $C_{80}H_{113}N_{25}O_{21}S$ 1791.8, found 1792.6 (M + H).

Dicarba LeuA A21C (**17**)

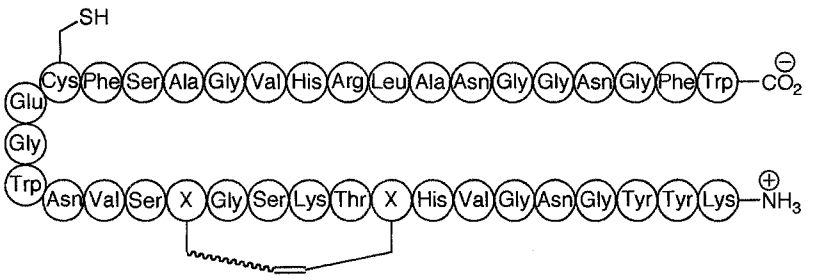

The synthesis of **17** was completed using a ligation reaction (as reported in the thesis of Dr. Jake Stymiest) using peptide **15** and the corresponding 20-mer *C*-terminal thioester. The reaction was completed according to literature procedure[11] using peptide **15** (3 mg, 2 μmol) and the 20-mer containing the *C*-terminal thioester (4 mg, 2 μmol) which were dissolved in 0.1 M Tris-HCl, 6 M guanidine buffer (4 mL) at pH 8.5. Acetonitrile (500 μL) was also added to assist in the solubilization of the peptides. Thiophenol (90 μL, 2% v/v) and benzylmercaptan (90 μL, 2% v/v) were then added and the reaction mixture was stirred at rt for 18 h. The reaction mixture was then concentrated and purified by HPLC using method B, t_R = 14.1 min, and lyophilized to yield product **17** as a white solid (3 mg, 42%). MALDI-TOF MS: calcd for $C_{176}H_{249}N_{52}O_{50}S$ 3922.8, Found 3924.1 (M + H).

Dicarba Leucocin A [Ala21Cys-acetamide] (18)

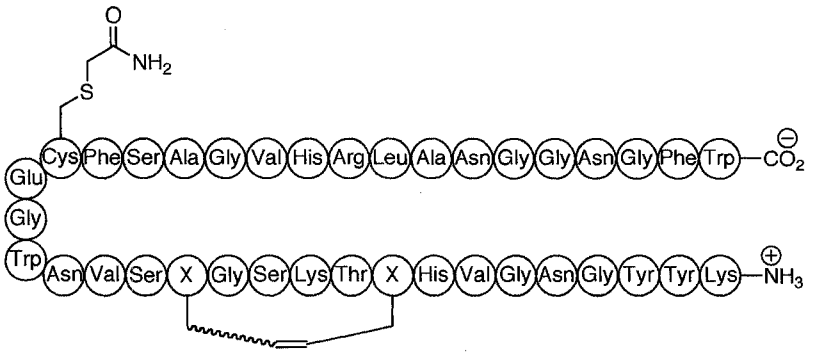

Dicarba LeuA [A21C] (**17**) (1 mg, 0.255 μmol) was dissolved in potassium phosphate buffer (200 μL, 100 mM solution of K_2HPO_4 adjusted to pH 6.0 with 5 M HCl) and acetonitrile (100 μL). The solution was vortexed and iodoacetamide (47 μL of 1.3 mg crystallized from carbon tetrachloride in 1.3 mL of buffer solution, 0.255 μmol) was added and placed onto an elliptical shaker for 1 h with vortexing every 15 min. After 2 h, freshly prepared iodoacetamide (47 μL, 0.255 μmol) was again added to the reaction and reacted for 1 h. After purification by HPLC using method A, two peaks (t_R = 13.5 min and 17.5 min) containing the desired mass by MALDI-MS analysis were lyophilized and carried forward to the desulfurization step. This reaction was completed as a mixture as it was suspected that there were cis and trans olefin isomers). MALDI-TOF MS: calcd for $C_{178}H_{250}N_{53}O_{51}S$ 3977.8, found 3979.0 (M + H).

[9,14]-Dicarba Leucocin A (22)

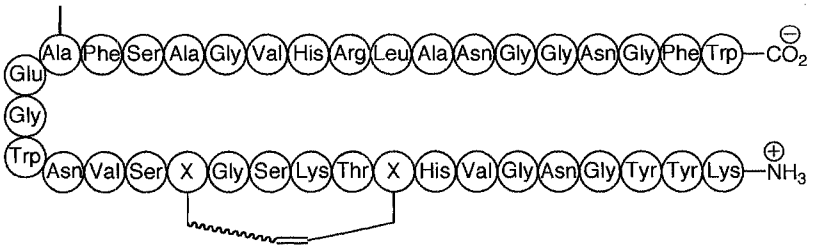

Attempted desulfurization from **18:**

Dicarba Leucocin A [Ala21Cys-acetamide] was dissolved in methanol (1 mL) and water (0.5 mL). Nickel (II) chloride (1 mg, 30 eq) was added and the resulting mixture was placed on the shaker for 3 min. Sodium borohydride (1 mg, 100 eq) was then added and the reaction was monitored by MALDI-TOF MS. Samples of the reaction mixture were taken at 30, 90 and 150 min, quenched with 1% aqueous TFA solution and then MALDI-MS spectra were acquired. Products of similar mass (potentially from reduction of the double bond) were detected by MALDI-MS, but were unable to be detected or isolated by HPLC. MALDI-TOF MS: calcd for $C_{176}H_{247}N_{52}O_{50}$ 3889.8, found 3891.0 (M + H).

Linear resynthesis of 22:

The peptide **22** was prepared by linear synthesis on a 0.4 mmol scale using low loading (0.19 mmol/g), preloaded Fmoc-Trp(Boc)-Novasyn-TGA resin. Manual SPPS was completed according to the method outlined in Section 7.1.6. The Fmoc protected amino acids were coupled in the following order: Fmoc-Phe-OH, Fmoc-Gly-OH, Fmoc-Asn(Trt)-OH, Fmoc-Gly-OH, Fmoc-Gly-OH, Fmoc-Asn(Trt)-OH, Fmoc-Ala-OH, Fmoc-Leu-OH, Fmoc-Arg(Pmc)-OH, Fmoc-His(Trt)-OH, Fmoc-Val-OH, Fmoc-Gly-OH and Fmoc-Ala-OH. The resin was split at this point into two equal portions of 0.2 mmol. One portion was then further elongated, using the same methodology, with the following residues: Fmoc-Phe-Ser($\varphi^{Me,\ Me}$pro)-OH, Fmoc-Ala-OH, Fmoc-Glu(O-*t*Bu)-OH, Fmoc-Gly-OH, and Fmoc-Trp(Boc)-OH. The remaining residues were all double coupled: Fmoc-Asn(Trt)-OH, Fmoc-Val-OH, Fmoc-Ser(O-*t*Bu)-OH, Fmoc-AllylGly-OH, Fmoc-Gly-OH, Fmoc-Ser(O-*t*Bu)-OH, Fmoc-Lys(Boc)-OH, Fmoc-Thr(O-*t*Bu)-OH, Fmoc-

AllylGly-OH. At this point the resin was split again into two 0.1 mmol portions and Fmoc-His(Trt)-OH was added. After this point it was beneficial to heat the reaction vessel to 45 °C to complete the peptide couplings. The remaining residues were added in the following order: Fmoc-Val-OH (triple coupling), Fmoc-Gly-OH, (split again into 0.05 mmol portions) Fmoc-Asn(Trt)-OH, Fmoc-Gly-OH, Fmoc-Tyr(O-*t*Bu)-OH, Fmoc-Tyr(O-*t*Bu)-OH and Fmoc-Lys(Boc)-OH. The linear peptide was then washed repeatedly with DCM, MeOH and then dried under a stream of argon. The resin was then dried overnight in the dessicator to remove any excess solvent. After obtaining the weight of the peptide on resin (2.235 g) a portion of the resin (0.100 g) was removed to have a better approximation of immobilized peptide. (2.235 g = 0.05 mmol => 0.1 g = 0.0022 mmol) The resin was then washed with DCM (3 x 5 mL) and then left to swell for 30 min. The vessel was then drained and washed/ bubbled with 0.8 M LiCl in DMF (3 x 2 mL/ 3 min) and rinsed once with dichloroethane (1 x 3 mL). The vessel was then drained and dichloroethane (3 mL) was then added to the resin and argon was bubbled through the mixture for 20 min. Grubbs' catalyst was then added to the reaction mixture (1.9 mg, 1 eq) and the vessel was wrapped in heating tape and equipped with a condenser and a thermocouple. The reaction was maintained at 83 °C for 16 h with additional solvent added when the total volume went below 2.5 mL. After a test cleavage indicated product by MALDI MS, the vessel was drained, washed with DCM (3 x 3 mL) and then suspended in a solution of dichloroethane (3 mL) and DMSO (200 μL, 2.8 mmol, 1200 eq) and bubbled for 24 h to assist in the removal of ruthenium. Finally, the peptide was cleaved from the resin with 95%: 2.5%: 2.5% TFA: H_2O: TIPS-H for four hours, filtered through glass wool, and concentrated *in vacuo*. The remaining solid was then triturated

repeatedly with ether until the solid was white, dried *in vacuo*, and purified by HPLC using solvent system C, t_R = 13.1 min, and lyophilized to yield the desired product as a white solid (0.2 mg, 1.1% based on purification of 18 mg of triturated/ dried, crude product). MALDI-TOF MS: calcd for $C_{176}H_{248}N_{52}O_{50}$ 3889.8. Found 3890.8 (M+H).

[C9a, C14a]- Leucocin A (23)

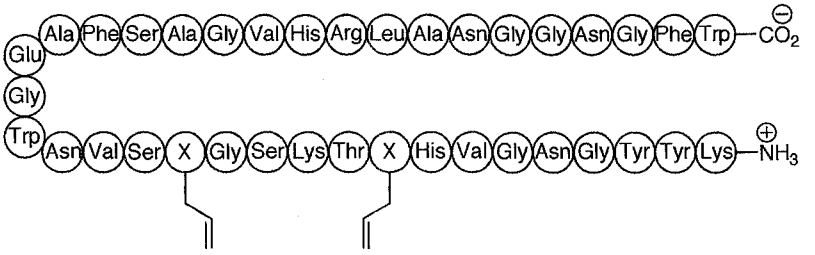

Leucocin analogue **23** was synthesized on a 0.05 mmol scale by manual synthesis as described in the synthesis of **22** before RCM cyclization. Product was purified by HPLC using solvent system C, t_R = 18.1 min, and lyophilized to yield product **23** (0.8 mg, 2.5% based on purification of 33 mg of triturated/ dried, crude product). MALDI-TOF MS: calcd for $C_{178}H_{252}N_{52}O_{50}$ 3917.9. Found 3918.9 (M+H).

[C9S, C14S]- Leucocin A (24)

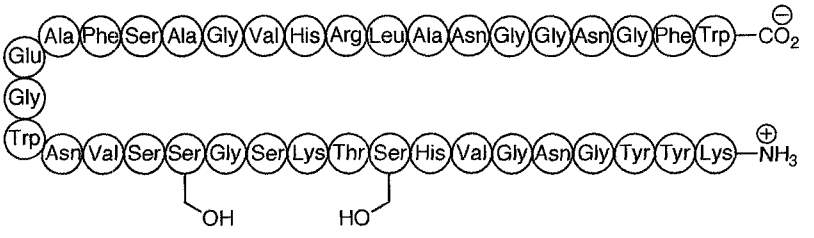

Leucocin analogue **24** was synthesized on 0.1 mmol scale by automated synthesis as outlined in Section 7.1.7. Fmoc-Ser(*t*-Bu)-OH was incorporated in place of cysteine at positions 9 and 14 and all other amino acids were coupled in the same order as compound

22 except that pseudoproline, Fmoc-Phe-Ser($\Psi^{Me,Me}$ Pro)-OH, was not used at position 22-23 but instead were incorporated as individual amino acids. Double couplings were used for the final residues (1-7). The crude peptide was cleaved from the resin, isolated using solvent system C, t_R = 12.6 min, and lyophilized to yield the product **24**. (0.2 mg, 0.7% based on purification of 28 mg of triturated/ dried, crude product). MALDI-TOF MS: calcd for $C_{174}H_{248}N_{52}O_{52}$ 3897.8, found 3899.4 (M+H).

[C9n, C14n]- Leucocin A (25)

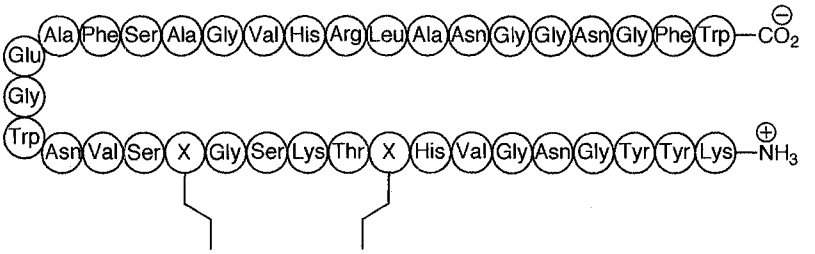

Leucocin analogue **25** was prepared on resin separated from the 0.2 mmol of the 14-mer separated in the synthesis of **22**. The 14-mer was elongated by manual synthesis according to the procedure outlined in Section 7.1.6. The Fmoc protected amino acids were coupled in the following order: Fmoc-Phe-Ser($\Psi^{Me,Me}$ Pro)-OH, Fmoc-Ala-OH, Fmoc-Glu(*t*-Bu)-OH, Fmoc-Gly-OH, Fmoc-Trp(Boc)-OH, Fmoc-Asn(Trt)-OH, Fmoc-Val-OH, and Fmoc-Ser(*t*-Bu)-OH. The resin was then further subdivided into portions and the remainder of leucocin analogue **25** was synthesized on a 0.03 mmol scale by automated synthesis as outlined in Section 7.1.7. The Fmoc protected amino acids were coupled in the following order: Fmoc-Nva-OH, Fmoc-Gly-OH, Fmoc-Ser(*t*-Bu)-OH, Fmoc-Lys(Boc)-OH, Fmoc-Thr(*t*-Bu)-OH, Fmoc-Nva-OH, Fmoc-His(Trt)-OH, Fmoc-Val-OH, Fmoc-Gly-OH, Fmoc-Asn(Trt)-OH, Fmoc-Gly-OH, Fmoc-Tyr(*t*-Bu)-OH,

Fmoc-Tyr(*t*-Bu)-OH and Fmoc-Lys(Boc)-OH. The product was then cleaved from the resin and purified by HPLC using solvent system A, t_R = 20.6 min, and lyophilized to produce the desired product **25** as a white solid (1.68 mg, 10% based on purification of 16.2 mg of triturated/ dried, crude product). MALDI-TOF MS: calcd for $C_{178}H_{256}N_{52}O_{50}$ 3921.9, found 3923.1 (M+H).

[C9F, C14F] - Leucocin A (26)

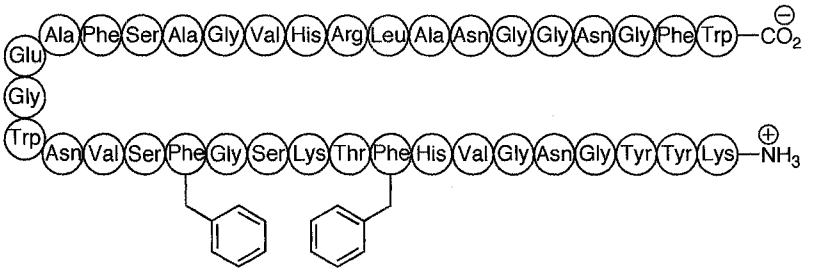

Leucocin analogue **26** was synthesized on a 0.03 mmol in an identical fashion to **25** except that Fmoc-Phe-OH was incorporated at positions 9 and 14. The product was cleaved and purified using solvent system A, t_R = 21.9 min, and was then lyophilized to yield **26** as a white solid (0.99 mg, 8% based on purification of 12.3 mg of triturated/ dried, crude product). MALDI-TOF MS calcd for $C_{186}H_{256}N_{52}O_{50}$ 4017.9, found 4019.1 (M+H).

[M31Nle]- Pediocin PA-1, NlePed (27)

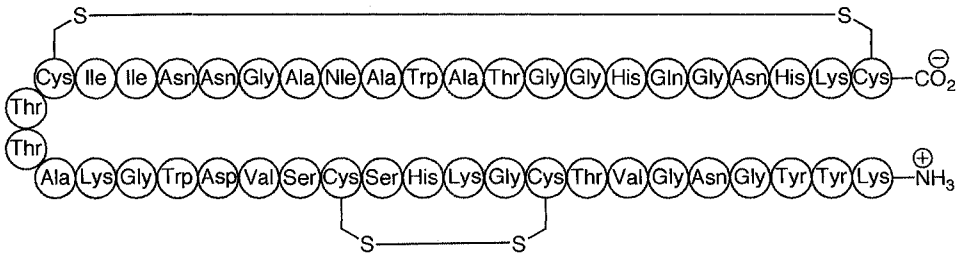

Residues 21-44 of compound **27** were synthesized on a 0.25 mmol scale using NovaSyn TGT resin (loading 0.2 mmol/g) preloaded with Fmoc-Cys(Trt)-OH using automated synthesis according to the method outlined in Section 7.1.7. Pseudoproline dipeptides were incorporated at positions 21-22 and 34-35 to disrupt on-resin aggregation. The Fmoc protected amino acids were coupled in the following order: Fmoc-Lys(Boc)-OH, Fmoc-His(Trt)-OH, Fmoc-Asn(Trt)-OH, Fmoc-Gly-OH, Fmoc-Gln(Trt)-OH, Fmoc-His(Trt)-OH, Fmoc-Gly-OH, Fmoc-Gly-OH, Fmoc-Ala-Thr($\Psi^{Me,Me}$ Pro)-OH, Fmoc-Trp(Boc)-OH, Fmoc-Ala-OH, Fmoc-Nle-OH, Fmoc-Ala-OH, Fmoc-Gly-OH, Fmoc-Asn(Trt)-OH, Fmoc-Asn(Trt)-OH, Fmoc-Ile, Fmoc-Ile-OH, Fmoc-Cys(Trt)-OH, Fmoc-Thr(*t*-Bu)-OH and Fmoc-Ala-Thr($\Psi^{Me,Me}$ Pro)-OH. At this point the resin was divided into portions and the solvents and cartridges were replaced. The synthesis was continued with 0.05 mmol of resin. The remaining Fmoc protected amino acids were coupled in the following order: Fmoc-Lys(Boc)-OH, Fmoc-Gly-OH, Fmoc-Trp(Boc)-OH, Fmoc-Asp(*t*-Bu)-OH, Fmoc-Val-OH, Fmoc-Ser(*t*-Bu)-OH, Fmoc-Cys(Trt)-OH, Fmoc-Ser(*t*-Bu)-OH, Fmoc-His(Trt)-OH, Fmoc-Lys(Boc)-OH, Fmoc-Gly-OH, Fmoc-Cys(Trt)-OH, Fmoc-Thr(*t*-Bu)-OH, Fmoc-Val-OH, Fmoc-Gly-OH, Fmoc-Asn(Trt)-OH, Fmoc-Gly-OH, Fmoc-Tyr(*t*-Bu)-OH, Fmoc-Tyr(*t*-Bu)-OH and Fmoc-Lys(Boc)-OH. The resin was then cleaved using 94% TFA, 2.5% EDT, 2.5% water and 1% TIPS-H for 2 h. The crude peptide (31.6 mg of triturated solid previously dried on high vacuum) was then dissolved in a 1 mg/mL solution of 1:1 trifluoroethanol: 1 mM NH_4HCO_3. The pH of the solution was then adjusted to 8.0 with NH_4OH. Oxygen was then gently bubbled through the solution (approx. 1 bubble/sec) for 16 h. Next, the solution was concentrated *in vacuo* to remove as much of the volatile component as possible without precipitating the peptide.

The solution was then frozen in a bath of dry ice / acetone (-78 °C) and lyophilized. The remaining solid was then purified by HPLC using solvent system D, t_R = 23.6 min, and lyophilized to yield the desired product **27** as a white solid (1.83 mg, 6% based on purification of 31.6 mg of triturated/ dried, crude product). MALDI-TOF MS calcd for $C_{197}H_{295}N_{61}O_{60}S_4$ 4603.1, found 4604.5 (M+H).

[C9F, C14F, M31Nle]- Pediocin PA-1, [C9F, C14F]-NlePed (29)

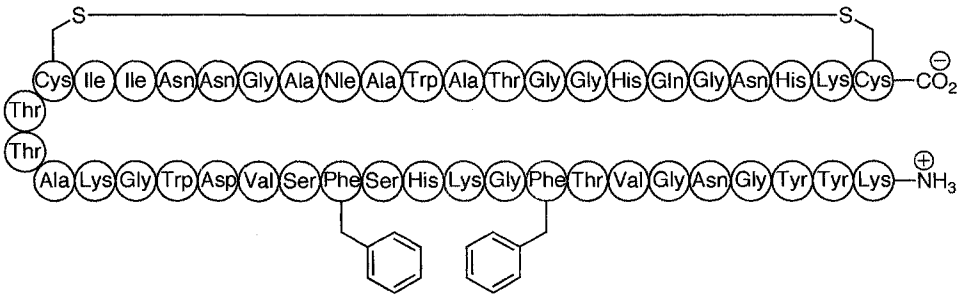

Pediocin analogue **29** was synthesized on a 0.05 mmol scale on resin already containing the first 24 amino acids from the preparation of peptide **27**. The synthesis was completed in an identical fashion to peptide **27** except that Fmoc-Phe-Ser($\Psi^{Me,Me}$ Pro)-OH was used in place of Cys 14 and Phe 15. Cys 9 was similarly replaced by Fmoc-Phe-OH. After cleavage and cyclization, the remaining solid was purified by HPLC using solvent system D, t_R = 26.0 min, and lyophilized to yield peptide **29** as a white solid (2.01 mg, 12% based on purification of 16.0 mg of triturated/ dried, crude product). MALDI-TOF MS: calcd for $C_{209}H_{305}N_{61}O_{60}S_2$ 4693.2, found 4694.4 (M+H).

[T8H, C9F, G10T, C14F, M31Nle]- Pediocin PA-1, [T8H, C9F, G10T, C14F] NlePed (31)

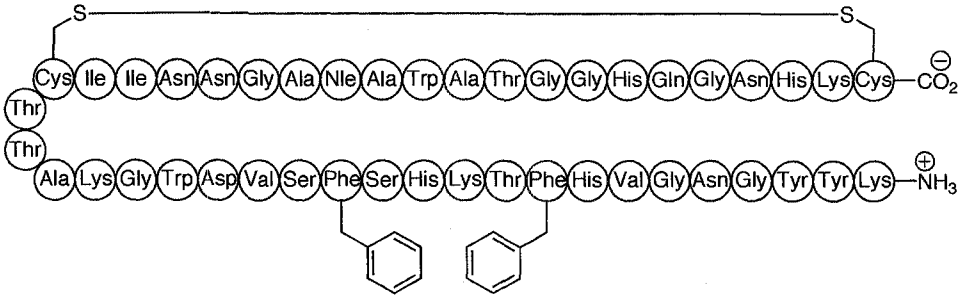

Pediocin analogue **31** was synthesized on a 0.05 mmol scale in an identical fashion to peptide **29** except that Thr 8 was replaced by Fmoc-His(Trt)-OH and Gly 10 was replaced by Fmoc-Thr(*t*-Bu)-OH. After cleavage and cyclization, the remaining solid was purified by HPLC using solvent system D, t_R = 25.2 min, and was then lyophilized to produce **31** as a white solid (2.31 mg, 14% based on purification of 15.8 mg of triturated/ dried, crude product). MALDI-TOF MS: calcd for $C_{213}H_{309}N_{63}O_{60}S_2$ 4772.3, found 4773.2 (M+H).

[C9F, G10T, H12S, S13G, C14F, M31Nle]- Pediocin PA-1, LeuLoopPed (32)

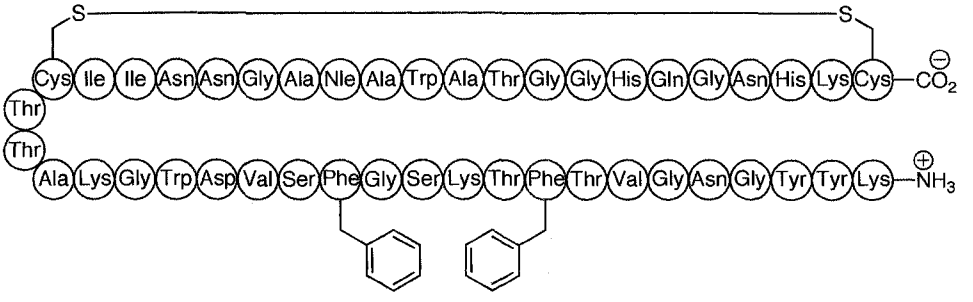

Pediocin analogue **32** was synthesized on a 0.05 mmol scale in an identical fashion to peptide **29** except that Gly 10 was replaced by Fmoc-Thr(*t*-Bu)-OH, His 12 was replaced by Fmoc-Ser(*t*-Bu)-OH, and Ser 13 was replaced by Fmoc-Gly-OH. After cleavage and cyclization, the remaining solid was purified by HPLC using solvent system E, t_R = 42.7

min, and lyophilized to yield peptide **32** as a white solid (1.4 mg, 7% based on purification of 20 mg of triturated/ dried, crude product). MALDI-TOF MS: calcd for $C_{207}H_{305}N_{59}O_{61}S_2$ 4657.2, found 4658.8 (M+H).

[C9F, C14F]-LeuA (1-18)- [M31Nle]-Ped (19-44), Leu-Ped (33)

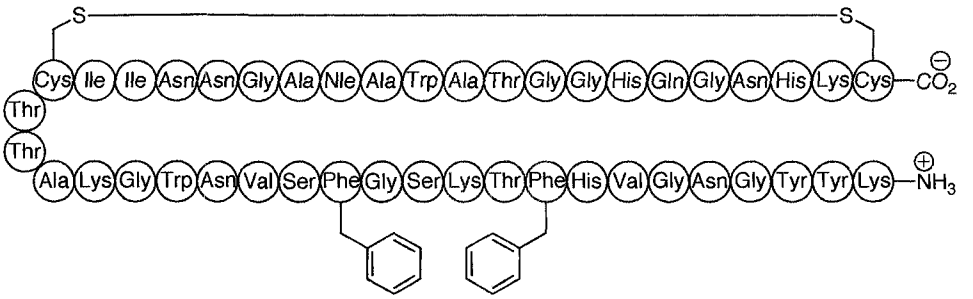

Pediocin analogue **33** was synthesized on a 0.05 mmol scale in an identical fashion to peptide **29** except that Thr 8 was replaced by Fmoc-His(Trt)-OH, Gly 10 was replaced by Fmoc-Thr(*t*-Bu)-OH, His 12 was replaced by Fmoc-Ser(*t*-Bu)-OH, Ser 13 was replaced by Fmoc-Gly-OH and Asp 17 was replaced by Fmoc-Asn(Trt)-OH. After cleavage and cyclization, the remaining solid was purified by HPLC using solvent system D, t_R = 25.5 min, and lyophilized to produce peptide **33** as a white solid (1.32 mg, 8% based on purification of 15.8 mg of triturated/ dried, crude product). MALDI-TOF MS: calcd for $C_{209}H_{306}N_{62}O_{59}S_2$ 4691.2, found 4692.9 (M+H).

7.2.4 Preparation of induction peptides and corresponding analogues

CbaX (1-10): EntF (11-25) (34)

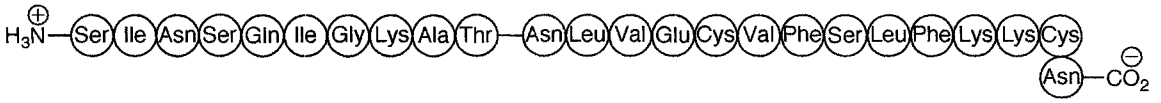

CbaX (1-10)- EntF (11-25) was synthesized on a 0.05 mmol scale by manual synthesis as outlined in Section 7.1.6. Resin containing the *C*-terminal 12-25 portion of EntF was used from the syntheis of fragment **40**. The remaining Fmoc protected amino acids were coupled in the following order: Fmoc-Ser(*t*-Bu)-OH, Fmoc-Ala-Thr($\Psi^{Me,Me}$ Pro)-OH, Fmoc-Lys(Boc)-OH, Fmoc-Gly-OH, Fmoc-Ile-OH, Fmoc-Gln(Trt)-OH, Fmoc-Ser(*t*-Bu)-OH, Fmoc-Asn(Trt)-OH, Fmoc-Ile-OH and Fmoc-Ser(*t*-Bu)-OH. After cleavage from the solid support, the remaining solid was purified by HPLC using solvent system H, t_R = 29.7 min, and lyophilized to yield peptide **34** as a white solid (6.22 mg, 28% based on purification of 22 mg of triturated/ dried, crude product). MALDI-TOF MS: calcd for $C_{119}H_{196}N_{32}O_{37}S_2$ 2729.4, found 2730.2 (M+H).

EntF (1-10): CbaX (11-24) (35)

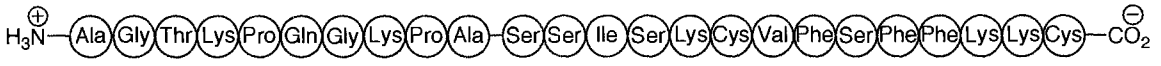

EntF (1-10)- CbaX (11-24) was synthesized on a 0.05 mmol scale by manual synthesis as outlined in Section 7.1.6. Resin containing the *C*-terminal 11-24 portion of CbaX was used from the synthesis of **37**. The remaining Fmoc protected amino acids were coupled in the following order: Fmoc-Ala-OH, Fmoc-Pro-OH, Fmoc-Lys(Boc)-OH, Fmoc-Gly-OH, Fmoc-Gln(Trt)-OH, Fmoc-Pro-OH, Fmoc-Lys(Boc)-OH, Fmoc-Thr(*t*-Bu)-OH, Fmoc-Gly-OH and Fmoc-Ala-OH. After cleavage from the solid support, the remaining

solid was purified by HPLC using solvent system H, t_R = 18.6 min, and lyophilized to produce the desired product **35** as a white solid (4.92 mg, 21% based on purification of 23.1 mg of triturated/ dried, crude product). MALDI-TOF MS calcd for $C_{115}H_{184}N_{30}O_{31}S_2$ 2545.3, found 2546.6 (M+H).

CbaX (7-24) (36)

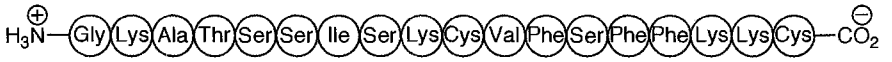

CbaX (7-24) was synthesized on a 0.1 mmol scale by manual synthesis as outlined in Section 7.1.6. Resin containing the *C*-terminal 11-24 portion of CbaX was used from the synthesis of peptide **37**. The remaining Fmoc protected amino acids were coupled in the following order: Fmoc-Thr(*t*-Bu)-OH, Fmoc-Ala-OH, Fmoc-Lys(Boc)-OH, and Fmoc-Gly-OH. At this point, 0.05 mmol of resin was removed for the preparation of CbaX (**9**). After cleavage from the solid support, the remaining solid was purified by HPLC using solvent system H, t_R = 18.6 min, and lyophilized to give **36** as a white solid (4.0 mg, 19% based on purification of 21.0 mg of triturated/ dried, crude product). MALDI-TOF MS calcd for $C_{89}H_{142}N_{22}O_{24}S_2$ 1967.0, found 1968.4 (M+H).

CbaX (11-24) (37)

CbaX (11-24) was synthesized on a 0.5 mmol scale by manual synthesis as outlined in Section 7.1.6. Resin containing the *C*-terminal 16-24 portion of CbaX was used from the synthesis of peptide **38**. The remaining Fmoc protected amino acids were coupled in the following order: Fmoc-Lys(Boc)-OH, Fmoc-Ser(*t*-Bu)-OH, Fmoc-Ile-OH and Fmoc-Ser

t-Bu)-Ser($\Psi^{Me,Me}$ Pro)-OH. At this point, 0.05 mmol of resin was cleaved from the solid support, purified by HPLC using solvent system G, t_R = 15.7 min, and lyophilized to yield the desired product **37** as a white solid (1.5 mg, 10% based on purification of 15.1 mg of triturated/ dried, crude product). MALDI-TOF MS calcd for $C_{74}H_{115}N_{17}O_{19}S_2$ 1609.8, found 1610.8 (M+H).

CbaX (16-24) (38)

CbaX (16-24) was synthesized on a 1.0 mmol scale by manual synthesis (as outlined in Section 7.1.6) using preloaded H-Cys(Trt)-2ClTrt resin (0.75 mmol/g loading). The Fmoc protected amino acids were coupled in the following order: Fmoc-Lys(Boc)-OH, Fmoc-Lys(Boc)-OH, Fmoc-Phe-OH, Fmoc-Phe-OH, Fmoc-Phe-Ser($\Psi^{Me,Me}$ Pro)-OH, Fmoc-Val-OH and Fmoc-Cys(Trt)-OPfp. A portion of the resin (0.05 mmol) was then removed, cleaved by acid hydrolysis, purified by HPLC using solvent system H, t_R = 18.4 min, and lyophilized to give the desired product **38** as a white solid (8.6 mg, 57% based on purification of 15.0 mg of triturated/ dried, crude product). MALDI-TOF MS calcd for $C_{53}H_{77}N_{11}O_{11}S_2$ 1107.5, found 1108.8 (M+H).

EntF (7-25) (39)

EntF (7-25) was synthesized on a 0.1 mmol scale by manual synthesis as outlined in Section 7.1.6. Resin containing the *C*-terminal 11-25 portion of EntF was used from the synthesis of peptide **40**. The remaining Fmoc protected amino acids were coupled in the

following order: Fmoc-Ala-OH, Fmoc-Pro-OH, Fmoc-Lys(Boc)-OH, and Fmoc-Gly-OH. At this point, 0.05 mmol of resin was removed for the preparation of EntF (**10**). The remaining resin was cleaved from the solid support, purified by HPLC using solvent system H, t_R = 24.7 min, and lyophilized to yield the desired product **39** (4.17 mg, 14% based on purification of 30 mg of triturated/ dried, crude product). MALDI-TOF MS calcd for $C_{93}H_{150}N_{24}O_{26}S_2$ 2083.1, found 2084.4 (M+H).

EntF (11-25) (40)

EntF (11-25) was synthesized on a 0.5 mmol scale by manual synthesis as outlined in Section 7.1.6. Resin containing the *C*-terminal 16-25 portion of EntF was used from the synthesis of peptide **41**. The Fmoc protected amino acids were coupled in the following order: Fmoc-Glu(*t*-Bu)-OH, Fmoc-Val-OH, Fmoc-Leu-OH, Fmoc-Asn(Trt)-OH and Fmoc-Ser(*t*-Bu)-OH. A portion of the resin was then removed (0.05 mmol), cleaved from the solid support, purified by HPLC using solvent system H, t_R = 27.0 min, and lyophilized to yield the desired product **40** (1.8 mg, 6% based on purification of 30 mg of triturated/ dried, crude product). MALDI-TOF MS calcd for $C_{77}H_{122}N_{19}O_{22}S_2$ 1729.9, found 1731.0 (M+H).

EntF (16-25) (41)

EntF (16-25) was synthesized on a 1.0 mmol scale by manual synthesis (as outlined in Section 7.1.6) using preloaded Fmoc-Asn(Trt)-Wang resin (loading 0.54 mmol/g). The

Fmoc protected amino acids were coupled in the following order: Fmoc-Cys(Trt)-OPfp, Fmoc-Lys(Boc)-OH, Fmoc-Lys(Boc)-OH, Fmoc-Phe-OH, Fmoc-Leu-OH, Fmoc-Ser(*t*-Bu)-OH, Fmoc-Phe-OH, Fmoc-Val-OH, and Fmoc-Cys(Trt)-OPfp. A portion of the resin was then removed (0.05 mmol), cleaved from the solid support, purified by HPLC using solvent system H, t_R = 18.8 min, and lyophilized to yield the desired product **41** (1.7 mg, 11% based on purification of 15 mg of triturated/ dried, crude product). MALDI-TOF MS calcd for $C_{54}H_{84}N_{13}O_{13}S_2$ 1187.6, found 1188.8 (M+H).

CbaX (1-11) (42)

CbaX (1-11) was prepared on a 0.1 mmol scale by manual synthesis (as outlined in Section 7.1.6) using preloaded Fmoc-Ser(*t*-Bu)-OH resin (loading 0.64 mmol/g). The Fmoc amino acids were coupled in the following order: Fmoc-Thr(*t*-Bu)-OH, Fmoc-Ala-OH, Fmoc-Lys(Boc)-OH, Fmoc-Gly-OH, Fmoc-Ile-OH, Fmoc-Gln(Trt)-OH, Fmoc-Ser(*t*-Bu)-OH, Fmoc-Asn(Trt)-OH, Fmoc-Ile-OH and Fmoc-Ser(*t*-Bu)-OH. Half of the resin was then cleaved, purified by HPLC using solvent system I, t_R = 15.1 min, and lyophilized to yield the desired product as a white solid (3.51 mg, 25% based on purification of 13.8 mg of triturated/ dried, crude product). MALDI-TOF MS calcd for $C_{45}H_{80}N_{14}O_{18}$ 1104.6, found 1105.7 (M+H).

EntF (1-11) (43)

EntF (1-11) was prepared on a 0.1 mmol scale by manual synthesis (as outlined in Section 7.1.6) using preloaded Fmoc-Ser(*t*-Bu)-OH resin (loading 0.64 mmol/g). The Fmoc amino acids were coupled in the following order: Fmoc-Ala-OH, Fmoc-Pro-OH, Fmoc-Lys(Boc)-OH, Fmoc-Gly-OH, Fmoc-Gln(Trt)-OH, Fmoc-Pro-OH, Fmoc-Lys(Boc)-OH, Fmoc-Thr(*t*-Bu)-OH, Fmoc-Gly-OH and Fmoc-Ala-OH. Half of the resin was then cleaved, purified by HPLC using solvent system I, t_R = 10.9 min, and lyophilized to yield product **43** as a white solid (3.55 mg, 26% based on purification of 13.7 mg of triturated/ dried, crude product). MALDI-TOF MS calcd for $C_{44}H_{76}N_{14}O_{15}$ 1040.6, found 1041.7 (M+H).

CbaX (16-24) + N (44)

Peptide **44** was prepared on a 0.1 mmol scale by manual synthesis (as outlined in Section 7.1.6) using preloaded Fmoc-Asn(Trt)-Wang resin (loading 0.54 mmol/g). The Fmoc amino acids were coupled in the following order: Fmoc-Cys(Trt)-OPfp, Fmoc-Lys(Boc)-OH, Fmoc-Lys(Boc)-OH, Fmoc-Phe-OH, Fmoc-Phe-OH, Fmoc-Ser-OH, Fmoc-Phe-OH, Fmoc-Val-OH and Fmoc-Cys(Trt)-OPfp. Half of the resin was then cleaved, purified by HPLC using solvent system H, t_R = 16.6 min and lyophilized to yield **44** as a white solid (2.48 mg, 20% based on purification of 12.4 mg of triturated/ dried, crude product). MALDI-TOF MS calcd for $C_{57}H_{82}N_{13}O_{13}S_2$ 1221.6, found 1222.8 (M+H).

EntF (16-25) – N, EntF (16-24) (45)

Peptide **45** was prepared on a 0.1 mmol scale by manual synthesis (as outlined in Section 7.1.6) using preloaded Fmoc-Cys(Trt)-Novasyn TGT resin (loading 0.2 mmol/g). The Fmoc amino acids were coupled in the following order: Fmoc-Lys(Boc)-OH, Fmoc-Lys(Boc)-OH, Fmoc-Phe-OH, Fmoc-Leu-OH, Fmoc-Ser(*t*-Bu)-OH, Fmoc-Phe-OH, Fmoc-Val-OH and Fmoc-Cys(Trt)-OPfp. Half of the resin was then cleaved, purified by HPLC using solvent system H, t_R = 17.4 min, and lyophilized to yield compound **45** as a white solid (3.36 mg, 22% based on purification of 15.1 mg of triturated/ dried, crude product). MALDI-TOF MS calcd for $C_{50}H_{78}N_{11}O_{11}S_2$ 1073.5, found 1074.8 (M+H).

7.2.5 Preparation of photoaffinity labeled peptides

Completed with the assistance of Ms. Emma Heydari

CbaX(16-24)[F18Bpa] (49)

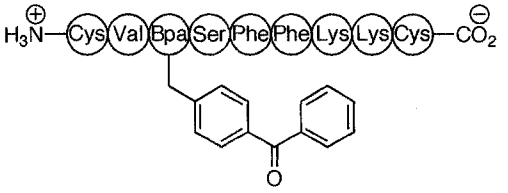

The peptide was loaded according to the method outlined in Section 7.1.5 onto 2-chlorotrityl chloride resin on 0.9 mmol scale (loading 1.6 mmol/g) and elongated using manual SPPS as outlined in Section 7.1.6. The next two residues were then added to the resin (Fmoc-Lys(Boc)-OH and Fmoc-Lys(Boc)-OH) which was then divided into 0.3 mmol portions for the preparation of peptides **49-51**. Peptide **49** was prepared on 0.3 mmol scale by the sequential addition of the following Fmoc amino acids: Fmoc-Phe-OH, Fmoc-Phe-OH, Fmoc-Ser(*t*-Bu)-OH, Fmoc-Bpa-OH, Fmoc-Val-OH and Fmoc-Cys(Trt)-OPfp. At this point, 0.1 mmol of the resin was removed and cleaved. The

crude peptide was then purified by HPLC using solvent system H, t_R = 21.8 min, and lyophilized to yield the desired product **49** as a white solid (4.8 mg, 41% based on purification of 11.7 mg of triturated/ dried, crude product). MALDI-TOF MS calcd for $C_{60}H_{81}N_{11}O_{12}S_2$ 1211.6, found 1212.5 (M+H).

CbaX(16-24)[F20Bpa] (50)

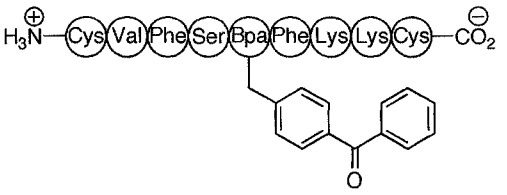

Peptide **50** was prepared on 0.3 mmol scale using manual SPPS as outlined in section 7.1.6 beginning with the tripeptide described for compound **49**. The synthesis was completed by the sequential addition of the following Fmoc amino acids: Fmoc-Phe-OH, Fmoc-Bpa-OH, Fmoc-Ser(*t*-Bu)-OH, Fmoc-Phe-OH, Fmoc-Val-OH and Fmoc-Cys(Trt)-OPfp. At this point, 0.1 mmol of the resin was removed and cleaved. The crude peptide was then purified by HPLC using solvent system H, t_R = 21.8 min, and lyophilized to yield the desired product **50** (5.5 mg, 38% based on purification of 14.3 mg of triturated/ dried, crude product). MALDI-TOF MS calcd for $C_{60}H_{81}N_{11}O_{12}S_2$ 1211.6, found 1212.7 (M+H).

CbaX(16-24)[F21Bpa] (51)

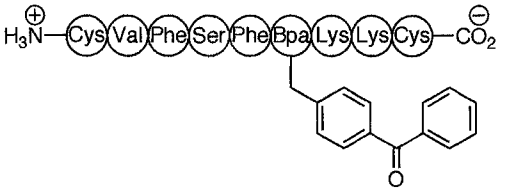

Peptide **51** was prepared on 0.3 mmol scale (using manual SPPS as outlined in section 7.1.6) on the tripeptide described for compound **49**. The synthesis was completed by the sequential addition of the following Fmoc amino acids: Fmoc-Bpa-OH, Fmoc-Phe-OH, Fmoc-Ser(*t*-Bu)-OH, Fmoc-Phe-OH, Fmoc-Val-OH and Fmoc-Cys(Trt)-OPfp. At this point, 0.1 mmol of the resin was removed and cleaved. The crude peptide was then purified by HPLC using solvent system H, t_R = 21.5 min, and lyophilized to yield the desired product as a white solid (8.1 mg, 52% based on purification of 15.5 mg of triturated/ dried, crude product). MALDI-TOF (MS) calcd for $C_{60}H_{81}N_{11}O_{12}S_2$ 1211.6, found 1212.6 (M+H).

CbaX[F18Bpa] (52)

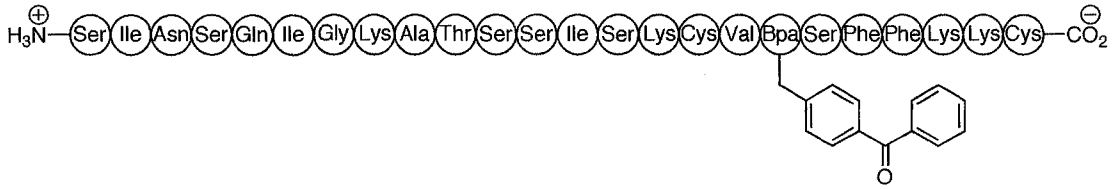

Resin from peptide **49** (0.2 mmol) containing the Fmoc-protected 9-mer was extended to the full-length peptide using manual SPPS as outlined in section 7.1.6. For residues 1-14, Fmoc deprotection was assisted by the use of LiCl washes (3 min bubbling with 3 mL of 3.39 g LiCl in 100 mL DMF, followed by one DMF rinse of 5 mL) before each deprotection. For residues 1-15, the use of *N*-methylpyrrolidinone (NMP) as the solvent

was found to be beneficial. The synthesis was completed by the sequential addition of the following Fmoc amino acids: Fmoc-Lys(Boc)-OH, Fmoc-Ser(*t*-Bu)-OH, Fmoc-Ile-OH, Fmoc-Ser(*t*-Bu)-OH, Fmoc-Ser(*t*-Bu)-OH, Fmoc-Thr(*t*-Bu)-OH, Fmoc-Ala-OH, Fmoc-Lys(Boc)-OH, Fmoc-Gly-OH, Fmoc-Ile-OH, Fmoc-Gln(Trt)-OH, Fmoc-Ser(*t*-Bu)-OH, Fmoc-Asn(Trt)-OH, Fmoc-Ile-OH and Fmoc-Ser(*t*-Bu)-OH. At this point 0.05 mmol of resin was cleaved, purified by HPLC using solvent system H, t_R = 26.9 min, and lyophilized to yield the desired product **52** (0.4 mg, 3% based on purification of 13.0 mg of triturated/ dried, crude product). MALDI-TOF MS calcd for $C_{123}H_{192}N_{30}O_{35}S_2$ 2713.4, found 2714.3 (M+H).

CbaX[F21Bpa] (54)

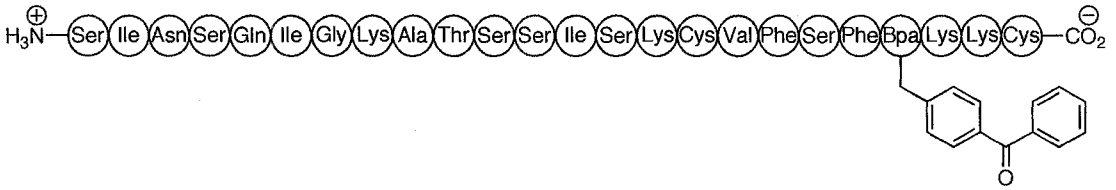

Peptide **54** was completed in an identical fashion to peptide **52** using 0.2 mmol of resin from peptide **51**. Peptide **54** was purified using solvent system H, t_R = 26.5 min, and lyophilized to yield the desired product **54** (2.9 mg, 22% based on purification of 12.9 mg of triturated/ dried, crude product). MALDI-TOF MS calcd for $C_{123}H_{192}N_{30}O_{35}S_2$ 2713.4, found 2714.8 (M+H).

7.2.6 Tripeptides for orthoester linker study

Tripeptides completed with the assistance of Ms. Landon Reid

The following analytical method (similar to method reported by Barany *et al.*[101]) was used for the HPLC analysis of tripeptides.

0-5 min: 5% MeCN/ 95% H_2O (0.1% TFA)

5-30 min: 5% - 45% MeCN ramp

30-35 min: 45% - 95% MeCN ramp

35-40 min 95% MeCN/ 5% H_2O (0.1% TFA)

40-45 min: 95% - 5% MeCN ramp

45-50 min: 5% MeCN/ 95% H_2O (0.1% TFA)

Flow rate: 1.20 mL/min

Gly-Phe-Cys Tripeptide (57)

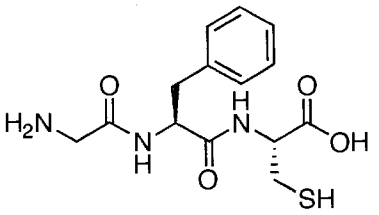

The Gly-Phe-L-Cys tripeptide **57** was prepared manually using PyBOP and NMM on preloaded H-Cys(Trt)-2-ClTrt resin on 0.75 mmol scale and was used as an HPLC standard for model studies. The synthesis was completed by the sequential addition of Fmoc Phe-OH and Fmoc-Gly-OH. Cleavage from resin, followed by HPLC purification using the analytical solvent system, t_R = 18.0 min, and lyophilization yielded the desired peptide standard. HRMS (ES) calcd for $C_{14}H_{19}N_3O_4S$ 325.1169, found 326.1164 (M+H).

Gly-Phe-D-Cys (58)

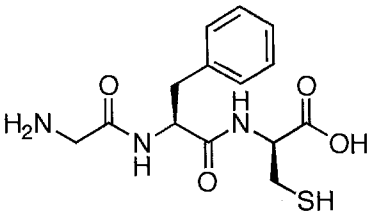

The Gly-Phe-D-Cys tripeptide **58** was prepared manually using PyBOP and NMM on 2-ClTrt resin (0.2 mmol scale) and was used as an HPLC standard for model studies. The resin was loaded with Fmoc-D-Cys-OH according to Section 7.1.5 and synthesized using the standard piperidine deprotection method (Section 7.1.6). The synthesis was completed by the sequential addition of Fmoc-Phe-OH and Fmoc-Gly-OH. Cleavage from resin, followed by HPLC purification using the analytical solvent system, t_R = 20.9 min, and lyophilization yielded the desired peptide standard. HRMS (ES) calcd for $C_{14}H_{19}N_3O_4S$ 325.1169, found 326.1167 (M+H).

Tripeptide Piperidine Adduct 59

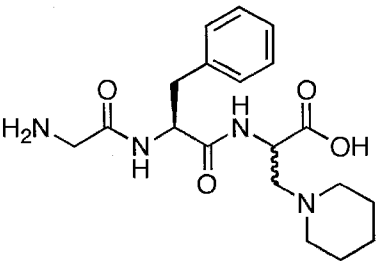

The tripeptide piperidine adduct **59** was separated by HPLC from the L-tripeptide Wang resin/piperidine synthesis of **57** and was identified by ES-MS and retention time according to published material[101] using the analytical solvent system, t_R = 23.4 min. HRMS ES calcd for $C_{19}H_{28}N_4O_4$ 376.2183, found 377.2181.

7.2.7 HPLC analysis of peptide synthesis methods

The following data is derived from the synthesis of **57** on Wang or 2-ClTrt resin using either:

1) Piperidine deprotection (as outlined in Section 7.1.7) or

2) DBU deprotection (2% DBU: 2% piperidine: 96% DMF in place of 20% piperidine in Section 7.1.7).

After resin cleavage, the results of the syntheses were compared by integration of peaks using analytical HPLC according to the retention time of synthesized standards: H-Gly-Phe-L-Cys (**57**), H-Gly-Phe-D-Cys (**58**), and piperidine adduct product (**59**).

H-Gly-Phe-L-Cys (Wang resin: Piperidine deprotection)

The peptide was synthesized on 0.2 mmol scale on resin preloaded with Fmoc-L-Cys(Trt)-Wang resin using the manual synthesis method outlined in section 7.1.6. The resin was divided into equal portions for testing of the following cleavage conditions:

1) 95% TFA, 2.5% H_2O, 2.5% TIPS-H

H-Gly-Phe-L-Cys- 63%, H-Gly-Phe-D-Cys- 6%, piperidine adduct- 31%

2) 5% TFA, 90% DCM, 5% TIPS-H

H-Gly-Phe-L-Cys- 44%, H-Gly-Phe-D-Cys- 6%, piperidine adduct- 50%

3) 95% TFA, 2% EDT, 2% H_2O, 1% TIPS-H

H-Gly-Phe-L-Cys- 87%, H-Gly-Phe-D-Cys- 9%, piperidine adduct- 4%

4) 71 % TFA, 5% EDT, 13% TMS-Br, 10% Thioanisole, 1% m-Cresol

H-Gly-Phe-L-Cys- 85%, H-Gly-Phe-D-Cys- 7%, piperidine adduct- 8%

H-Gly-Phe-L-Tripeptide (Wang resin: DBU deprotection)

The entire procedure for the above tripeptide synthesis was repeated using 2% DBU/ 2% piperidine/ 96% DMF instead of 20% piperidine.

1) 95% TFA, 2.5% H_2O, 2.5% TIPS-H

H-Gly-Phe-L-Cys- 51%, H-Gly-Phe-D-Cys- 28%, piperidine adduct- 21%

2) 5% TFA, 90% DCM, 5% TIPS-H

H-Gly-Phe-L-Cys- 30%, H-Gly-Phe-D-Cys- 24%, piperidine adduct- 46%

3) 95% TFA, 2% EDT, 2% H_2O, 1% TIPS-H

H-Gly-Phe-L-Cys- 65%, H-Gly-Phe-D-Cys- 32%, piperidine adduct- 3%

4) 71% TFA, 5% EDT, 13% TMS-Br, 10% Thioanisole, 1% m-Cresol

H-Gly-Phe-L-Cys- 60%, H-Gly-Phe-D-Cys- 31%, piperidine adduct- 9%

H-Gly-Phe-L-Cys (2-ClTrt resin: Piperidine deprotection)

The peptide was synthesized on 0.2 mmol scale preloaded with Fmoc-L-Cys(Trt)-2-ClTrt resin using the manual synthesis method outlined in section 7.1.6. The resin was divided into equal portions for testing of the following cleavage conditions:

1) 95% TFA, 2.5% H_2O, 2.5% TIPS-H

H-Gly-Phe-L-Cys- 93%, H-Gly-Phe-D-Cys- 7%, piperidine adduct- N.A.

2) 5% TFA, 90% DCM, 5% TIPS-H

H-Gly-Phe-L-Cys- 96%, H-Gly-Phe-D-Cys- 4%, piperidine adduct- N.A.

3) 95% TFA, 2% EDT, 2% H_2O, 1% TIPS-H

H-Gly-Phe-L-Cys- 96%, H-Gly-Phe-D-Cys- 4%, piperidine adduct- N.A.

4) 71% TFA, 5% EDT, 13% TMS-Br, 10% Thioanisole, 1% m-Cresol

H-Gly-Phe-L-Cys- 96%, H-Gly-Phe-D-Cys- 4%, piperidine adduct- N.A.

H-Gly-Phe-L-Cys (2-ClTrt resin: DBU deprotection)

The entire procedure for the above tripeptide synthesis was repeated using 2% DBU/ 2% piperidine/ 96% DMF instead of 20% piperidine.

1) 95% TFA, 2.5% H_2O, 2.5% TIPS-H

H-Gly-Phe-L-Cys- 87%, H-Gly-Phe-D-Cys- 13%, piperidine adduct- N.A.

2) 5% TFA, 90% DCM, 5% TIPS-H

H-Gly-Phe-L-Cys- 88%, H-Gly-Phe-D-Cys- 12%, piperidine adduct- N.A.

3) 95% TFA, 2% EDT, 2% H_2O, 1.0% TIP-S

H-Gly-Phe-L-Cys- 86%, H-Gly-Phe-D-Cys- 14%, piperidine adduct- N.A.

4) 71% TFA, 5% EDT, 13% TMS-Br, 10% Thioanisole, 1% m-Cresol

H-Gly-Phe-L-Cys- 84%, H-Gly-Phe-D-Cys- 13%, piperidine adduct- 3%

7.2.8 Preparation of orthoester containing compounds

(*R*)-[(3-Methyloxetan-3-yl) methyl]-2-(((9*H*-fluoren-9-yl) methoxy) carbonylamino)-3-(tritylthio)propanoate, Fmoc-Cys(Trt)- O-(3-methyl oxetane-3-yl) methanol. (60)

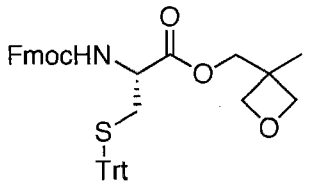

Fmoc-Cys(Trt)-OH (1.0 g, 1.7 mmol) was dissolved in dry DCM (10 mL) along with 1-hydroxybenzotriazole (HOBt, 0.26 g, 1.1 eq, 1.9 mmol) and 2-oxetane-2-methyl methanol (0.26 mL, 1.5 eq, 2.6 mmol). Finally, diisopropylcarbodiimide (DIPCDI, 0.26 mL, 1.7 mmol) was added and the resulting mixture was left to stir for 2 h. The reaction

mixture was then cooled to 0 °C for 5 min and filtered through a cotton plug. The solvent was then removed *in vacuo* and the remaining residue was purified by column chromatography (2:1 Hex:EtOAc) to yield the desired product as a white solid (920 mg, 81% yield). $[\alpha]_D^{25}$ 6.32 (*c* 1.05, CH_2Cl_2); IR (CH_2Cl_2, cast) 3308, 3058, 2962, 2874, 1725, 1491, 1447 cm^{-1}; ^1H NMR (CD_2Cl_2, 400MHz) δ 7.80 (br d, 2H, *J* = 7.6 Hz, ArH), 7.63 (br d, 2H, *J* = 6.4 Hz, ArH), 7.45-7.36 (m, 8H, ArH), 7.36-7.20 (m, 11H, ArH), 5.29 (m, 1H, NH), 4.38 (ap t, 4H, *J* = 5.7 Hz, oxetane CH_2), 4.32-4.27 (m, 3H, OCH_2 and Hα), 4.24 (br t, 1H, *J* = 7.0 Hz, Fmoc CH), 4.18 (br d, 2H, *J* = 7.4 Hz, Fmoc CH_2), 2.70-2.55 (m, 2H, Hβ), 1.26 (s, 3H, CCH_3); ^{13}C NMR (CD_2Cl_2, 100 MHz) δ 170.7, 155.9, 144.5, 144.2, 141.5, 129.7, 128.3, 128.2, 127.9, 127.8, 127.3, 127.1, 125.3, 120.2, 79.3, 70.0, 67.3, 47.4, 39.3, 34.2, 21.0; HRMS (ES) calcd for $C_{42}H_{39}NO_5SNa$ 692.2441, found 692.2439.

(*R*)-[(3-Methyloxetan-3-yl)methyl]-2-(((9*H*-fluoren-9-yl) methoxy) carbonylamino)-3-(*tert*-butyldisulfanyl)propanoate, Fmoc-Cys(S-*t*-Bu)-O-(3-methyl oxetane-3-yl) methanol. (61)

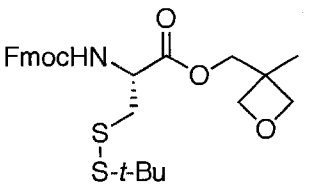

Fmoc-Cys(S-*t*-Bu)-OH (2.12 g, 4.91 mmol) was dissolved in dry DMF (15 mL) along with 1-hydroxybenzotriazole (HOBt, 0.663 g, 4.91 mmol) and 2-oxetane-2-methyl methanol (0.58 mL, 5.9 mmol). Finally, diisopropylcarbodiimide (DIPCDI, 0.76 mL, 4.91 mmol) was added to the solution and the resulting mixture was left to stir. After 2 h,

the solution was concentrated to dryness and purified by column chromatography (2:1 Hexane: EtOAc) to yield the desired product as a white solid (1.5 g, 59%). $[\alpha]_D^{25}$ -8.72 (*c* 1.37, CH_2Cl_2); IR (CH_2Cl_2, cast) 3322, 3064, 2961, 2874, 1725, 1527, 1451 cm^{-1}; ^1H NMR (CD_2Cl_2, 400MHz) δ 7.79 (d, 2H, *J* = 7.5 Hz, ArH), 7.63 (br d, 2H, *J* = 7.1 Hz, ArH), 7.42 (t, 2H, *J* = 7.5 Hz, ArH), 7.34 (br t, 2H, *J* = 7.5 Hz, ArH), 5.71 (br d, 1H, *J* = 8.4 Hz , NH), 4.74-4.69 (m, 1H Hα), 4.50-4.45 (m, 2H, oxetane CHH), 4.41-4.37 (m, 2H, oxetane CHH), 4.35 (d, 2H, *J* = 6.0 Hz), 4.28-4.24 (m, 3H, OCH_2C and Fmoc CH), 3.25 (dd, 1H, *J* = 13.4, 3.5 Hz, Hβ), 3.14 (dd, 1H, *J* = 13.6, 6.0 Hz, Hβ), 1.26 (s, 12H, CCH_3 and S-*t*-Bu); ^{13}C NMR (CD_2Cl_2, 100 MHz) δ 170.8, 155.9, 144.2, 144.1, 141.5, 127.9, 127.3, 125.3, 120.2, 79.4, 70.2, 67.3, 48.5, 47.4, 42.8, 39.3, 29.8, 21.0; HRMS (ES) calcd for $C_{27}H_{33}NO_5S_2Na$ 538.1692, found 538.1692.

(3-Methyloxetan-3-yl)methyl 4-methylbenzenesulfonate (67)[104]

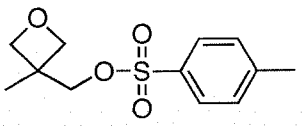

p-Toluenesulfonyl chloride (14.3 g, 75 mmol) was dissolved in pyridine (100 mL) under argon, and (3-methyloxetan-3-yl)methanol (5.0 mL, 50 mmol) was added dropwise. After 90 min of stirring, ice (100 g) was added and the resulting mixture was left to stir for another 30 min. The solution was then concentrated *in vacuo* to dryness and was then placed onto a vacuum filter (in the fumehood). The solid was washed repeatedly with cold water (milli-Q) until the solid remained completely white. The product was then left on high vacuum to remove all traces of water to yield the product as a white solid (9.2 g, 72%). IR (CH_2Cl_2, cast) 2966, 2875, 1598, 1460, 1359, 1176 cm^{-1}; ^1H NMR (CD_2Cl_2,

400 MHz) δ 7.79 (d, 2H, J = 8.6 Hz, ArH), 7.39 (d, 2H, J = 8.5 Hz, ArH), 4.32 (d, 2H, J = 11.9 Hz, 2 x oxetane CHH), 4.31 (d, 2H, J = 12.0 Hz, 2 x oxetane CHH), 4.07 (s, 2H, OCH_2C), 2.46 (s, 3H, $ArCH_3$), 1.27 (s, 3H, CCH_3); ^{13}C NMR (CD_2Cl_2, 100 MHz) δ 145.5, 132.8, 130.2, 128.1, 78.9, 74.6, 39.4, 21.6, 20.6; HRMS (ES) calcd for $C_{12}H_{16}O_4SNa$ 279.0662, found 279.0664.

(*S*)-(3-methyloxetan-3-yl)methyl-2-(benzyloxycarbonylamino)-3-hydroxy-propanoate, Cbz-L-Serine-O-[(3-Methyloxetan-3-yl)methanol (68)

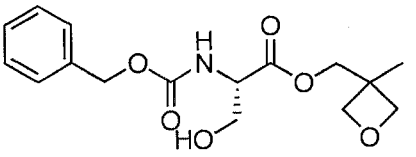

Cesium carbonate (9.22 g, 283 mmol) was slowly added to a solution of Cbz-Ser-OH (11.38 g, 47.6 mmol) in H_2O (50 mL) at room temperature. The resulting mixture was stirred for 19 h, then frozen in an acetone / dry ice bath, and lyopholized to produce a white foam. The lyophilized product was dissolved in dry DMF (350 mL) followed by the addition of oxetane tosylate **67** (12.56 g, 49.0 mmol), and sodium iodide (1.47 g, 9.8 mmol). The mixture was stirred for 72 h, and was then frozen and lypholized to a white foam. The product was dissolved in EtOAc (600 mL) and washed successively with H_2O (200 mL), 10% $NaHCO_3$ (2 x 100 mL) and brine (100 mL). The EtOAc layer was then dried over $MgSO_4$. Following filtration and solvent removal under reduced pressure, a yellow oil was obtained (13.7 g, 89%). $[\alpha]_D^{25}$ = -9.06 (*c* 1.0, CH_2Cl_2); IR (CH_2Cl_2, cast) 3500-3100, 2962, 2879, 1722, 1529, 1456 cm^{-1}; ^1H-NMR ($CDCl_3$, 400 MHz) δ 7.39-7.30 (m, 5H, ArH), 5.73 (br d, 1H, J = 6.8, NH), 5.12 (s, 2H, $ArCH_2O$), 4.53-4.50 (m, 2H, Hβ), 4.49-4.39 (m, 4H, 2 x oxetane CH_2), 4.12 (d, 2H, OCHHC), 3.98

(m, 1H, Hα), 3.29 (t, 1H, J = 6.0, OH), 1.26 (s, 3H, CCH$_3$); ^{13}C-NMR ($CDCl_3$, 100 MHz) δ 170.7, 156.3, 136.1, 128.5, 128.2, 128.1, 79.4, 69.0, 67.1, 63.2, 56.3, 39.5, 20.8; HRMS (ES) calcd for $C_{16}H_{21}NO_6Na$ 346.1261, Found 346.1260.

(*S*)-Benzyl-2-hydroxy-1-(4-methyl-2,6,7-trioxabicyclo[2.2.2]octan-1-yl) ethylcarbamate, Cbz-L-serine OBO Ester[104] (69)

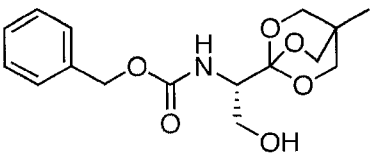

Serine derivative **68** (5.8 g, 17.9 mmol) was dissolved in DCM (150 mL) and cooled to 0 °C. In a separate vessel, BF_3•OEt_2 (45 μL, 0.36 mmol, 2 mol%) was dissolved in dry DCM (2 mL) and added dropwise to the cooled solution. The mixture was allowed to warm to room temperature and left to react for 2.5 h. To quench the reaction, triethylamine (1 mL) was added and the mixture was left to stir for an additional 30 min. The solvent was then removed *in vacuo* and the crude product was dissolved in EtOAc (150 mL) and washed with brine (100 mL). The organic layer was dried with Na_2SO_4, filtered, and purified by column chromatography (3:1, EtOAc/Hex) to yield the product as a white solid (3.8 g, 60% yield). $[\alpha]_D^{25}$ = -31.44 (*c* 1.0, EtOAc; Lit. -24.8, *c* 1.0, EtOAc); IR (CH_2Cl_2, cast) 3600-3200, 3033, 2939, 2882, 1723, 1525 cm^{-1}; ^{1}H-NMR (CD_2Cl_2, 600 MHz) δ 7.34 (m, 5H, ArH), 5.29 (br d, 1H, J = 8.4 Hz, NH), 5.08 (s, 2H, ArCH$_2$O), 3.92 (s, 6H, 3 x OCH$_2$C), 3.82 (ddd, 1H, J = 9.0, 4.8, 4.2 Hz, Hα), 3.75 (ddd, 1H, J = 11.4, 4.8, 4.2 Hz, Hβ), 3.63 (ddd, 1H, J = 11.4, 8.4, 4.8 Hz, Hβ), 2.44 (dd, 1H, J = 8.4, 5.4 Hz, OH), 0.80 (s, 3H, CCH$_3$); ^{13}C-NMR (CD_2Cl_2, 125 MHz) δ 156.7, 137.2,

128.8, 128.4, 128.3, 108.7, 73.1, 67.1, 62.2, 56.1, 30.9, 14.4; HRMS (ES) calcd for $C_{16}H_{22}NO_6$ 324.1442, Found 324.1444.

(*S*)-2-(Benzyloxycarbonylamino)-2-(4-methyl-2,6,7-trioxabicyclo [2.2.2]octan-1-yl) ethyl methanesulfonate, Cbz-Ser(Ms)-OBO (70)

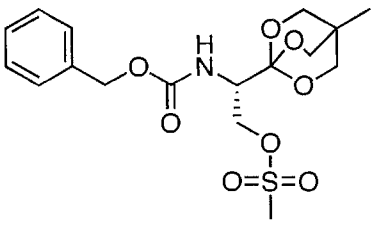

Cbz-Ser-OBO **69** (460 mg, 1.4 mmol) was dissolved in dry DCM (5 mL) under argon and cooled to 0 °C. Triethylamine (0.35 mL, 2 eq, 2.8 mmol) was then added to the solution followed by methanesulfonyl chloride (0.130 mL, 1.2 eq, 1.7 mmol). The solution was maintained at 0 °C for 15 min and then allowed to warm to room temperature for 10 min. The solvent was then evaporated *in vacuo* and purified by column chromatography (2:1 EtOAc: hexane containing 1% triethylamine) to yield the desired product as a white solid (380 mg, 68%). $[\alpha]_D^{25}$ = -23.67 (*c* 1.45, EtOAc); IR (EtOAc, cast) 3366, 3032, 2940, 2884, 1728, 1528, 1457 cm^{-1}; ^{1}H-NMR (CD_2Cl_2, 400 MHz) δ 7.34 (m, 5H, ArH), 5.25 (d, 1H, *J* = 7.8 Hz, NH) 5.08 (m, 2H, $ArCH_2O$), 4.44 (m, 1H, Hβ), 4.16 (m, 2H, Hα and Hβ), 3.90 (s, 6H, 3 x OCH_2C), 2.91 (s, 3H, SO_2CH_3), 0.78 (s, 3H, CCH_3); ^{13}C-NMR (CD_2Cl_2, 125 MHz) δ 156.3, 136.9, 128.7, 128.3, 128.2, 107.3, 73.0, 68.6, 67.1, 54.5, 37.6, 30.7, 14.1; HRMS (ES) calcd for $C_{17}H_{23}NO_8NaS$ 424.1037, found 424.1032 (M+Na).

(*S*)-2-(benzyloxycarbonylamino)-2-(4-methyl-2,6,7-trioxabicyclo[2.2.2]octan-1-yl)ethyl 4-methylbenzenesulfonate, Cbz-L-serine tosylate OBO Ester (71)

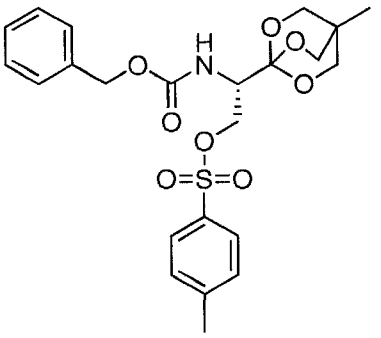

Cbz-Ser-OBO **69** (3.8 g, 11.8 mmol) was dissolved in DCM (40 mL) and cooled to 0 °C. Triethylamine (4.9 mL, 35.2 mmol) was added followed by *p*-toluenesulfonyl chloride (4.58 g, 24.0 mmol). The reaction mixture was left to stir for 15 min at 0 °C and then the ice bath was removed, allowing the reaction to warm to room temperature and react for 2 h. The mixture was concentrated *in vacuo* and then purified by column chromatography (1:1 EtOAc/hexane with 1% NEt_3) to yield a white solid (4.0 g, 71%). $[\alpha]_D^{25}$ -8.79 (*c* 1.04, DCM); IR (CH_2Cl_2, cast) 3500-3200, 2961, 2884, 1782, 1521, 1456 cm^{-1}; ^{1}H-NMR (CD_2Cl_2, 400 MHz) δ 7.73 (d, 2H, *J* = 8.0 Hz, SO_2ArH), 7.60-7.34 (m, 7H, ArH), 5.07 (s, 2H, $ArCH_2O$), 4.98 (br d, 1H, *J* = 12.0 Hz, NH), 4.23 (dd, 1H, *J* = 10.0, 3.6 Hz, Hβ), 4.05 (ddd, 1H, *J* = 9.6, 8.0, 3.6 Hz, Hα), 3.97 (dd, 1H, *J* = 10.0, 8.0 Hz, Hβ), 3.84 (s, 6H, 3 x OCH_2C), 2.42 (s, 3H, $ArCH_3$), 0.76 (s, 3H, CCH_3); ^{13}C-NMR (CD_2Cl_2, 100 MHz) δ 145.2, 136.9, 133.1, 130.3, 130.0, 128.6, 128.2, 128.1, 128.0, 107.2, 73.0, 69.2, 68.7, 67.0, 30.7, 21.6, 14.1; HRMS (ES) calcd for $C_{23}H_{27}NO_8SNa$ 500.1349, Found 500.1347.

(*S*)-2-amino-2-(4-methyl-2,6,7-trioxabicyclo[2.2.2]octan-1-yl)ethyl-4-methylbenzene-sulfonate, L-Serine tosylate OBO Ester (72)

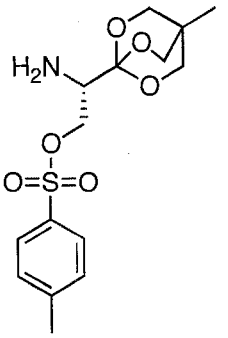

Compound **71** (1.04 g, 2.2 mmol) was dissolved in EtOAc (100 mL) followed by the addition of 1% palladium on carbon (0.109 g, 10% by weight of starting material) in EtOAc (5 mL). The reaction vessel was evacuated and then placed under a hydrogen atmosphere. The resulting reaction mixture was stirred for 3 h. The resulting mixture was filtered through Celite and the solvent was removed *in vacuo* to provide a white powder (0.6 g, 81%). $[\alpha]_D^{25}$ -13.57 (*c* 1.06, DCM); IR (CH_2Cl_2, cast) 3388, 3300, 2925, 1597, 1460, 1357, 1178 cm^{-1}; ^{1}H-NMR (CD_2Cl_2, 600 MHz) δ 7.77 (d, 2H, *J* = 7.8 Hz, Ar<u>H</u>), 7.36 (d, 2H, *J* = 7.8 Hz, Ar<u>H</u>), 4.22 (dd, 1H, *J* = 10.2, 3.0 Hz, Hβ), 3.83 (s, 6H, 3 x O<u>CH</u>$_2$C), 3.81 (dd, 1H, *J* = 10.2, 9.0 Hz, <u>H</u>β), 3.04 (dd, 1H, *J* = 9.0, 3.0 Hz, <u>H</u>α), 2.45 (s, 3H, Ar<u>CH</u>$_3$), 1.85 (br s, 2H, N<u>H</u>$_2$), 0.76 (s, 3H, C<u>CH</u>$_3$); HRMS (ES) calcd for $C_{15}H_{22}NO_6S$ 344.1162, found 344.1160 (M+H). Attempts to dissolve **72** in DMF, followed by reaction with trityl thiol resin and synthesize **57,** yielded only a trace amount of the desired cysteine product due to instability of **72**.

(*R*)-*S*-2-(Benzyloxycarbonylamino)-2-(4-methyl-2,6,7-trioxabicyclo[2.2.2]octan-1-yl)ethyl ethanethioate, Cbz-Cys(Ac)-OBO ester (74)

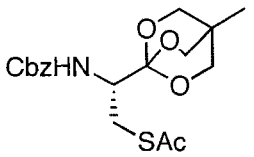

Cbz-Ser(Tos)-OBO **71** (300 mg, 0.63 mmol) was dissolved in dry DMF (7 mL) with triethylamine (0.26 mL, 3 eq, 1.9 mmol). Potassium thioacetate (0.215 g, 3 eq, 1.9 mmol) was then added to the solution and the resulting mixture was heated to 50 °C for 6 h. The solvent was then removed *in vacuo* and the remaining residue was dissolved in EtOAc (75 mL) and washed with sat. aq. $NaHCO_3$ (2 x 10 mL) and brine (2 x 10 mL) and dried with anhydrous Na_2SO_4. Charcoal (2 g) was then added to the solution and the mixture was left to stand for 10 min with occasional swirling. The mixture was then filtered through a pad of celite, concentrated *in vacuo* and purified by column chromatography (1:1 hexane: EtOAc) to yield the desired product as a white solid (325 mg, 80 %). $[\alpha]_D^{25}$ = -48.74 (*c* 1.20, DCM); IR (DCM, cast) 3400-3200, 3032, 2938, 2881, 1728, 1692, 1520, 1456, 1231 cm^{-1}; ^{1}H-NMR (CD_2Cl_2, 300 MHz) δ 7.34 (m, 5H, Ar<u>H</u>), 5.12 (d, 1H, *J* = 12.5 Hz, ArC<u>H</u>H), 5.05 (d, 1H, *J* = 12.5 Hz, ArCH<u>H</u>) 4.98 (m, 1H, N<u>H</u>), 3.91 (m, 7H, <u>H</u>α and 3 x OC<u>H</u>$_2$C), 3.25 (dd, 1H, *J* = 14.1, 3.9 Hz, <u>H</u>β), 2.96 (dd, 1H, *J* = 14.1, 10.5 Hz, <u>H</u>β), 2.25 (s, 3H, SCOC<u>H</u>$_3$), 0.78 (s, 3H, CC<u>H</u>$_3$); ^{13}C-NMR (CD_2Cl_2, 100 MHz) δ 196.2, 156.7, 137.5, 129.0, 128.5, 128.4, 108.4, 73.4, 67.1, 55.3, 31.1, 30.8, 30.2, 14.5; HRMS (ES) calcd. for $C_{18}H_{23}NO_6SNa$ 404.1138, Found 404.1136.

7.2.9 Crotalphine peptides

All of the crotalphine peptides were synthesized in a similar fashion using the following protected amino acids: Fmoc-Cys(Mmt)-OH, Fmoc-Gln(Trt)-OH, Fmoc-Ser(O-*t*-Bu), Fmoc-Glu(O-*t*-Bu), Fmoc-Asn(Trt)-OH. Natural crotalphine and analogues containing a *C*-terminal cysteine were synthesized on preloaded H-Cys(Trt)-2-Cl-Trt resin (0.75 mmol/g loading). Other analogues were prepared on Wang resin and loaded according to the method outlined in Section 7.1.4. Peptides were prepared on a 0.25 mmol scale and the syntheses were split after coupling of Phe 2 to allow analogues to be introduced in place of pyroglutamic acid 1. The peptides were cyclized by dissolving 10 mg of crude peptide (cleaved, washed with ether and dried) in 1 mL of 1 mM ammonium bicarbonate buffer at pH 8. The solutions were bubbled with oxygen for 15 min and then left to stir for 16 hours. It is important to note that MALDI TOF-MS data can also be acquired using negative ion mode instead of positive ion mode. The crotalphine structure does not have any negatively charged side chains or even a free *N*-terminus so signals are very weak in positive mode.

"Natural" Crotalphine Containing Extract (77)

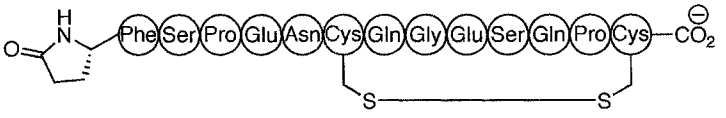

Lyophilized, crude snake venom from *Crotalus durissus terrificus* (600 mg, Cedar Lane Laboratories) was suspended in milli-Q water (30 mL) and placed into six separate molecular weight cut-off filters (5000 MWCO, Amicon, cellulose centrifugal Filter Device) and placed into a centrifuge at 5000 *g* for 20 min. Solution that went *through* the

filter was combined, frozen and lyophilized to yield a colorless oil without the high molecular weight toxic components (160 mg of filtered compound). The desired mass of crotalphine was not able to be detected by MALDI-TOF MS. Based on the information that one snake produces 20 mg of crude venom at a time, the initial sample was taken to represent the equivalent of 30 snake bites. This semi-purified sample of 160 mg lyophilized venom was used as the positive control in subsequent biological testing.

[C7a, C14a]-Crotalphine (78)

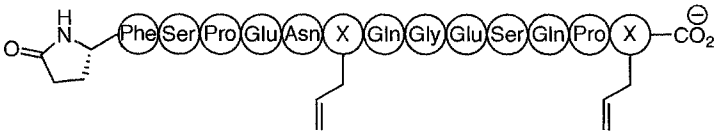

The peptide was prepared on a 0.3 mmol scale using Wang resin (0.8 mmol/g, 1% DVB, 100-200 mesh) that was loaded according to standard procedures with Fmoc-AllylGly-OH as outlined in Section 7.1.6. Amino acids were coupled using the amino acid (0.9 mmol, 3 eq), PyBOP (0.85 mmol, 2.8 eq) and NMM (2.25 mmol, 7.5 eq) and standard manual SPPS in the following order: Fmoc-Pro-OH, Fmoc-Gln(Trt)-OH, Fmoc-Ser(O-*t*Bu)-OH, Fmoc-Glu(O-*t*Bu)-OH, Fmoc-Gly-OH (double coupling), Fmoc-Gln(Trt)-OH and Fmoc-AllylGly-OH. The resin was then split into thirds, with one third carrying forward in the synthesis and one third being used for the preparation of [7, 14]-dicarba crotalphine, **81**. One portion of the resin (0.1 mmol) was further extended with the residues: Fmoc-Asn(Trt)-OH, Fmoc-Glu(O-*t*Bu)-OH, Fmoc-Pro-OH, Fmoc-Ser(O-*t*Bu)-OH, Fmoc-Phe-OH. The resin was again split so that half (0.05 mmol) was carried to the product **78** by addition of pyroglutamic acid, while the remaining half (0.05 mmol) was stored on resin to be used in examination of pyroglutamic acid analogues. The resin was then cleaved, purified by HPLC using solvent system J, t_R = 22.7 min, and lyophilized to

yield the desired product as a white solid (3.6 mg, 21% based on purification of 17.2 mg of triturated/ dried, crude product). MALDI-TOF MS: calcd for $C_{66}H_{93}N_{17}O_{25}Na$ 1546.6, found 1546.9 (M+Na).

[C7F, C14F]-Crotalphine (79)

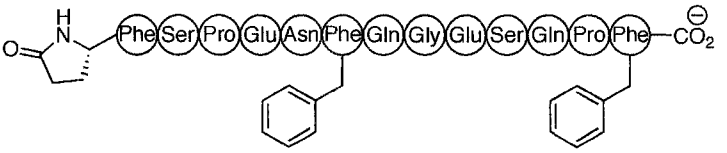

The product was synthesized in an identical fashion to [C7a, C14a]-Crotalphine (**78**) by Ms. Avena Ross except that phenylalanine residues were incorporated at positions 7 and 14. The resin was then cleaved, purified by HPLC using solvent system J, t_R = 27.3 min and lyophilized to yield the desired product as a white solid (3.7 mg, 33% based on purification of 11.1 mg of triturated/ dried, crude product). MALDI-TOF MS: calcd for $C_{74}H_{97}N_{17}O_{25}Na$ 1646.7, found 1647.0 (M+Na).

[C7S, C14S]-Crotalphine (80)

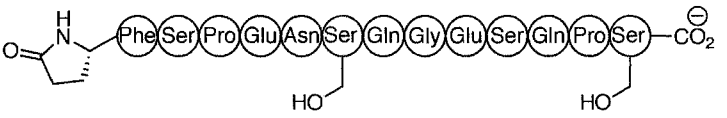

The product was synthesized on resin in an identical fashion to [C7a, C14a]-Crotalphine (**78**) by Ms. Avena Ross except that serine residues were incorporated at positions 7 and 14 The resin was then cleaved, purified by HPLC using solvent system J, t_R = 19.1 min and lyophilized to yield the desired product as a white solid (2.3 mg, 26% based on purification of 9.0 mg of triturated/ dried, crude product). MALDI-TOF MS: calcd for $C_{62}H_{89}N_{17}O_{27}Na$ 1526.6, found 1526.9 (M+Na).

[C7b, C14b]- Crotalphine, Dicarba Crotalphine (81)

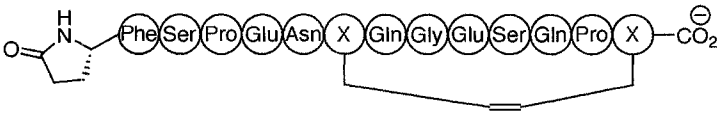

The on-resin [C7a, C14a]-Crotalphine [7-14] fragment from the synthesis of **78** (0.1 mmol) was suspended in DCM (5 mL) and was bubbled with argon for 20 minutes before adding 20 mol% Grubbs second generation catalyst[72] (17 mg) to the reaction vessel. The vessel was equipped with heat tape and a condenser and was heated to reflux for 14 hours. After this time, the reaction vessel was drained and washed with DCM (3 x 5 mL). A test cleavage of the resin was consistent with all of the starting material being transformed to product (no SM mass and only product mass). The resin was then left in a solution of DCM (5 mL) and DMSO (150 μL, 2 mmol, 100 eq relative to catalyst) for 24 h and was then drained, washed repeatedly with DCM (5 x 5 mL) and DMF (3 x 5 mL). The synthesis was then completed by sequential coupling of the following residues: Fmoc-Asn(Trt)-OH, Fmoc-Glu(O-*t*Bu)-OH, Fmoc-Pro-OH, Fmoc-Ser(O-*t*Bu)-OH, Fmoc-Phe-OH. The resin was again split so that half (0.05 mmol) could be carried to the product and half (0.05) could be used to examine analogues of pyroglutamic acid. The resin was then cleaved, purified by HPLC using solvent system J, t_R = 22.8 min and lyophilized to yield the desired product as a white solid (1.8 mg, 14% based on purification of 13.0 mg of triturated/ dried, crude product). MALDI-TOF MS calcd for $C_{64}H_{89}N_{17}O_{25}Na$ 1518.6, found 1518.9 (M+Na).

[q1P]-Crotalphine (82)

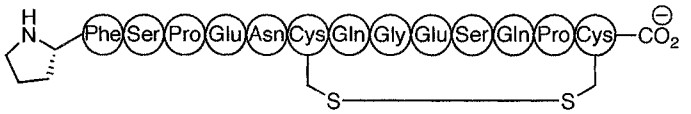

The peptide was prepared on a 0.25 mmol scale using preloaded H-Cys(Trt)-2-ClTrt resin (0.75 mmol/g) by automated synthesis according to the method outlined in Section 7.1.7. The residues Fmoc-Pro-OH, Fmoc-Gln(Trt)-OH, Fmoc-Ser(O-*t*Bu)-OH, Fmoc-Glu(O-*t*Bu)-OH, Fmoc-Gly-OH, Fmoc-Gln(Trt)-OH, Fmoc-Cys(Trt)-OH, Fmoc-Asn(Trt)-OH, Fmoc-Glu(O-*t*Bu)-OH, Fmoc-Pro-OH, Fmoc-Ser(O-*t*Bu)-OH and Fmoc-Phe-OH were added on the peptide synthesizer. The resin was then split into 5 portions of 0.05 mmol each. Fmoc-Pro-OH was then added by manual synthesis and after Fmoc removal, was cleaved from the resin. The solid was triturated repeatedly with diethyl ether leaving a white powder and the sample was then dried on high vacuum for 12 h. A portion of the dried material (10.5 mg) was suspended in $(NH_4)_2CO_3$ buffer (1 mM, pH 8.0) and the pH was adjusted to 8.0. Oxygen was bubbled through the solution for 30 minutes and the resulting solution was left to stir for 16 h. The solution was then concentrated *in vacuo* to a volume of less than 1 mL, purified by HPLC using solvent system J, t_R = 19.9 min, and lyophilized to yield the desired product as a white solid (3.4 mg, 33% based on purification of 10.5 mg of triturated/ dried, crude product). MALDI-TOF MS: calcd for $C_{62}H_{89}N_{17}O_{24}S_2$ 1519.6, found 1520.8 (M+H).

[q1AcP]-Crotalphine (83)

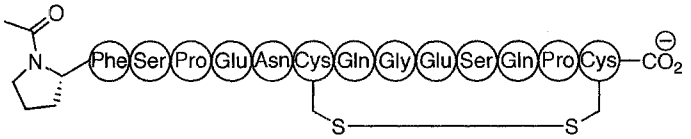

Peptide **83** was prepared on a portion (0.05 mmol) of the 14-mer prepared in [q1P]-Crotalphine **(82)**. Fmoc-Pro-OH was added by manual synthesis and after Fmoc removal, the free *N*-terminus was acylated using 20% acetic anhydride in DMF. Cleavage and cyclization were completed in the same manner as was used for the synthesis of **82**. The product **83** was purified by HPLC using solvent system J, t_R = 23.0 min, and lyophilized to yield the desired product as a white solid (3.48 mg, 35% based on purification of 10.0 mg of triturated/ dried, crude product). MALDI-TOF MS calcd for $C_{64}H_{91}N_{17}O_{25}S_2Na$ 1584.6, found 1584.9 (M+Na).

8. REFERENCES

1. Dawson, P. E.; Kent, S. B. H. Synthesis of native proteins by chemical ligation. *Annu. Rev. Biochem.* **2000**, *69*, 923-960.
2. Marx, V. Watching peptide drugs grow up. *Chem. Eng. News* **2005**, *83*, 17-24.
3. Marx, V. Roche's Fuzeon challenge. *Chem. Eng. News* **2005**, *83*, 16-17.
4. Jarvis, L. M. Breakthroughs in manufacturing are making large-scale synthesis of peptides a viable proposition. *Chem. Eng. News* **2006**, *84*, 23-25.
5. Cotter, P. D.; Hill, C.; Ross, R. P. Bacteriocins: Developing innate immunity for food. *Nat. Rev. Microbiol.* **2005**, *3*, 777-788.
6. Hackeng, T. M.; Griffin, J. H.; Dawson, P. E. Protein synthesis by native chemical ligation: Expanded scope by using straightforward methodology. *Proc. Natl. Acad. Sci. U.S.A.* **1999**, *96*, 10068-10073.
7. Muir, T. W. Semisynthesis of proteins by expressed protein ligation. *Annu. Rev. Biochem.* **2003**, *72*, 249-289.
8. Saxon, E.; Bertozzi, C. R. Cell surface engineering by a modified Staudinger reaction. *Science* **2000**, *287*, 2007-2010.
9. Shin, Y.; Winans, K. A.; Backes, B. J.; Kent, S. B. H.; Ellman, J. A.; Bertozzi, C. R. Fmoc-based synthesis of peptide-α-thioesters: Application to the total chemical synthesis of a glycoprotein by native chemical ligation. *J. Am. Chem. Soc.* **1999**, *121*, 11684-11689.
10. Ingenito, R.; Bianchi, E.; Fattori, D.; Pessi, A. Solid phase synthesis of peptide C-terminal thioesters by Fmoc/t-Bu chemistry. *J. Am. Chem. Soc.* **1999**, *121*, 11369-11374.

11. Yan, L. Z.; Dawson, P. E. Synthesis of peptides and proteins without cysteine residues by native chemical ligation combined with desulfurization. *J. Am. Chem. Soc.* **2001**, *123*, 526-533.

12. Mutter, M.; Nefzi, A.; Sato, T.; Sun, X.; Wahl, F.; Wohr, T. Pseudo-prolines (psi-Pro) for accessing inaccessible peptides. *Int. J. Pept. Res. Ther.* **1995**, *8*, 145-153.

13. Haack, T.; Mutter, M. Serine derived oxazolidines as secondary structure disrupting, solubilizing building-blocks in peptide-synthesis. *Tetrahedron Lett.* **1992**, *33*, 1589-1592.

14. Sampson, W. R.; Patsiouras, H.; Ede, N. J. The synthesis of 'difficult' peptides using 2-hydroxy-4-methoxybenzyl or pseudoproline amino acid building blocks: a comparative study. *J. Pept. Sci.* **1999**, *5*, 403-409.

15. White, P.; Keyte, J. W.; Bailey, K.; Bloomberg, G. Expediting the Fmoc solid phase synthesis of long peptides through the application of dimethyloxazolidine dipeptides. *J. Pept. Sci.* **2004**, *10*, 18-26.

16. Woehr, T.; Wahl, F.; Nefzi, A.; Rohwedder, B.; Sato, T.; Sun, X.; Mutter, M. Pseudo-prolines as a solubilizing, structure-disrupting protection technique in peptide synthesis. *J. Am. Chem. Soc.* **1996**, *118*, 9218-9227.

17. Offer, J.; Quibell, M.; Johnson, T. On-resin solid-phase synthesis of asparagine N-linked glycopeptides: Use of N-(2-acetoxy-4-methoxybenzyl) (AcHmb) aspartyl amide-bond protection to prevent unwanted aspartimide formation. *J. Chem. Soc., Perkin Trans. 1* **1996**, 175-182.

18. Packman, L. C. N-2-Hydroxy-4-methoxybenzyl (Hmb) backbone protection strategy prevents double aspartimide formation in a difficult peptide sequence. *Tetrahedron Lett.* **1995**, *36*, 7523-7526.

19. Quibell, M.; Owen, D.; Packman, L. C.; Johnson, T. Suppression of piperidine-mediated side product formation for Asp(O-t-Bu)-containing peptides by the use of N-(2-hydroxy-4-methoxybenzyl) (Hmb) backbone amide protection. *J. Chem. Soc., Chem. Commun.* **1994**, 2343-2344.

20. Wright, G. D. Bacterial resistance to antibiotics: Enzymatic degradation and modification *Adv. Drug Deliv. Rev.* **2005**, *57*, 1451-1470.

21. Garneau, S.; Martin, N. I.; Vederas, J. C. Two-peptide bacteriocins produced by lactic acid bacteria. *Biochimie* **2002**, *84*, 577-592.

22. Nes, I. F.; Diep, D. B.; Havarstein, L. S.; Brurberg, M. B.; Eijsink, V.; Holo, H. Biosynthesis of bacteriocins in lactic acid bacteria. *Anton. Leeuw. Int. J. G.* **1996**, *70*, 113-128.

23. Cintas, L. M.; Casaus, M. P.; Herranz, C.; Nes, I. F.; Hernandez, P. E. Review: Bacteriocins of lactic acid bacteria. *Food Sci. Technol. Int.* **2001**, *7*, 281-305.

24. van Belkum, M. J.; Stiles, M. E. Nonlantibiotic antibacterial peptides from lactic acid bacteria. *Nat. Prod. Rep.* **2000**, *17*, 323-335.

25. Klaenhammer, T. R. Genetics of bacteriocins produced by lactic acid bacteria. *FEMS Microbiol. Rev.* **1993**, *12*, 39-86.

26. Cotter, P. D.; Hill, C.; Ross, R. P. What's in a name? Class distinction for bacteriocins - Author reply. *Nat. Rev. Microbiol.* **2006**, *4*.

27. Heng, N. C. K.; Tagg, J. R. What's in a name? Class distinction for bacteriocins. *Nat. Rev. Microbiol.* **2006**, *4*.

28. Stiles, M. E.; Holzapfel, W. H. Lactic acid bacteria of foods and their current taxonomy. *Int. J. Food. Microbiol.* **1997**, *36*, 1-29.

29. Chatterjee, C.; Paul, M.; Xie, L. L.; van der Donk, W. A. Biosynthesis and mode of action of lantibiotics. *Chem. Rev.* **2005**, *105*, 633-683.

30. Drider, D.; Fimland, G.; Hechard, Y.; McMullen, L. M.; Prevost, H. The continuing story of class IIa bacteriocins. *Microbiol Mol Biol Rev* **2006**, *70*, 564-582.

31. Fukase, K.; Kitazawa, M.; Sano, A.; Shimbo, K.; Fujita, H.; Horimoto, S.; Wakamiya, T.; Shiba, T. Total synthesis of peptide antibiotic nisin. *Tetrahedron Lett.* **1988**, *29*, 795-798.

32. Sailer, M.; Helms, G. L.; Henkel, T.; Niemczura, W. P.; Stiles, M. E.; Vederas, J. C. N-15-labeled and C-13-labeled media from *Anabaena sp.* for universal isotopic labeling of bacteriocins - NMR resonance assignments of leucocin-A from *Leuconostoc gelidum* and nisin A from *Lactococcus lactis*. *Biochemistry* **1993**, *32*, 310-318.

33. Gallagher, N. L. F.; Sailer, M.; Niemczura, W. P.; Nakashima, T. T.; Stiles, M. E.; Vederas, J. C. Three-dimensional structure of leucocin A in trifluoroethanol and dodecylphophocholine micelles: Spatial location of residues critical for biological activity in type IIa bacteriocins from lactic acid bacteria. *Biochemistry* **1997**, *36*, 15062-15072.

34. Henkel, T.; Sailer, M.; Helms, G. L.; Stiles, M. E.; Vederas, J. C. NMR assignment of leucocin-A, a bacteriocin from *Leuconostoc gelidum*, supported by a stable

isotope labeling technique for peptides and proteins. *J. Am. Chem. Soc.* **1992**, *114*, 1898-1900.

35. Wang, Y. J.; Henz, M. E.; Gallagher, N. L. F.; Chai, S. Y.; Gibbs, A. C.; Yan, L. Z.; Stiles, M. E.; Wishart, D. S.; Vederas, J. C. Solution structure of carnobacteriocin B2 and implications for structure-activity relationships among type IIa bacteriocins from lactic acid bacteria. *Biochemistry* **1999**, *38*, 15438-15447.

36. Haugen, H. S.; Fimland, G.; Nissen-Meyer, J.; Kristiansen, P. E. Three-dimensional structure in lipid micelles of the pediocin-like antimicrobial peptide curvacin A. *Biochemistry* **2005**, *44*, 16149-16157.

37. Uteng, M.; Hauge, H. H.; Markwick, P. R. L.; Fimland, G.; Mantzilas, D.; Nissen-Meyer, J.; Muhle-Goll, C. Three-dimensional structure in lipid micelles of the pediocin-like antimicrobial peptide sakacin P and a sakacin P variant that is structurally stabilized by an inserted C-terminal disulfide bridges. *Biochemistry* **2003**, *42*, 11417-11426.

38. Fimland, G.; Blingsmo, O. R.; Sletten, K.; Jung, G.; Nes, I. F.; Nissen-Meyer, J. New biologically active hybrid bacteriocins constructed by combining regions from various pediocin-like bacteriocins: The *C*-terminal region is important for determining specificity. *Appl. Environ. Microbiol.* **1996**, *62*, 3313-3318.

39. Fimland, G.; Johnsen, L.; Axelsson, L.; Brurberg, M. B.; Nes, I. F.; Eijsink, V. G. H.; Nissen-Meyer, J. A C-terminal disulfide bridge in pediocin-like bacteriocins renders bacteriocin activity less temperature dependent and is a major determinant of the antimicrobial spectrum. *J. Bacteriol.* **2000**, *182*, 2643-2648.

40. Kaur, K.; Andrew, L. C.; Wishart, D. S.; Vederas, J. C. Dynamic relationships among type IIa bacteriocins: Temperature effects on antimicrobial activity and on structure of the *C*-terminal amphipathic α-helix as a receptor-binding region. *Biochemistry* **2004**, *43*, 9009-9020.

41. Hechard, Y.; Derijard, B.; Letellier, F.; Cenatiempo, Y. Characterization and purification of mesentericin Y105, an anti-*Listeria* bacteriocin from *Leuconostoc mesenteroides*. *J. Gen. Microbiol.* **1992**, *138*, 2725-2731.

42. Diep, D. B.; Skaugen, M.; Salehian, Z.; Holo, H.; Nes, I. F. Common mechanisms of target cell recognition and immunity for class II bacteriocins. *Proc. Natl. Acad. Sci. U.S.A.* **2007**, *104*, 2384-2389.

43. Erni, B. The mannose transporter complex: an open door for the macromolecular invasion of bacteria. *J. Bacteriol.* **2006**, *188*, 7036-7038.

44. Ramnath, M.; Arous, S.; Gravesen, A.; Hastings, J. W.; Hechard, Y. Expression of mptC of *Listeria monocytogenes* induces sensitivity to class IIa bacteriocins in *Lactococcus lactis*. *Microbiology-(UK)* **2004**, *150*, 2663-2668.

45. Gravesen, A.; Ramnath, M.; Rechinger, K. B.; Andersen, N.; Jansch, L.; Hechard, Y.; Hastings, J. W.; Knochel, S. High-level resistance to class IIa bacteriocins is associated with one general mechanism in *Listeria monocytogenes*. *Microbiology-(UK)* **2002**, *148*, 2361-2369.

46. Dalet, K.; Cenatiempo, Y.; Cossart, P.; Hechard, Y. A sigma(54)-dependent PTS permease of the mannose family is responsible for sensitivity of *Listeria monocytogenes* to mesentericin Y105. *Microbiology-(UK)* **2001**, *147*, 3263-3269.

47. Hechard, Y.; Pelletier, C.; Cenatiempo, Y.; Frere, J. Analysis of sigma(54)-dependent genes in *Enterococcus faecalis*: a mannose PTS permease (EIIMan) is involved in sensitivity to a bacteriocin, mesentericin Y105. *Microbiology-(UK)* **2001**, *147*, 1575-1580.

48. Yan, L. Z.; Gibbs, A. C.; Stiles, M. E.; Wishart, D. S.; Vederas, J. C. Analogues of bacteriocins: Antimicrobial specificity and interactions of leucocin A with its enantiomer, carnobacteriocin B2, and truncated derivatives. *J. Med. Chem.* **2000**, *43*, 4579-4581.

49. Tominaga, T.; Hatakeyama, Y. Determination of essential and variable residues in pediocin PA-1 by NNK scanning. *Appl. Environ. Microbiol.* **2006**, *72*, 1141-1147.

50. Keller, L.; Surette, M. G. Communication in bacteria: an ecological and evolutionary perspective. *Nat. Rev. Microbiol.* **2006**, *4*, 249-258.

51. Havarstein, L. S.; Diep, D. B.; Nes, I. F. A family of bacteriocin ABC transporters carry out proteolytic processing of their substrates concomitant with export. *Mol. Microbiol.* **1995**, *16*, 229-240.

52. van Belkum, M. J.; Worobo, R. W.; Stiles, M. E. Double-glycine-type leader peptides direct secretion of bacteriocins by ABC transporters: Colicin V secretion in *Lactococcus lactis*. *Mol. Microbiol.* **1997**, *23*, 1293-1301.

53. Bassler, B. L.; Losick, R. Bacterially speaking. *Cell* **2006**, *125*, 237-246.

54. Reading, N. C.; Sperandio, V. Quorum sensing: The many languages of bacteria. *FEMS Microbiol. Lett.* **2006**, *254*, 1-11.

55. Kleerebezem, M.; Quadri, L. E. N.; Kuipers, O. P.; deVos, W. M. Quorum sensing by peptide pheromones and two-component signal-transduction systems in Gram-positive bacteria. *Mol. Microbiol.* **1997**, *24*, 895-904.

56. Gursky, L. J.; Martin, N. I.; Derksen, D. J.; van Belkum, M. J.; Kaur, K.; Vederas, J. C.; Stiles, M. E.; McMullen, L. M. Production of piscicolin 126 by *Carnobacterium maltaromaticum* UAL26 is controlled by temperature and induction peptide concentration. *Arch. Microbiol.* **2006**, *186*, 317-325.

57. Ahn, C.; Stiles, M. E. Mobilization and expression of bacteriocin plasmids from Carnobacterium piscicola isolated from meat. *J. Appl. Bacteriol.* **1992**, *73*, 217-228.

58. Worobo, R. W.; Henkel, T.; Sailer, M.; Roy, K. L.; Vederas, J. C.; Stiles, M. E. Characteristics and genetic determinant of a hydrophobic peptide bacteriocin, carnobacteriocin-A, produced by *Carnobacterium piscicola* LV17A. *Microbiology-UK* **1994**, *140*, 517-526.

59. Franz, C. M. A. P.; van Belkum, M. J.; Worobo, R. W.; Vederas, J. C.; Stiles, M. E. Characterization of the genetic locus responsible for production and immunity of carnobacteriocin A: the immunity gene confers cross-protection to enterocin B. *Microbiology-UK* **2000**, *146*, 621-631.

60. Franz, C. M. A. P.; van Belkum, M. J.; Holzapfel, W. H.; Abriouel, H.; Galvez, A. Diversity of enterococcal bacteriocins and their grouping in a new classification scheme. *FEMS Microbiol. Rev.* **2007**, *31*, 293-310.

61. Barlos, K.; Gatos, D.; Schafer, W. Synthesis of prothymosin alpha (Pro T-alpha) - a protein consisting of 109 amino-acid-residues. *Angew. Chem., Int. Ed. Engl.* **1991**, *30*, 590-593.

62. Barlos, K.; Chatzi, O.; Gatos, D.; Stavropoulos, G. 2-Chlorotrityl chloride resin - studies on anchoring of Fmoc-amino acids and peptide cleavage. *Int. J. Pept. Protein Res.* **1991**, *37*, 513-520.

63. Controlled Drugs and Substances Act. In 1996; Vol. Part 1 Class A Precursors.

64. Woolf, C. Pain: Moving from symptom control toward mechanism-specific pharmacological management. *Ann. Intern. Med.* **2004**, *140*, 441-451.

65. Chiswick, M. L. Assessment of pain in neonates. *Lancet* **2000**, *355*, 6-8.

66. Bennett, G. J. *Methods in Pain Research: Animal Models of Pain.* CRC Press: 2001; Vol. 6.

67. Hargreaves, K.; Dubner, R.; Brown, F.; Flores, C.; Joris, J. A new and sensitive method for measuring thermal nociception in cutaneous hyperalgesia. *Pain* **1988**, *32*, 77-88.

68. Brigatte, P.; Hoffmann, F. A.; Bernardi, M. M.; Giorgi, R.; Fernandes, I.; Takehara, H. A.; Barros, S. B. M.; Almeida, M. G.; Cury, Y. Tolerance to the antinociceptive effect of *Crotalus durissus terrificus* snake venom in mice is mediated by pharmacodynamic mechanisms. *Toxicon* **2001**, *39*, 1399-1410.

69. Cury, Y.; Picolo, G. K., Konno, K; Giorgi, R.; Brigatte, P.; Gutierrez, V.; Camargo, A.; Analog compounds of analgesic peptides derived from the venom of *Crotalus durissus terrificus* snakes, their uses, compositions, methods of preparation and purification. WO20051027357(A3), CA2565731(A1), AU2005239771(A1), **2005**.

70. Stymiest, J. L.; Mitchell, B. F.; Wong, S.; Vederas, J. C. Synthesis of biologically active dicarba analogues of the peptide hormone oxytocin using ring-closing metathesis. *Org. Lett.* **2003**, *5*, 47-49.

71. Stymiest, J. L.; Mitchell, B. F.; Wong, S.; Vederas, J. C. Synthesis of oxytocin analogues with replacement of sulfur by carbon gives potent antagonists with increased stability. *J. Org. Chem.* **2005**, *70*, 7799-7809.

72. Grubbs, R. H. Olefin metathesis. *Tetrahedron* **2004**, *60*, 7117-7140.

73. Miller, S. J.; Blackwell, H. E.; Grubbs, R. H. Application of ring-closing metathesis to the synthesis of rigidified amino acids and peptides. *J. Am. Chem. Soc.* **1996**, *118*, 9606-9614.

74. EMD-Biosciences, Improving synthetic efficiency in SPPS. In *NovaBiochem Catalog* 2006-2007; pp 3.5-3.6.

75. Pattabiraman, V. R.; Stymiest, J. L.; Derksen, D. J.; Martin, N. I.; Vederas, J. C. Multiple on-resin olefin metathesis to form ring-expanded analogues of the lantibiotic peptide, lacticin 3147 A2. *Org. Lett.* **2007**, *9*, 699-702.

76. Ghalit, N.; Poot, A. J.; Furstner, A.; Rijkers, D. T. S.; Liskamp, R. M. J. Ring-closing alkyne metathesis approach toward the synthesis of alkyne mimics of thioether A-, B-, C-, and DE-ring systems of the antibiotic nisin Z. *Org. Lett.* **2005**, *7*, 2961-2964.

77. Ghalit, N.; Rijkers, D. T. S.; Kemmink, J.; Cees, V. B.; Liskamp, R. M. J. Pre-organization induced synthesis of a crossed alkene-bridged nisin Z DE-ring mimic by ring-closing metathesis. *Chem. Commun.* **2005**, 192-194.

78. Ghalit, N.; Rijkers, D. T. S.; Liskamp, R. M. J. Alkene- and alkyne-bridged mimics of nisin as potential peptide-based antibiotics. *J. Mol. Cat. A* **2006**, *254*, 68-77.

79. Fleury, Y.; Dayem, M. A.; Montagne, J. J.; Chaboisseau, E.; LeCaer, J. P.; Nicolas, P.; Delfour, A. Covalent structure, synthesis, and structure-function studies of mesentericin Y 105, a defensive peptide from Gram-positive bacteria *Leuconostoc mesenteroides*. *J. Biol. Chem.* **1996**, *271*, 14421-14429.

80. Hastings, J. W.; Sailer, M.; Johnson, K.; Roy, K. L.; Vederas, J. C.; Stiles, M. E. Characterization of leucocin-A-UAL-187 and cloning of the bacteriocin gene from *Leuconostoc gelidum*. *J. Bacteriol.* **1991**, *173*, 7491-7500.

81. Derksen, D. J.; Stymiest, J. L.; Vederas, J. C. Antimicrobial leucocin analogues with a disulfide bridge replaced by a carbocycle or by noncovalent interactions of allyl glycine residues. *J. Am. Chem. Soc.* **2006**, *128*, 14252-14253.

82. Hutchinson, E. G.; Thornton, J. M. A revised set of potentials for β-turn formation in proteins. *Protein Sci.* **1994**, *3*, 2207-2216.

83. Miller, K. W.; Schamber, R.; Osmanagaoglu, O.; Ray, B. Isolation and characterization of pediocin AcH chimeric protein mutants with altered bactericidal activity. *Appl. Environ. Microbiol.* **1998**, *64*, 1997-2005.

84. Fimland, G.; Jack, R.; Jung, G.; Nes, I. F.; Nissen-Meyer, J. The bactericidal activity of pediocin PA-1 is specifically inhibited by a 15-mer fragment that spans the bacteriocin from the center toward the *C*-terminus. *Appl. Environ. Microbiol.* **1998**, *64*, 5057-5060.

85. Fimland, G.; Johnsen, L.; Dalhus, B.; Nissen-Meyer, J. Pediocin-like antimicrobial peptides (class IIa bacteriocins) and their immunity proteins: biosynthesis, structure, and mode of action. *J. Pept. Sci.* **2005**, *11*, 688-696.

86. Chapman, R. N.; Arora, P. S. Optimized synthesis of hydrogen-bond surrogate helices: Surprising effects of microwave heating on the activity of Grubbs catalysts. *Org. Lett.* **2006**, *8*, 5825-5828.

87. Elaridi, J.; Patel, J.; Jackson, W. R.; Robinson, A. J. Controlled synthesis of (S,S)-2,7-diaminosuberic acid: A method for regioselective construction of dicarba analogues of multicystine-containing peptides. *J. Org. Chem.* **2006**, *71*, 7538-7545.

88. Jiang, S.; Li, P.; Lee, S. L.; Lin, C. Y.; Long, Y. Q.; Johnson, M. D.; Dickson, R. B.; Roller, P. P. Design and synthesis of redox stable analogues of sunflower trypsin inhibitors (SFTI-1) on solid support, potent inhibitors of matriptase. *Org. Lett.* **2007**, *9*, 9-12.

89. Robinson, A. J.; Elaridi, J.; Van Lierop, B. J.; Mujcinovic, S.; Jackson, W. R. Microwave-assisted RCM for the synthesis of carbocyclic peptides. *J. Pept. Sci.* **2007**, *13*, 280-285.

90. Kaiser, J.; Kinderman, S. S.; van Esseveldt, B. C. J.; van Delft, F. L.; Schoemaker, H. E.; Blaauw, R. H.; Rutjes, F. Synthetic applications of aliphatic unsaturated α-H-α-amino acids. *Org. Biomol. Chem.* **2005**, *3*, 3435-3467.

91. Morrow, J. A.; Segall, M. L.; Lund-Katz, S.; Phillips, M. C.; Knapp, M.; Rupp, B.; Weisgraber, K. H. Differences in stability among the human apolipoprotein E isoforms determined by the amino-terminal domain. *Biochemistry* **2000**, *39*, 11657-11666.

92. Bisello, A., Chorev, M., Synthesis of photoreactive peptides. In *Synthesis of Peptides and Peptidomimetics*, Workbench Edition ed.; Murray Goodman, A. F., Luis Moroder, Claudio Toniolo, Ed. Thieme: Stuttgart-New York, 2004; Vol. E22c, pp 87-152.

93. Brunner, J.; Senn, H.; Richards, F. M. 3-Trifluoromethyl-3-phenyldiazirine - a new carbene generating group for photolabeling reagents. *J. Biol. Chem.* **1980**, *255*, 3313-3318.

94. Fleet, G. W. J.; Porter, R. R.; Knowles, J. R. Affinity labelling of antibodies with aryl nitrene as reactive group. *Nature (London)* **1969**, *224*, 511-512.

95. Nakamoto, C.; Behar, V.; Chin, K. R.; Adams, A. E.; Suva, L. J.; Rosenblatt, M.; Chorev, M. Probing the bimolecular interactions of parathyroid-hormone with the human parathyroid-hormone parathyroid hormone-related protein-ceceptor. Design, synthesis and characterization of photoreactive benzophenone-containing analogs of parathyroid hormone. *Biochemistry* **1995**, *34*, 10546-10552.

96. Kurzchalia, T. V.; Wiedmann, M.; Girshovich, A. S.; Bochkareva, E. S.; Bielka, H.; Rapoport, T. A. The signal sequence of nascent preprolactin interacts with the 54K polypeptide of the signal recognition particle. *Nature (London)* **1986**, *320*, 634-636.

97. Oneil, K. T.; Degrado, W. F. The interaction of calmodulin with fluorescent and photoreactive model peptides - evidence for a short interdomain separation. *Proteins: Struct., Funct., Genet.* **1989**, *6*, 284-293.

98. Kotzybahibert, F.; Kapfer, I.; Goeldner, M. Recent trends in photoaffinity-labeling. *Angew. Chem., Int. Ed. Engl.* **1995**, *34*, 1296-1312.

99. Swali, V.; Wells, N. J.; Langley, G. J.; Bradley, M. Solid-phase dendrimer synthesis and the generation of super-high-loading resin beads for combinatorial chemistry. *J. Org. Chem.* **1997**, *62*, 4902-4903.

100. Han, Y. X.; Albericio, F.; Barany, G. Occurrence and minimization of cysteine racemization during stepwise solid-phase peptide synthesis. *J. Org. Chem.* **1997**, *62*, 4307-4312.

101. Barany, G.; Han, Y. X.; Hargittai, B.; Liu, R. Q.; Varkey, J. T. Side-chain anchoring strategy for solid-phase synthesis of peptide acids with *C*-terminal cysteine. *Biopolymers* **2003**, *71*, 652-666.

102. Blaskovich, M. A.; Lajoie, G. A. Synthesis of a chiral serine aldehyde equivalent and its conversion to chiral α-amino-acid derivatives. *J. Am. Chem. Soc.* **1993**, *115*, 5021-5030.

103. Corey, E. J.; Raju, N. A new general synthetic route to bridged carboxylic ortho esters. *Tetrahedron Lett.* **1983**, *24*, 5571-5574.

104. Blaskovich, M. A.; Evindar, G.; Rose, N. G. W.; Wilkinson, S.; Luo, Y.; Lajoie, G. A. Stereoselective synthesis of threo and erythro β-hydroxy and β-disubstituted-β-hydroxy α-amino acids. *J. Org. Chem.* **1998**, *63*, 3631-3646.

105. Tyacke, R. J.; Robinson, E. S. J.; Schnabel, R.; Lewis, J. W.; Husbands, S. M.; Nutt, D. J.; Hudson, A. L. N1 '-fluoroethyl-naltrindole (BU97001) and N1 '-fluorethyl-(14-formylamino)-naltrindole (BU97018) potential delta-opioid receptor PET ligands. *Nucl. Med. Biol.* **2002**, *29*, 455-462.

106. Robinson, E. S. J.; Tyacke, R. J.; Finch, L.; Willmott, G.; Husbands, S.; Nutt, D. J.; Hudson, A. L. Pharmacological characterisation of novel α-(2)-adrenoceptor

antagonists as potential brain imaging agents. *Neuropharmacology* **2004**, *46*, 847-855.

107. Neil, A.; Terenius, L. D-Propoxyphene acts differently from morphine on opioid receptor-effector mechanisms. *Eur. J. of Pharmacol.* **1981**, *69*, 33-39.

108. Saito, O. A., T; Yamamoto, T. Analgesic effects of nonsteroidal antiinflammatory drugs, acetaminophen, and morphine in a mouse model of bone cancer pain. *J. Anesth.* **2005**, *19*, 218-224.

109. Rubinstein, M.; Mogil, J. S.; Japon, M.; Chan, E. C.; Allen, R. G.; Low, M. J. Absence of opioid stress-induced analgesia in mice lacking β-endorphin by site-directed mutagenesis. *Proc. Natl. Acad. Sci. U.S.A.* **1996**, *93*, 3995-4000.

110. Worobo, R. W.; van Belkum, M. J.; Sailer, M.; Roy, K. L.; Vederas, J. C.; Stiles, M. E. A signal peptide secretion-dependent bacteriocin from *Carnobacterium divergens*. *J. Bacteriol.* **1995**, *177*, 3143-3149.

111. Staros, J. V. N-Hydroxysulfosuccinimide active esters - bis(N-hydroxysulfosuccinimide) esters of 2 dicarboxylic-acids are hydrophilic, membrane-impermeant, protein cross linkers. *Biochemistry* **1982**, *21*, 3950-3955.

112. Still, W. C.; Kahn, M.; Mitra, A. Rapid chromatographic technique for preparative separations with moderate resolution. *J. Org. Chem.* **1978**, *43*, 2923-2925.

113. EMD-Biosciences, Attachment of hydroxymethyl resins using symmetrical anhydride. In *NovaBiochem Catalog* 2006-2007; p 2.36.

114. EMD-Biosciences, Loading of trityl resins. In *NovaBiochem Catalog* 2006-2007; p 2.17.

115. Kaiser, E.; Colescot, R. L; Bossinge, C. D.; Cook, P. I. Color test for detection of free terminal amino groups in solid-phase synthesis of peptides. *Anal. Biochem.* **1970**, *34*, 595.

116. Kazmaier, U.; Hebach, C.; Watzke, A.; Maier, S.; Mues, H.; Huch, V. A straightforward approach towards cyclic peptides via ring-closing metathesis - scope and limitations. *Org. Biomol. Chem.* **2005**, *3*, 136-145.

117. Tagg, J. R.; Dajani, A. S.; Wannamaker, L. W. Bacteriocins of Gram-positive bacteria. *Bacteriol. Rev.* **1976**, *40*, 722-756.

118. Gill, S. C.; Vonhippel, P. H. Calculation of protein extinction coefficients from amino-acid sequence data. *Anal. Biochem.* **1989**, *182*, 319-326.

119. van Belkum, M. J.; Derksen, D. J.; Franz, C. M. A. P.; Vederas, J. C. Structure-function relationships of inducer peptide phermones involved in bacteriocin production in *Carnobacterium maltaromaticum* and *Enterococcus faecium*. *Microbiology* **2007**, *153*, 3660-3666.

120. Franz, C.; Schillinger, U.; Holzapfel, W. H. Production and characterization of enterocin 900, a bacteriocin produced by *Enterococcus faecium* BFE 900 from black olives. *Int. J. Food. Microbiol.* **1996**, *29*, 255-270.

9. APPENDIX 1 – LACTICIN 3147 A2 PEPTIDES

Lantibiotics are peptide derived antimicrobial agents that are ribosomally synthesized and post-translationally modified to their biologically active forms.[1] These peptides contain a characteristic lanthioine bridge (Lan **A-1** or MeLan **A-2**, Figure A-1), and often incorporate the unsaturated residues 2,3-didehydroalanine (Dha, **A-3**) and dehydrobutyrine (Dhb, **A-4**). Although lantibiotics containing these structures (such as nisin A (**A-5**), lacticin 3147 A1 (**A-6**) and lacticin 3147 A2 (**A-7**), Figure A-2) display potent antimicrobial activity, these unusual features also represent some of the major limitations with respect to the practical application of these peptides. The characteristic thioether moiety of **A-1** and **A-2** is prone to oxidation, while the unsaturated moieties **A-3** and **A-4** are subject to nucleophilic addition, both leading to a decrease or complete loss of antimicrobial activity.

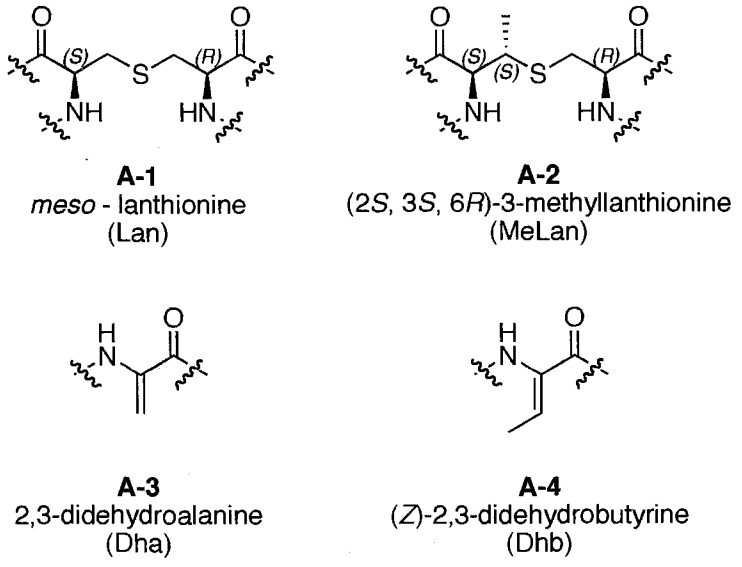

Figure A-1. Common unsaturated amino acids found in lantibiotic peptides

9.1 Attempts towards a convergent synthesis of dicarba lacticin 3147A2

Previous work in the Vederas group with oxytocin has shown that disulfide bonds can be replaced by carbon-carbon double bonds to furnish a more stable analog while retaining activity.[2, 3] Based on this report, a similar study was devised to determine if lanthionine bridges could also be replaced by carbon-carbon double bonds.

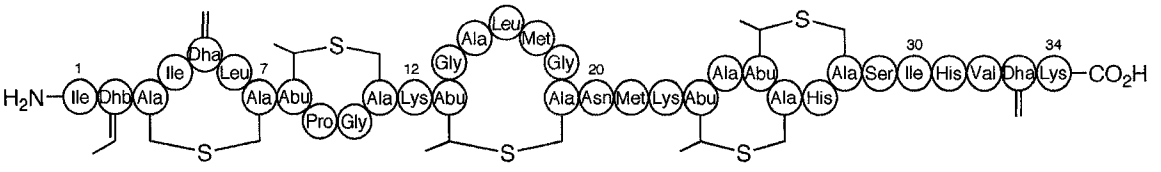

A-5, Nisin A

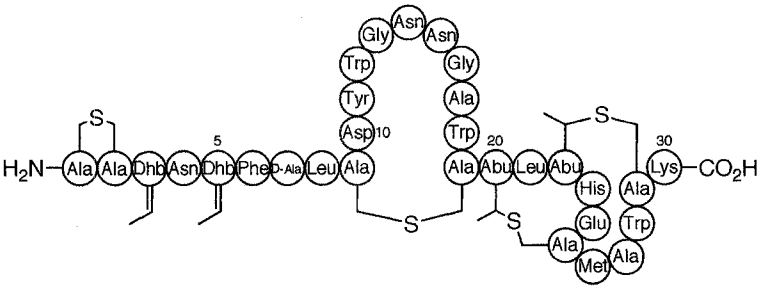

A-6, Lacticin 3147 A1

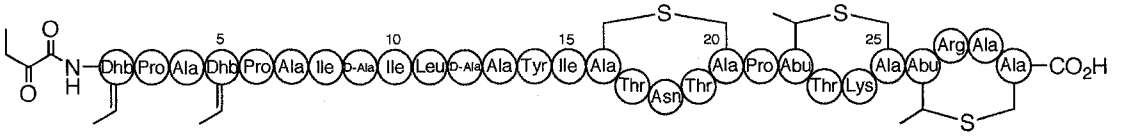

A-7, Lacticin 3147 A2

Figure A-2. Representative examples of lantibiotic bacteriocins. Nisin A (A-5), Lacticin 3147 A1 (A-6) and Lacticin 3147 A2 (A-7).

As the structures of lacticin 3147 A1 and A2 (Figure A-2) were determined in the Vederas laboratory,[4] these peptides were ideal test substrates for a structure activity relationship (SAR) study. Lacticin 3147 A2 has rings which are of a similar size to oxytocin none of which are overlapping, hence this was selected for the model SAR

study. A convergent synthesis of dicarba-lacticin 3147 A2 (**A-7a**) was designed (Scheme A-1).

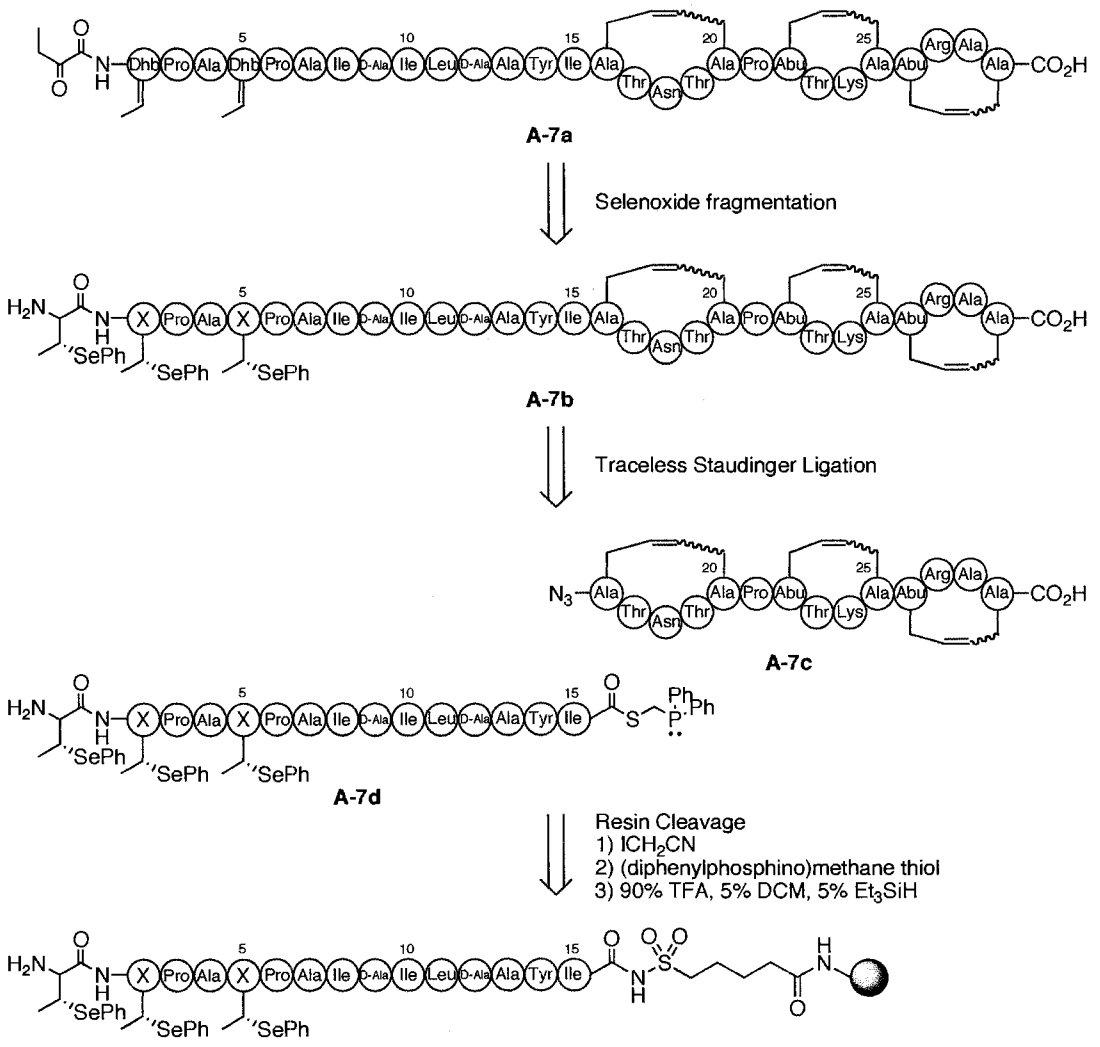

Scheme A-1. Overall retrosynthesis to dicarba-analog of lacticin 3147 A2

The overall scheme incorporates many features that had not previously been used in the same synthesis. The *C*-terminal tricyclic portion of the peptide (**A-7c**) was expected to arise from a linear synthesis followed by sequential on-resin RCM reactions and was prepared by a former graduate student, Dr. Jake Stymiest. The linear portion of the peptide (residues 6-15) that was destined to form the *C*-terminal thioester (**A-7d**) was prepared by another former graduate student, Dr. Nathaniel Martin. Incorporation of the

Dhb residues was envisioned to arise from selenoxide fragmentation of the corresponding selenides which were prepared by another graduate student, Mr. Vijay Pattabiraman. Coupling of the tricyclic portion of the peptide and the linear 15-mer was to be completed using traceless Staudinger ligation methodology (Scheme A-2).[5] As the entire project was a collaborative effort with three other graduate students, this appendix will only deal with the preparation of the (diphenylphosphino)methane thiol (Scheme A-3) and the re-synthesis of the linear 10-mer as a test substrate.

The key ligation step, responsible for coupling the two halves of the molecule, employs a bifuctional linker to join the *C*-terminal thioester (**A**) of one peptide with the *N*-terminal azide (**B**) of another peptide (Scheme A-2). The thioester containing peptide is prepared to incorporate the bifunctional phosphine-thiol at the *C*-terminus. Upon addition of the coupling partner to the reaction mixture, the free phosphine reacts with the azide to effectively join the coupling fragments with extrusion of nitrogen gas (**C-E**). The phosphorus-nitrogen bond (**E**) then rearranges via formation of a 5-membered ring (**F**). Collapse of the tetrahedral intermediate is expected to eliminate the thiol (**G**) to yield the amide containing desired product (**H**, Scheme A-2). Alternatively, formation of a bicyclic compound (**I**) via attack of oxygen to phosphorus has been postulated as a mechanism of generating unwanted byproducts.[6, 7]

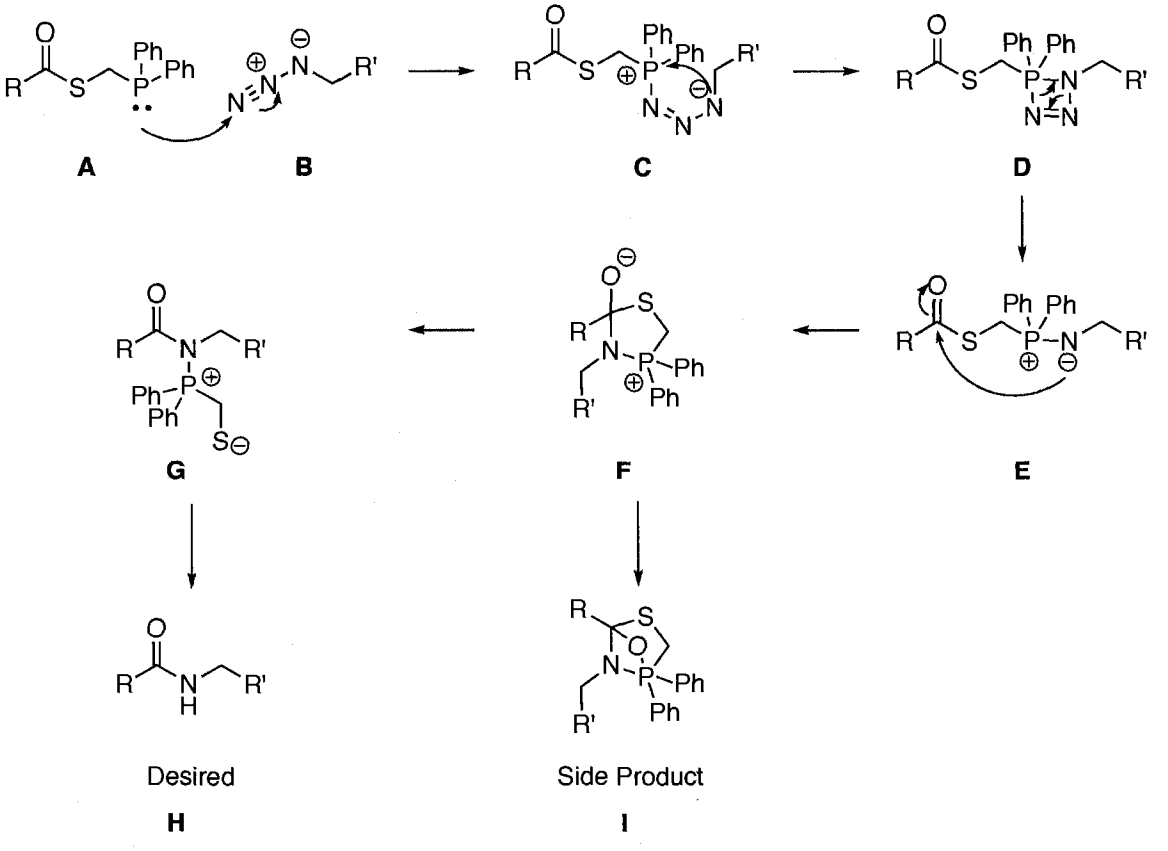

Scheme A-2. Traceless Staudinger ligation used to couple peptide fragments.

The bifunctional thiol-phosphine **A-12**, was prepared using a literature procedure (Scheme A-3).[5] Starting with the commercially available precursor chloromethyl-phosphoric dichloride **A-8**, reaction with phenylmagnesium bromide yields intermediate **A-9** in a modest yield of 35%. The main cause of this low yield is the problematic column chromatography that was required to remove unwanted side products. Reaction of the chloromethyl derivative **A-9** with thioacetate introduces the masked thiol to yield **A-10**. Reduction of the phosphine oxide occurs after an extended reaction time with trichlorosilane to yield phosphine **A-11**. Base hydrolysis of the thioacetate yields the required bifunctional linker in the unoptimized overall yield of 6%.

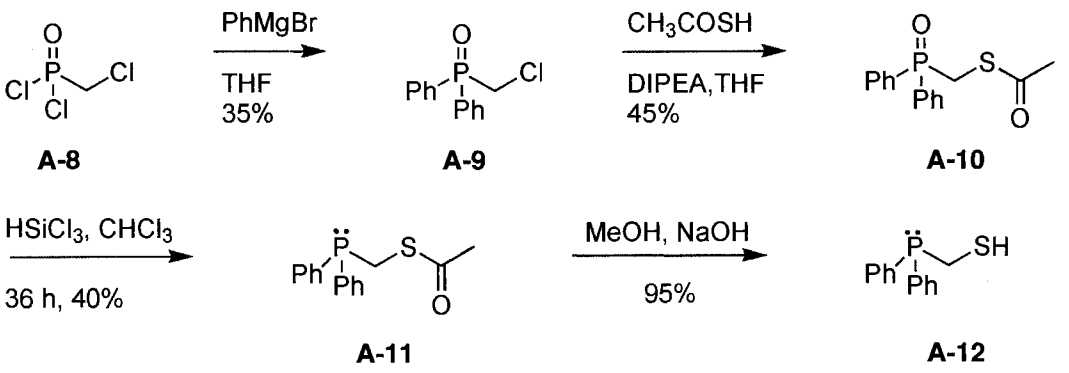

Scheme A-3. Synthesis of the required fragment for traceless Staudinger ligation.

The free thiol **A-12** was then used in an effort to cleave the desired peptide from the solid support (Scheme A-4). Unfortunately, upon activation with iodoacetonitrile and addition of the **A-12**, the desired thioester **A-7d** was not detected by MALDI-TOF MS or HPLC.

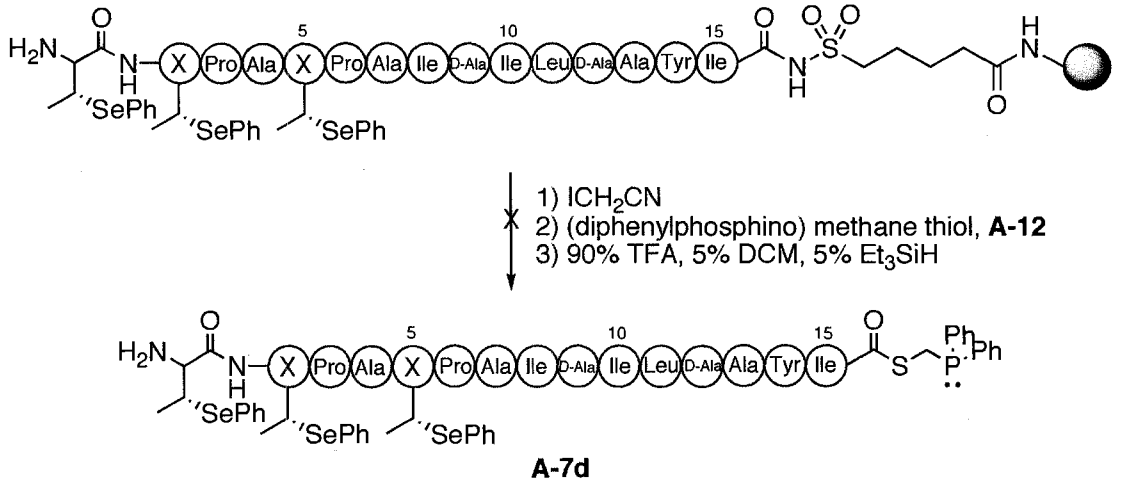

Scheme A-4. Attempted resin cleavage to form thioester A-7d.

This may have been caused by a variety of factors. It is possible that that peptide was not synthesized due to hydrophobic aggregation during synthesis. Given the complexity of the conditions required for cleavage, it is difficult to check intermediate peptides by MALDI-MS. Alternatively, the conditions necessary for resin cleavage may be responsible for degradation of the peptide. The relatively reactive phenylselenide side chains may have reacted with the iodoacetonitrile used in resin activation or potentially with the phosphine-thiol **A-12**.

With the substantial effort invested into this synthesis, this negative result was a significant setback. It became clear that the preparation of dicarba-lacticin 3147 A2 would require substantial optimization, particularly in the *N*-terminal dehydroamino acid portion of the peptide. To assist in this optimization, the linear 10-mer (**A-13**, residue 6-15) was prepared on Wang resin to be used as a model substrate for coupling of

dehydroamino acid precursors. This resin was then used by another graduate student in the laboratory, Mr. Vijay Pattabiraman, to optimize the coupling conditions for the preparation of the final five residues. However, this convergent scheme was eventually abandoned, and after substantial optimization, the total synthesis was completed in a linear fashion as outlined in the thesis of Vijay Pattabiraman.

9.2 Attempts toward increasing dehydro amino acid resistance to nucleophilic addition

As previously mentioned, a common component of the lantibiotics are the unsaturated residues Dha (**A-3**) and Dhb (**A-4**). The unsaturated residues Dha (**A-3**) and Dhb (**A-4**) are subject to Michael addition by nucleophiles, which can have an adverse effect on their biological activity.

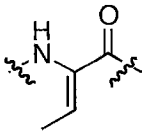

A-4
(*Z*)-2,3-didehydrobutyrine
(Dhb)

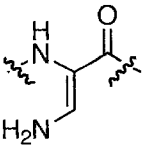

A-14
(*Z*)-2,3-diaminoacrylic acid

Figure A-3. Comparison of naturally occuring dehydrobutyrine residue and the proposed vinylogous amide analogue

This is particularly a problem as dehydro residues have been shown to be reactive with the naturally occurring peptide glutathione, a compound found naturally in meat and animal cells.[8, 9] This limits the application of lantibiotics as food preservation agents for meat as well as for *in vivo* use. The electrophilic character of the β-carbon, due to conjugation to the amide carbonyl, is responsible for the residues propensity to be attacked by nucleophiles. Conceptually, replacement of the methyl substituent on Dhb (**A-4**) would be expected to alter the electrophilic character of the β-carbon. One potential replacement of the vinyl methyl group in **A-4** is the introduction of an amine to produce 2,3-diaminoacrylic acid, **A-14** (Figure A-3). This compound would be expected to have reduced electrophilic character at the β-carbon based on the increased conjugation produced by formation of the vinylogous amide. Attempts to prepare the proposed compound followed a modification of a literature procedure.[10] Beginning with

commercially available H-Ser(Bn)-OH **A-15**, esterification, acylation and hydrogenation occur readily under standard conditions, requiring only aqueous washes between steps to yield **A-16**. Displacement of the methyl ester with methyl amine occurs by combining **A-16** with a 40% solution of the respective amine to produce **A-17**. Finally, oxidation and trapping of the serine side chain occurs by pre-mixing *p*-toluenesulfonyl chloride and DMSO for 3 min, followed by addition of **A-17**, yielding the electrophilic precursor **A-18**.

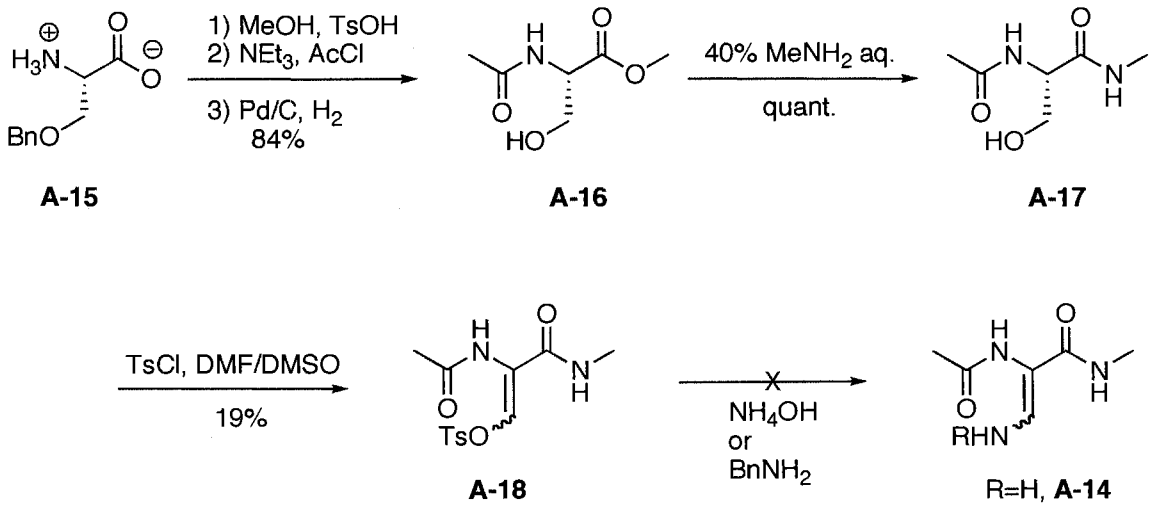

Scheme A-5. Method used in attempt to prepare vinylogous amide derivative A-14.

In contrast to literature reports of successful reactions with methyl amine, the final step to yield the desired product by reaction with ammonia or benzylamine was unsuccessful. Byproducts isolated from the reaction have masses that are consistent with amine attack onto the tosylate. Removal of the tosylate group from **A-18** would be expected to generate a serine β-aldehyde which, if not trapped immediately with a nucleophile, may undergo a retro-aldol type reaction to eliminate the side chain substituent of the serine derivative.

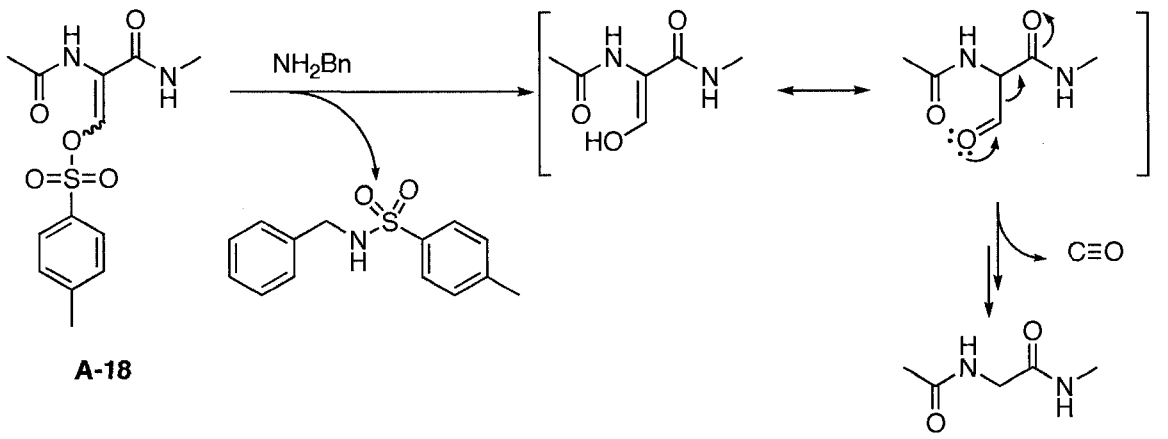

Scheme A-6. Proposed side reaction that occurs by reaction of amine with A-18.

9.3 Future Work

The underlying goals of these projects still present unmet challenges. The synthesis of the dicarba-lacticin 3147 A2 has been completed as part of the thesis of Vijay Pattabiraman, but lessons from the traceless Staudinger ligation are useful for further investigation. Recent reports in the literature have investigated the reaction mechanism more closely and have stated that problems have been observed in non-glycine residue couplings with **A-12** and that yields can be improved by addition of electron donating substituents on the aromatic phosphorus ligands.[6, 7] It has been proposed that this occurs by stabilization of the phosphorus positive charge by the electron donating aromatic substituents (Scheme A-7). The introduction of hindered amine substituents (such as dimethylamine) may produce compounds that have improved coupling efficiency versus the reported methoxy derivative and may improve its solubility properties.

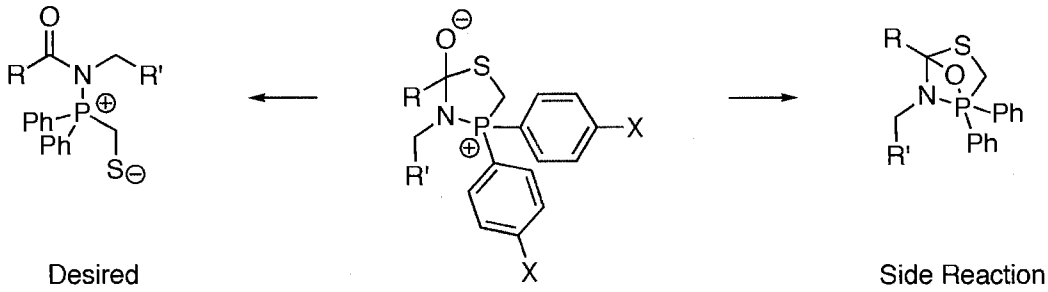

Scheme A-7. Substituents on aromatic ring can adjust ligation efficiency. Electron donating substituents (e.g. X= OMe) favor desired product.

Further possibilities exist in the replacement of Dha and Dhb residues. Some structures that would be expected to have reduced electrophilicity but similar planar shape include aromatic or strained derivatives such as those shown in Figure A-4. Although these structures are interesting from a chemical perspective, they are likely not

realistic replacements to be incorporated for most human applications as the synthetic requirements to prepare a lantibiotic analog by chemical synthesis have proven to be a monumental effort.

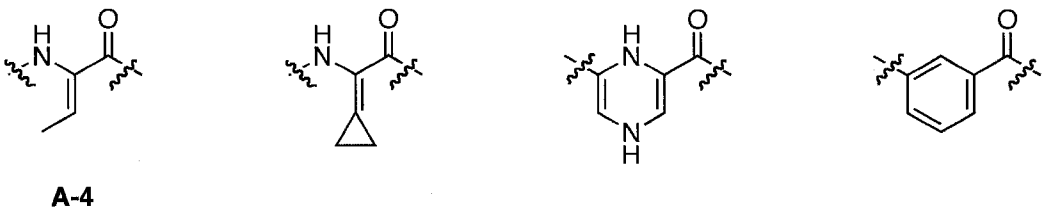

A-4

Figure A-4. Proposed structures that may reduce electrophilic character at β-carbon while maintaining similar shape to parent compound A-4

However, a better understanding of the mode of action of lantibiotics and acceptable dehydroamino acid substitutions may lead to biologically accessible products. A more thorough understanding of the requirements for the dehydratase that enzymatically produces the Dha and Dhb residues may allow a biological method to produce unsaturated residues of electronically or sterically hindered analogues to be developed.

9.4 Experimental

(Diphenylphosphoryl)chloromethane,[5] A-9

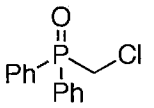

Chloromethylphosphoric dichloride (3.1 mL, 5 g, 30 mmol) was dissolved in freshly distilled THF (60 mL). A solution of phenylmagnesium bromide (3.0 M in diethyl ether, 20 mL, 60 mmol) was combined with THF (40 mL) and added dropwise to the previous solution over 1 h. The solution was then heated at reflux for 36 h. The reaction was then cooled to 0 °C and quenched via the slow addition of water (5 mL). The solvent was then removed *in vacuo* and the residue was dissolved in DCM (30 mL), washed with water (1 x 10 mL) and brine (1 x 10 mL). The solution was then dried over $MgSO_4$, concentrated, and purified by column chromatography (3% MeOH in DCM) to yield the desired product **A-9** as a colorless oil (2.6 g, 35%). ^{1}H-NMR ($CDCl_3$, 300 MHz) δ 7.88-7.78 (m, 4 H, ArH), 7.66-7.49 (m, 6H, ArH), 4.06 (d, 2H, J = 6.7 Hz, CH_2).

S-(Diphenylphosphoryl)methyl ethanethioate,[5] A-10

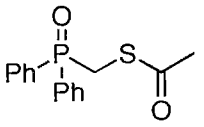

Compound **A-9** (2.6 g, 10.4 mmol) was dissolved in THF (65 mL) under argon and cooled to 0 °C. Thioacetic acid (4.8 mL, 66 mmol) was then added to the reaction mixture and the resulting solution was stirred for 1 h. After 1 h, diisopropylethyl amine (11.5 mL) was added and the reaction was heated at reflux for 17 h. The reaction was cooled to room temperature and thioacetic acid (4.8 mL, 66 mmol) and triethylamine (9.5

mL) were added to the solution and heated at reflux for 9 h. The solvent mixture was then removed (with a rotary evaporator inside the fume hood) and the resulting thick, black residue was taken up into DCM (50 mL), washed with 2 M HCl (1 x 20 mL), sat. $NaHCO_3$ (1 x 20 mL), brine (1 x 20 mL) and dried over $MgSO_4$. Charcoal was then added and the solution was heated at reflux for 4 h. The mixture was then filtered through a pad of celite, concentrated and purified by column chromatography in the fumehood (70% EtOAc: hexane) to yield the product as a clear oil (1.37 g, 45%); IR (CH_2Cl_2, cast) 3441, 3055, 2953, 1698, 1200 cm^{-1}; ^{1}H-NMR ($CDCl_3$, 300 MHz) δ 7.82-7.74 (m, 4H, Ar<u>H</u>), 7.60-7.44 (m, 6H, Ar<u>H</u>), 3.77 (d, 2 H, J = 8.4 Hz, C<u>H</u>$_2$), 2.27 (s, 3H, C<u>H</u>$_3$); ^{13}C-NMR ($CDCl_3$, 100 MHz) 193.1, 132.3, 132.2, 131.7, 131.3, 131.0, 130.7, 128.7, 128.6, 30.0. HRMS (EI) calc'd for $C_{15}H_{15}O_2PS$ 290.0530, found 290.0526.

_S_-(diphenylphosphino)methyl ethanethioate,[5] A-11

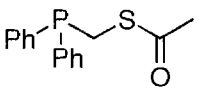

Compound **A-10** (1.36 g, 4.7 mmol) was dissolved in $CHCl_3$ (12 mL) under argon. Trichlorosilane (7.1 mL, 70 mmol, 15 eq) was then added to the reaction mixture and left to stir for 36 h. The solution was then concentrated and purified by column chromatography (3% MeOH in DCM) to yield the product as a colorless oil (0.52 g, 40%). ^{1}H-NMR data only. ^{1}H-NMR ($CDCl_3$, 300 MHz) δ 7.46-7.40 (m, 4H, Ar<u>H</u>), δ 7.39-7.34 (m, 6H, Ar<u>H</u>), δ 3.52 (d, 2H, J = 3.6 Hz, C<u>H</u>$_2$), δ 2.30 (s, 3H, C<u>H</u>$_3$); 27.3 (d, J = 70.3 Hz).

(Diphenylphosphino)methanethiol,[5] A-12

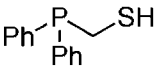

Compound **A-11** was dissolved in degassed methanol (30 ml) and sodium hydroxide (320 mg, 2 eq) was added. The resulting solution was stirred for 2 h. The solvent was then removed *in vacuo* and the remaining residue was dissolved in DCM and washed with 2 M HCl and brine and dried over $MgSO_4$ to yield product as a colorless oil (350 mg, 95%). ^{1}H-NMR ($CDCl_3$, 300 MHz) δ 7.47-7.40 (m, 4H, ArH), 7.40-7.32 (m, 6H, ArH), 3.07 (dd, 2H, J = 7.9, 2.8 Hz, CH_2), 1.39 (t, 1H, J = 7.5 Hz); ^{13}C-NMR ($CDCl_3$, 100 MHz) δ 134.3, 133.5, 131.5, 130.7, 129.0, 128.8, 128.7, 128.6, 21.7 (d, J = 59.5 Hz).

Lacticin 3147-A2 (6-15), (A-13, 6-15)

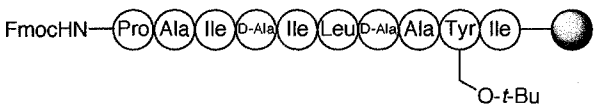

Wang resin (1.25 g, 1 mmol, 0.8 mmol/g loading) was placed in dry DMF (minimum amount, 10 mL) and allowed to swell for 30 min. Fmoc-Ile-OH (10 mmol, 3.53 g) was dissolved in dry DCM (20 mL). Dicyclohexylcarbodiimide (DCC, 5 mmol, 1.03 g) was then added to the Fmoc-Ile-OH in DCM. The resulting mixture was cooled to 0 °C, and left to stir under an argon atmosphere for 20 min. The dicyclohexyl urea was removed by filtration and the residue was concentrated *in vacuo*. The remaining residue was dissolved in dry DMF (2 x 10 mL) and added to the mixture containing the resin. Catalytic N,N-(dimethylamino)pyridine (0.1 mmol, 12 mg) was then added to reaction mixture and left to stir under argon for 1 h. After loading, the mixture was added to a solid phase reaction vessel equipped with a glass frit to remove excess reagents and

solvents while leaving the resin in the vessel. The resin was washed repeatedly with DMF (3 x 10 mL) and DCM (3 x 10 mL) before finally being treated with a solution of 20% acetic anhydride in DMF (1 x 10 ml) for 15 minutes. After another washing cycle of DMF (3 x 10 mL) and DCM (3 x 10 mL), the amino acids for Lacticin 3147 A2 (6-15) were coupled using PyBOP and standard Fmoc-SPPS in the following order: Fmoc-Ile-OH, Fmoc-Tyr(*t*-Bu)-OH, Fmoc-Ala-OH, Fmoc-D-Ala-OH, Fmoc-Leu-OH, Fmoc-Ile-OH, Fmoc-D-Ala-OH, Fmoc-Ile-OH, Fmoc-Ala-OH and Fmoc-Pro-OH. The resin was washed with DMF, DCM and MeOH before being stored with the Fmoc group remaining on the resin. Test cleavage; MALDI-TOF (MS) calc'd for $C_{65}H_{92}N_{10}NaO_{14}$ 1259.7, found 1259.5 (M + Na).

(*S*)-Methyl 2-acetamido-3-hydroxypropanoate, N-Acetyl serine methyl ester, Ac-Ser-OMe (A-16)

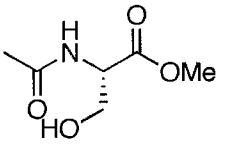

Serine-benzyl ether (H-Ser(OBn)-OH, 1.0 g, 5.12 mmol) was dissolved in methanol (30 mL) along with *p*-toluenesulfonic acid (1.95 g, 10.2 mmol) and refluxed for 24 h. The solvent was then removed *in vacuo* and the remaining residue was dissolved in DCM (30 mL) and washed with an aqueous solution of saturated $NaHCO_3$ (3 x 15 mL). The organic layer was then dried with Na_2SO_4, filtered, and concentrated to dryness. The residue was then redissolved in dry DCM (20 mL) along with triethylamine (0.79 mL, 5.6 mmol, 1.1 eq) and cooled in an ice bath for 15 min. Acetyl chloride (0.38 mL, 5.3 mmol, 1.05 eq) was then added as a solution in DCM (10 mL) in a dropwise fashion and the

resulting mixture was left to stir for 1 h. The solution was then washed with 1 M HCl (3 x 10 mL) and evaporated *in vacuo*. The residue was then suspended in EtOAc (10 mL) and 10% Pd/C (150 mg) in EtOAc (3 mL) was added. The reaction was stirred vigorously under a hydrogen atmosphere for 16 h. The reaction mixture was then filtered through celite and the solvent was removed *in vacuo* to give the product as a white solid (0.69 g, 84%). All 3 steps of the reaction were monitored by TLC using 2:1:1:1 EtOAc: BuOH: H_2O: CH_3COOH or 10% MeOH in DCM. $[\alpha]_D^{25}$ -0.1 (*c* 1.03, MeOH); IR (MeOH, cast) 3306, 3084, 2956, 1744, 1658, 1546 cm^{-1}; ^{1}H-NMR ($CDCl_3$, 400 MHz) δ 6.60-6.50 (br d, 1H, *J* = 7.2 Hz, NH), 4.67 (ddd, 1H, *J* =7.2, 3.6, 3.6 Hz, Hα), 3.98 (dd, 1H, *J* = 11.2, 4.0 Hz, Hβ), 3.91 (dd, 1H, *J* = 11.2, 3.6 Hz, Hβ), 3.80 (s, 3H, OCH_3), 2.80-2.40 (br s, 1H, OH), 2.03 (s, 3H, $COCH_3$); ^{13}C-NMR ($CDCl_3$, 100 MHz) δ 170.9, 170.5, 63.3, 54.7, 52.7, 23.0; HRMS (ES) calc'd for $C_6H_{11}NNaO_4$ 184.0580, found 184.0580.

(*S*)-2-Acetamido-3-hydroxy-*N*-methylpropanamide, N-Acetyl serine methyl amide, Ac-Ser-NHMe (A-16a)

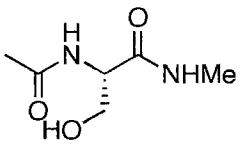

N-Acetyl serine methyl ester (300 mg, 1.9 mmol) was dissolved in 40% aqueous methylamine and stirred for 16 h. The reaction was then concentrated to dryness to yield the desired product (298 mg, quant). $[\alpha]_D^{25}$ -7.46 (*c* 0.88); IR (MeOH, cast) 3296, 3069, 1651, 1544 cm^{-1}; ^{1}H NMR ($CDCl_3$, 400 MHz) δ 6.90-6.80 (m, 1H, NH), 6.80-6.70 (m, 1H, NH), 4.38 (m, 1H, Hα), 4.13 (dd, 1H, *J* = 12.0, 3.6 Hz, Hβ), 3.61 (dd, 1H, *J* = 11.6, 4.0 Hz, Hβ), 2.81 (d, 3H, *J* = 5.2 Hz, NCH_3), 2.07 (s, 3H, $COCH_3$); ^{13}C NMR ($CDCl_3$,

100 MHz) δ 171.6, 171.1, 62.5, 53.4, 26.0, 23.0; HRMS (ES) calc'd for $C_6H_{13}N_2O_3$ 161.0921, found 161.0919.

2-Acetamido-3-(methylamino)-3-oxoprop-1-enyl 4-methylbenzenesulfonate[10] (A-17)

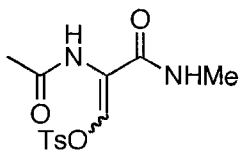

N-Acetyl serine methyl amide (24 mg, 0.15 mmol) was dissolved in DMF (3 mL) and cooled to -5 °C. In a separate vessel, *p*-toluenesulfonyl chloride (0.086 g, 0.45 mmol, 3 eq) was dissolved in a solution of 1:1 DMSO/ DMF (2 mL). The tosyl chloride solution was then added to the initial reaction vessel and NMM (0.2 mL, 10 eq) was added after 3 min. The reaction was then allowed to react for 1 h at rt. The reaction was then diluted with water (40 mL) and extracted with EtOAc (3 x 10 mL). The organic solvent was then removed *in vacuo* and the residue was purified by column chromatography (3:1 EtOAc: hexane) to yield the product as a white solid (9 mg, 19%). IR (CH_2Cl_2 cast) 3304, 3115, 1664, 1510, 1381 cm^{-1}; ^1H NMR ($CDCl_3$, 400 MHz) δ 8.50 (s, 1H, Hβ), 7.94 (br s, 1H, NH), 7.85 (d, 2H, J = 8.4 Hz, Ar<u>H</u>H), 7.40 (d, 2H, J = 8.8 Hz, ArH<u>H</u>), 7.04 (br s, 1H, NH), 2.92 (d, 3H, J = 4.8 Hz, NC<u>H</u>$_3$), 2.47 (s, 3H, ArC<u>H</u>$_3$), 2.08 (s, 3H, CC<u>H</u>$_3$); ^{13}C NMR ($CDCl_3$, 100 MHz) δ 168.2, 161.4, 146.5, 132.0, 130.8, 130.2, 128.3, 120.5, 26.9, 24.2, 21.7; HRMS (ES) calc'd for $C_{13}H_{16}N_2NaO_5S$ 335.0672, found 335.0674 (M + Na).

9.5 References

1. Chatterjee, C.; Paul, M.; Xie, L. L.; van der Donk, W. A. Biosynthesis and mode of action of lantibiotics. *Chem. Rev.* **2005**, *105*, 633-683.
2. Stymiest, J. L.; Mitchell, B. F.; Wong, S.; Vederas, J. C. Synthesis of biologically active dicarba analogues of the peptide hormone oxytocin using ring-closing metathesis. *Org. Lett.* **2003**, *5*, 47-49.
3. Stymiest, J. L.; Mitchell, B. F.; Wong, S.; Vederas, J. C. Synthesis of oxytocin analogues with replacement of sulfur by carbon gives potent antagonists with increased stability. *J. Org. Chem.* **2005**, *70*, 7799-7809.
4. Martin, N. I.; Sprules, T.; Carpenter, M. R.; Cotter, P. D.; Hill, C.; Ross, R. P.; Vederas, J. C. Structural characterization of lacticin 3147, a two-peptide lantibiotic with synergistic activity. *Biochemistry* **2004**, *43*, 3049-3056.
5. Nilsson, B. L.; Kiessling, L. L.; Raines, R. T. High-yielding Staudinger ligation of a phosphinothioester and azide to form a peptide. *Org. Lett.* **2001**, *3*, 9-12.
6. Soellner, M. B.; Tam, A.; Raines, R. T. Staudinger ligation of peptides at non-glycyl residues. *J. Org. Chem.* **2006**, *71*, 9824-9830.
7. Soellner, M. B.; Nilsson, B. L.; Raines, R. T. Reaction mechanism and kinetics of the traceless Staudinger ligation. *J. Am. Chem. Soc.* **2006**, *128*, 8820-8828.
8. Stergiou, V. A.; Thomas, L. V.; Adams, M. R. Interactions of nisin with glutathione in a model protein system and meat. *J. Food Prot.* **2006**, *69*, 951-956.
9. Rose, N. L.; Sporns, P.; Dodd, H. M.; Gasson, M. J.; Mellon, F. A.; McMullen, L. M. Involvement of dehydroalanine and dehydrobutyrine in the addition of glutathione to nisin. *J. Agr. Food Chem.* **2003**, *51*, 3174-3178.

10. Nakazawa, T.; Suzuki, T.; Ishii, M. Synthesis and characterization of [beta]-O-tosyldehydroserine as a precursor of dehydroamino acids. *Tetrahedron Lett.* **1997**, *38*, 8951-8954.